

Doctoral Thesis ETH No. 20218

Functional Surface Coating for Electrochemically Controlled Delivery to Living Cells

A dissertation submitted to the
ETH ZURICH

for the degree of
Doctor of Sciences
(Dr. sc. ETH Zürich)

presented by
Norma Graf
MSc. Material Science ETH
born on March 24, 1983
citizen of Bleienbach (BE)

accepted on the recommendation of
Prof. Dr. Janos Vörös, examiner
Dr. Tomaso Zambelli, co-examiner
Dr. Fouzia Boulmedais, co-examiner

February, 2012

PHANTASIE IST WICHTIGER ALS WISSEN, DENN WISSEN IST BEGRENZT.

ALBERT EINSTEIN

Acknowledgements

My first thanks go to you, Tomaso. You guided and supported me always during my whole thesis. Your support in any situation was extremely valuable for me. I am very grateful that you were my supervisor! I learned a lot of things from you. One of the most important lessons was, how to work systematically and towards a clear goal in the future and enjoy and live a great private life at the same time. Thank you very much!

Then, thank you Janos. You were always able to widen my perspective without being too protective. You let me look at things from different angles which might have caused some little wrangles. After all I am very glad, you're the best professor I ever had! I guess I can stop rhyming like a silly cow because you got who was the secret Santa now. :) Thank you for everything.

Another very important person during my time here, were you Esther. You always managed to keep an overview over all the bills and forms I occasionally tended to lose or forget. It was always nice having you around and filling the group with a soul! Thanks also to you, Stephen Wheeler. I could always come to you and ask you for an emergency fix for my flow-cells, which was very important! Without your help in many many situations, my PhD would have taken far longer! Thanks also to Martin Lanz, I could always approach you in the last minute and you would always be there to help me out!

Elsa you know that you are extremely important for me. I could always discuss science as well as many many private matters with you! I will definitely remember the stairs of J-Floor where we spent quite some time! You are a super-great friend!

Thanks also to you Leena for your enthusiasm about basically every kind of sport you can think of, and joining us for climbing and hiking, thanks to you Victoria for bringing a great spirit to our group by your lovely and sweet (in many senses) way. I learned from you how to bake cinnamon raisin loafs, how to 'scrap book' and how I should treat my

plants properly. You are a great example for me how to be an excellent scientist and still enjoy many private hobbies at the same time. Thanks to you Raphael Z. for always being in a cheerful mood and being always there to help in any situation. No matter if it was scientifically or personally, I could always approach you and you would cheer me up!

Thanks also to Prayanka, for always having a nice story to tell in the coffee corner, to Harald who was always there even when the lab was deserted, since it was already late at night, to Gemma for always patiently answering my cell questions and teaching me how to speak without words, to Raphael G. for letting me drink with him and discover his nice personality :), to Alex L. for always being up to organize a BBQ, a fondue, wine tasting or other great events, to Pablo for being always in a great mood and never fed up with questions and problems for the CLSM, to Sophie for sharing some great game and drink memories from Taufers and Titisee, to Bernd for always taking care of my special coffee and tea requests and sharing office with me, to Dario for being a patient office mate and sharing great Cortona memories, to Rami for funny memories how tea is served in Shanghai, to Kaori and Pascal for unforgettable memories from Hong Kong, to Chris for introducing me to 'beignets', to Juliane for increasing the women ratio in our office and taking lots of funny pictures, to José for always being in a great mood even in the morning, and to Benjamin for many interesting discussions about our projects.

A great thank you also to the old members of LBB! Orane, it was a pleasure starting my PhD under your guidance! It would have only been half as much fun without Mr. Potato Man. Bink, after I convinced you that I am not *that* annoying we enjoyed many funny moments together. Thanks for tons of fun LBB events and your fine social sense. Dorothee, I have to admit I did not agree with all of your 'angry emails' to the group, but after being lab responsible myself I understand your perspective way better :). Robert, it was a fun time in our office. Thanks for showing some taek won do tricks during work and bringing the indispensable couch to our office. Thanks also to Marta and Ana who were always up to party and taking lots of embarrassing pictures there. Many thanks also to you Andreas D. for being the greatest office mate in the world! I had so much fun!

Another great thank belongs to our cooperation partners from Strasbourg, namely Hajare Mhamed, Fouzia Boulmedais, Pierre Schaaf and Philippe Laval. It was a great pleasure to work with you and discuss results as well as possible perspectives with you. It was very nice to see that honesty and openness with other scientists lead to enormously successful cooperations.

Another person that was very important in my PhD is Erik Reimhult. Thank you Erik for endless skype discussions about the structure and content of my first paper. Thanks for your patience and your never ending support and motivation for my project. Thanks also to Sara Morgenthaler who is actually responsible in the first place that I decided to do a PhD at all. You know I always looked up to you and it was so nice to be able to share ideas and wishes for the future with you. Thanks also to Holger Frauenrath. You supported me very much in the first part of my PhD. You showed me that science can be great fun and you were always listening to any issues I had at work.

My PhD would not have been half as successful without the help of my devoted students. Tristan Petit, you were my first semester student and I owe you a lot of very basic pillars of my work. Francesco Albertini, you were my second semester student and I also enjoyed working with you very much! Your enthusiasm and openness for scientific ideas always impressed me. Alex Tanno, you really brought back my enthusiasm for work after a long boring phase in the lab. It was really great to work with you and to see how fast you acquire and learn completely new things. Thanks for your devoted help! Luca Hirt, I was impressed how much you cared for your project and how easily you seemed to learn all these new things in such a short time! Thank you for your help! Alex Dochter it was wonderful to have a brainiac to complete our team! Your persistence and creativity in solving scientific questions was very impressive. Nuria Rothfuchs, you appeared in the very last moment, and I enjoyed working with you very much. Thank you all very very much!

The last round of 'thank yous' goes to my family. Popi, es isch wunderschön xi, immer öpper im Rügge zha wo es unendlichs Inträsse a minere Arbet zeigt. Es hed mich immer sehr gfreut, dass Du Dich so für alles interessiersch was ich mach. Götti und Elisabeth, es hed mer mega gfalle, dass ihr üch immer informiert hend was ich denn eigentlich da so mache und sogar versuecht hend mis Paper z entziffere! Danke viel mal. Mam and Roland, thank you for your support, even though you did not always understand the fuzz that people make about stuff like papers and conferences. Finally, I thank Dominik. Thank you so much for everything. You always handled my (of course very seldom occurring) 'work-grumpiness' with humor and patience. Thank you for your support in every aspect!

Last, I thank ETH Zürich and the Germaine de Staël France-Switzerland Project for financial support.

Abstract

When a tissue in the human body is injured, a cascade of chemical signals is initiated to start the healing process. What is essential in daily life, can cause severe problems if the injury is caused by surgical operations for implants of biomaterials conceived to improve a patient health. The body tries to 'heal' the affected area, proteins adsorb on the surface and a deposit of activating and inhibiting substances is formed. The implant will be either resorbed or encapsulated due to the so-called 'foreign body reaction'. To avoid this, many researchers attempted to create 'non-adhesive' surfaces which eliminate the adsorption of proteins and, thereby, inhibit the foreign body reaction. However, due to advances in healthcare, for example in tissue engineering using scaffolds, the need for beneficial interaction between tissue and biomaterial has arisen. In this perspective, the cellular contact with artificial substrates can be desired to influence the cell behavior from the surface. 'Surface-mediated drug delivery' has been used for DNA transfection, but not for drug delivery in a general fashion. In order to use this approach more universally, a way to modify the properties of biomaterial surfaces is needed.

There are several options to modify the chemical properties of a surface. A popular, powerful approach is to coat the surfaces with polyelectrolyte multilayers (PEMs). Polyelectrolytes adsorb spontaneously onto oppositely charged substrates reversing the net charge. This overcompensation enables the subsequent adsorption of an oppositely charged polyelectrolyte in a layer-by-layer fashion. The method of layer-by-layer adsorption has been used extensively among a variety of biomedical applications. To increase the functionality of such coatings, many research groups incorporated active factors into the PEM films. The loading capacity of the films with active factors could be further increased by the incorporation of *carriers*, such as phospholipid vesicles, into the PEM films. The triggered release from vesicles has been demonstrated by a variety of stimuli such as light, temperature, redox reactions, ultrasound and many more.

This thesis is about the design and creation of a platform for electrochemically induced and surface-mediated drug delivery. The platform is based on a functional surface coating consisting of PEMs with embedded liposomes as carriers for a model-drug (i.e. a fluorescent dye) which can be released by an electrochemical stimulus.

First, the materials for the buildup of the platform were selected. Since the application of a current in aqueous solutions causes the generation of a pH gradient from the electrode, the pH-sensitivity of the materials was of high importance. The PEM between the substrate and the liposomes for example should remain stable in the pH-gradient, while the liposomes should release their substance due to the change in pH. After finding the appropriate materials, we demonstrated the stable incorporation of 100 % negatively charged liposomes into the PEM film without additional stabilization of the vesicles. Then, we showed that the dye could be released from the embedded vesicles upon the application of a galvanostatic current.

The platform was then further optimized in order to control the release in terms of place and time. Two different patterning techniques were employed to show the spatially controlled release of the dye. Moreover, the application of different current densities allowed for the tuning of the release kinetics. We also show an attempt to refill the vesicles, which was not successful.

In a next step, we found a simple strategy to increase the loading capacity within the PEM film up to 17 times, using the spontaneous adsorption of vesicle-multilayers onto the PEM. By combining atomic force microscopy and quartz crystal microbalance measurements, we found that the PLL in the underlying PEM diffuses up to the adsorbing liposomes stabilizing them by compensation of the negative charges. Due to this stabilization the vesicles in the PEM preserved their spherical shape. Then, more PLL could migrate up along the liposomes and newly arriving vesicles could attach again to the now slightly positively charged liposomes, forming a multilayer on the PEM.

Finally, the platform has been adapted for cell adhesion by exchanging the covering PEM with cross-linked (PLL/HA)₁₂PLL-g-PEG-RGD. We could show that the short application of 50 $\mu\text{A}/\text{cm}^2$ led to the release of the dye and the delivery into cells on top of the platform.

The achievements of this thesis serve as new tools for addressing basic research questions for example to create 'artificial synapses' whereas substances can be released from vesicles and taken up by other vesicles mimicking the natural way signals are transmitted between neuronal cells.

Zusammenfassung

Wenn körperliches Gewebe verletzt wird, wird eine Kaskade von chemischen Signalen ausgelöst um das Gewebe zu heilen. Während diese Reaktion im alltäglichen Leben unverzichtbar ist, kann sie nach chirurgischen Eingriffen zu ernsthaften Problemen führen. Jede Operation ist mit einer Verletzung von Körpergewebe verbunden, die besonders beim Einsetzen von Implantaten Fremdkörperreaktionen hervorrufen kann. Der Körper versucht dabei die betroffene Stelle zu 'heilen', das heisst Proteine adsorbieren auf der Implantatoberfläche und ein Depot von aktivierenden und inhibierenden Substanzen wird gebildet. Das Implantat wird entweder resorbiert oder eingekapselt, beides höchst unerwünschte Reaktionen bei Langzeitimplantaten. Um dieses Problem zu vermeiden, haben viele Forscher an sogenannten 'nicht-adhesiven' Oberflächen gearbeitet. Diese verhindern die Adsorption von Proteinen und Zellen und dadurch die Fremdkörperreaktion. Kürzlich hat ein anderer Ansatz immer mehr Beachtung gefunden. Dabei ist der Kontakt zwischen Zellen und Oberflächen erwünscht, um das Verhalten der Zellen durch Abgabe von Medikamenten von der Oberfläche direkt zu beeinflussen. Diese 'Oberflächen-vermittelte-Medikamentabgabe' wurde bisher nur für DNA-Transfektion benutzt und nicht für Medikamentabgabesysteme im Allgemeinen. Um diesen Ansatz generell nutzbar zu machen, braucht es einen Weg, Oberflächeneigenschaften zu modifizieren.

Um die chemischen Oberflächeneigenschaften eines Materials zu verändern gibt es verschiedene Möglichkeiten. Eine sehr beliebte Möglichkeit ist die Oberflächen mit Polyelektrolytmultischichten (PEMs) zu bedecken. Polyelektrolyte adsorbieren spontan auf gegensätzlich geladenen Oberflächen und invertieren dabei die Ladung. Diese Überkompensation ermöglicht die Adsorption von weiteren, gegensätzlich geladenen Polyelektrolyten. Diese Methode wird sehr oft in biomedizinischen Anwendungen verwendet und ist sehr bekannt. Um die Funktionalität der Beschichtung weiter zu erhöhen, integrieren viele Forschungsgruppen aktive Substanzen in die Beschichtungen. Die grösstmögliche Bela-

dition kann erhöht werden wenn man zusätzlich Vesikel einbettet, die mit einer aktiven Substanz gefüllt sind. Die Freisetzung dieser Substanz kann über verschiedene Auslöser geschehen, zum Beispiel Licht, Temperatur, Redox Reaktionen, und Ultraschall.

Diese Dissertation behandelt die Entwicklung und Herstellung einer Plattform für 'Oberflächen vermittelte Medikamentabgabe'. Die Plattform basiert auf einer funktionellen Oberflächenbeschichtung aus PEMs mit eingebetteten Liposomen, die mit einem 'Stellvertreter Medikament' (einer fluoreszenten Farbe) gefüllt sind. Die Farbe kann über einen elektrochemischen Stiumulus freigesetzt werden.

Zuerst wurden die Materialien für den Aufbau der Plattform ausgewählt. Da das Anlegen eines Stroms ein pH-Gradient verursacht, war die pH-Empfindlichkeit der Substanzen ein sehr wichtiger Faktor. Die PEM-Schicht zwischen der Oberfläche und den Vesikeln sollte zum Beispiel inakt bleiben wenn sich der pH verändert, währenddessen die Vesikel auf die pH-Veränderung reagieren und die Farbe freisetzen sollten. Nachdem wir die Materialien ausgewählt hatten, wurden Liposomen mit einer rein negativen Oberflächenladung ohne zusätzliche Stabilisierung in die PEM-Schicht eingebettet. Das war bisher noch nicht möglich. Dann zeigten wir, dass die Farbe durch den angelegten Strom tatsächlich von den eingebetteten Vesikeln freigesetzt wurde.

Die Plattform wurde dann weiter optimiert um auch die Zeit und den Ort der Freisetzung kontrollieren zu können. Zwei unterschiedliche Arten der Oberflächenstrukturierung wurden angewendet um die räumlich kontrollierte Freisetzung zu zeigen. Zudem konnten wir durch verschiedene Ströme die Zeit der Freisetzung steuern. Wir versuchten auch leere Vesikel durch einen angelegten Strom mit Farbe zu *befüllen*, was leider aber nicht geklappt hat.

In einem nächsten Schritt haben wir eine sehr einfache Möglichkeit gefunden die Beladung der Beschichtung mit aktiven Faktoren um 17 Mal zu vervielfachen, indem wir spontane Vesikel-Multischichten auf der Oberfläche adsorbierten. Durch komplementäre Analyse mit Rasterkraftmikroskopie und Quarzkristall-Mikrowägung konnten wir bestätigen, dass das positiv geladene Poly-L-Lysin (PLL) in der PEM-Schicht zu den ankommenden Liposomen diffundierte und sie durch Ladungskompensation stabilisierte. Neu ankommende Vesikel konnten dann auf den nun leicht positiv geladenen Vesikeln adsorbieren und so eine Vesikelmultischicht bilden.

Die Plattform wurde schliesslich für Zelladhäsion angepasst, indem die PEM-Schicht in Kontakt mit den Zellen durch eine vernetzte PEM-Schicht ersetzt wurde. Es gelang uns

zu zeigen, dass ein Strom von $50 \mu\text{A}/\text{cm}^2$ zur Freisetzung der Ladung genügte. Auf diese Art freigesetzte Farbmoleküle wurden von der auf der Polyelektrolytschicht wachsenden Zellkultur aufgenommen.

Unsere Plattform könnte verwendet werden um grundlegende Forschungsfragen zu beantworten, beispielsweise um künstliche Synapsen zu realisieren. Hierbei würden die Vesikel in der Multischicht Substanzen freisetzen, welche wiederum von anderen Vesikeln aufgenommen werden könnten. Dies würde es ermöglichen natürliche Signaltransduktionsprozesse zu imitieren.

1	Introduction:	
	State of the Art of Polyelectrolyte Multilayer Based Drug Delivery	1
1.1	Implants and Associated Problems	1
1.1.1	Healing upon Injury	3
1.1.2	Tissue - Biomaterial Interface	3
1.1.3	First Approach: Non-Fouling Biomaterial Surfaces	4
1.1.4	Second Approach: Surface-Mediated Drug Delivery	5
1.2	Functional Surface Modifications	5
1.2.1	Layer-by-Layer Deposition	6
1.2.2	Polyelectrolyte Multilayers (PEMs)	6
1.2.3	Phospholipid Vesicles as Nano-carriers	9
1.2.4	Triggered Release from Liposomes	9
1.3	Research Status in the Laboratory of Biosensors and Bioelectronics at my Arrival	12
1.4	Scope of the Thesis	13
2	Materials & Methods	19
2.1	Materials	19
2.1.1	Sodium Chloride Solution	19
2.1.2	Substrates/Working Electrodes	20
2.1.3	Polyelectrolytes	20
2.1.4	Lipids	21
2.1.5	Cells and Cell Additives	22
2.2	Methods	23
2.2.1	Substrate Cleaning	23
2.2.2	Patterning	24

2.2.3	Vesicle Preparation and Adsorption	24
2.2.4	Deposition of PEMs onto the Substrates	25
2.2.5	Cross-linking	26
2.2.6	(Electrochemical) Flow-cells	26
2.2.7	Electrochemistry (EC)	26
2.2.8	(EC-) Atomic Force Microscopy ((EC)-AFM)	27
2.2.9	(EC-) Confocal Laser Scanning Microscopy ((EC-CLSM)	28
2.2.10	(EC-) Quartz Crystal Microbalance ((EC)-QCM)	29
3	Morphology of Polyelectrolyte Multilayers and their Electrochemical Dissolution	31
3.1	PEM Morphology vs. Substrate	32
3.2	Electrochemically Induced PEM Dissolution	33
3.2.1	Dissolution vs. Delamination	34
3.2.2	Influencing the Stability for PEM Dissolution	37
3.3	Chapter Conclusion	39
4	Electrochemically Stimulated Release from Liposomes Embedded in a Polyelectrolyte Multilayer	41
4.1	Challenges, Strategies & Encountered Problems	41
4.2	The Components of the System	42
4.2.1	Underlying PEM (uPEM)	43
4.2.2	Liposomes	45
4.2.3	Covering PEM (cPEM)	49
4.3	EC-Triggered Release from the Platform	51
4.4	Chapter Conclusion	53
5	Platform Optimization for Temporal and Spatial Release Control	55
5.1	Challenges, Strategies & Encountered Problems	55
5.2	Spatially Controlled Release	57
5.2.1	Adding Patterned Insulator	57
5.2.2	Separate ITO Electrode	59
5.3	Temporally Controlled Release	59
5.4	Refilling Vesicles	59
5.5	Chapter Conclusion	65

6	Increasing the Loading Capacity of the Platform by Spontaneous Vesicle-Multilayer Formation	67
6.1	Challenges, Strategies & Encountered Problems	67
6.2	Amount of Vesicle Adsorption vs. uPEM Thickness	69
6.2.1	AFM Investigations	69
6.2.2	QCM Investigations	71
6.3	Adding a PEM-Barrier for the PLL	73
6.4	Chapter Conclusion	75
7	Electrochemically Driven Delivery of Calcein to Cells on Top of the Platform	77
7.1	Challenges, Strategies & Encountered Problems	77
7.1.1	Avoiding Cell-Platform Contact: Micro-welled Substrate	79
7.2	cPEM Optimization for Cell Adhesion	80
7.3	Finding an Appropriate Factor to be Delivered	82
7.4	Calcein for the Delivery to Cells	84
7.4.1	Needed Concentration	84
7.4.2	Applying the Current: Released Calcein into the Cells	86
7.5	Chapter Conclusion	88
8	Conclusion and Outlook	91
	References	95
	Curriculum Vitae	103

Abbreviations

AFM	Atomic Force Microscopy
AF	Alexa Fluor
CHEMS	Cholesteryl hemisuccinate
CLSM	Confocal Laser Scanning Microscope
cPEM	Covering Polyelectrolyte Multilayer
DOPE	1,2-dioleoyl-sn-glycero-3-phosphoethanolamine
DOPS	1,2-Dioleoyl-sn-Glycero-3-(Phospho-L-serine)
EC	Electrochemistry / electrochemical
ECM	Extra cellular matrix
FITC	Fluorescein Isothiocyanate
FRAP	Fluorescence Recovery after Photobleaching
HA	Sodium Hyaluronate
ITO	Indium Tin Oxide
NBD-POPC	1-Oleoyl-2-[12-[(7-nitro-2-1,3-benzoxadiazol-4-yl)amino]lauroyl]-sn-Glycero-3-Phosphocholine
OWLS	Optical Waveguide Lightmode Spectroscopy
PAH	Poly(allylamine hydrochloride)
PEG	Poly(ethylene glycol)
PEM	Polyelectrolyte Multilayer
PGA	Poly-L-glutamic-acid sodium salt
PLL	Poly-L-lysine hydrobromide
PLL- <i>g</i> -PEG	Poly(L-lysine)- <i>graft</i> -poly(ethylene glycol)
POPC	1-palmitoyl-2-oleoyl-sn-glycero-3-phosphocholine
PSS	Poly(sodium 4-styrene sulfonate)
QCM	Quartz Crystal Microbalance
uPEM	Underlying Polyelectrolyte Multilayer

CHAPTER 1

Introduction: State of the Art of Polyelectrolyte Multilayer Based Drug Delivery

In this introduction I will describe the state of the art of polyelectrolyte multilayers (PEM) based drug delivery. First, the implantation of biomaterials and its associated problems is detailed and the two main approaches to solve these problems are explained. Then, strategies for surface modifications are shown, with a special focus on the layer-by-layer method used for polyelectrolytes. Finally, several mechanisms for the incorporation of functional molecules into polyelectrolyte multilayers are highlighted and different triggering mechanisms for the release are discussed. In the following part, I will describe the present research status of our laboratory at my arrival and subsequently, explain the scope of my thesis. Figure 1.1 shows a graphical overview of the outline of the introduction. The upside down triangle represents the focusing from general drug delivery concepts based on PEMs to the tip of the triangle representing the detailed scope of the thesis.

1.1 Implants and Associated Problems

The history of implants begins very early. Recently, archaeologists found a 5000-year-old artificial eye in Iran. This was the earliest artificial eye ball found so far. The eye was made of lightweight material thought to be derived from bitumen paste painted with gold. The eye is believed to serve two purposes, an aesthetic one and a spiritual one.^[1]

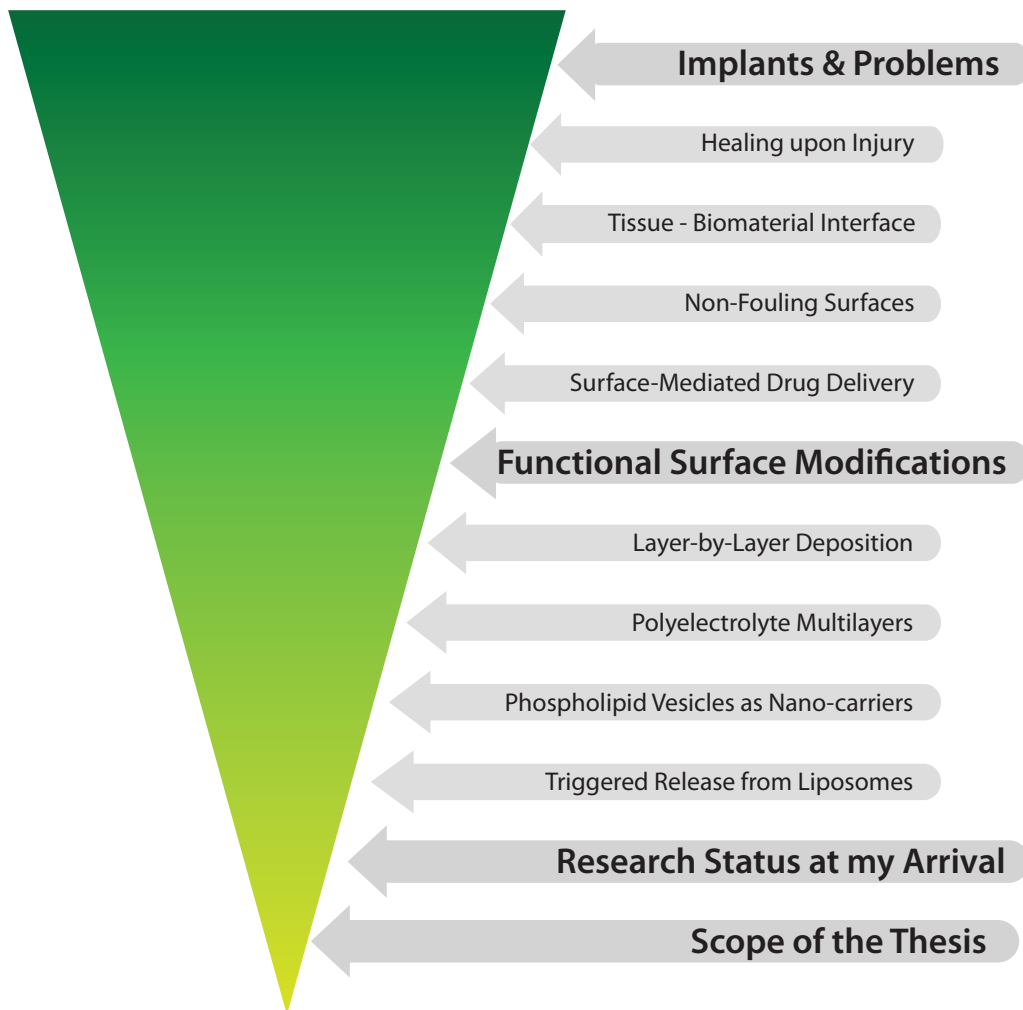


Figure 1.1: Graphical Outline of the introduction. The upside down triangle represents the focusing during the thesis from general concepts to the final scope of the thesis.

Nowadays, still many artificial eyes are made and implanted to people. They are made of medical grade plastic acrylic and can barely be distinguished from the natural eye, illustrating the high level of sophistication of implant technology, available materials, and experience and knowledge in the field of biotechnology nowadays. However, there are still many unsolved problems and issues related to the interface of natural tissue and artificial materials.

The need for glucose sensing for diabetic patients, to mention just one example, has generated a billion USD/year industry showing the magnitude of the problem. Although it is commonly accepted that continuous monitoring with implanted sensors would be highly beneficial for the therapy, nearly all of today's glucose measurements are per-

formed *in vitro* because the fibrous encapsulation of implanted sensors within a few days prohibits their wide-spread use.

1.1.1 Healing upon Injury

When a tissue in the human body is damaged by a physical injury, a localized inflammatory response is initiated by chemical signals, released by cells of the body as a consequence to the injury. The signals cause the nearby capillaries to dilate and become more permeable. This aids the delivery of clotting elements to the injured area, so that blood clotting can occur, beginning the repair process and avoiding the spreading of microbes to other parts of the body. Then, phagocytic cells are attracted by chemical signals and consume pathogens together with cell debris: the tissue heals (Figure 1.2)^[10]. Due to the death of cells and their removal following injury the tissue mass is locally decreased: new cells are recruited to compensate for this decrease and the tissue is remodeled. The inflammation reaction is a well-controlled cascade of signals and events which is essential in daily life.

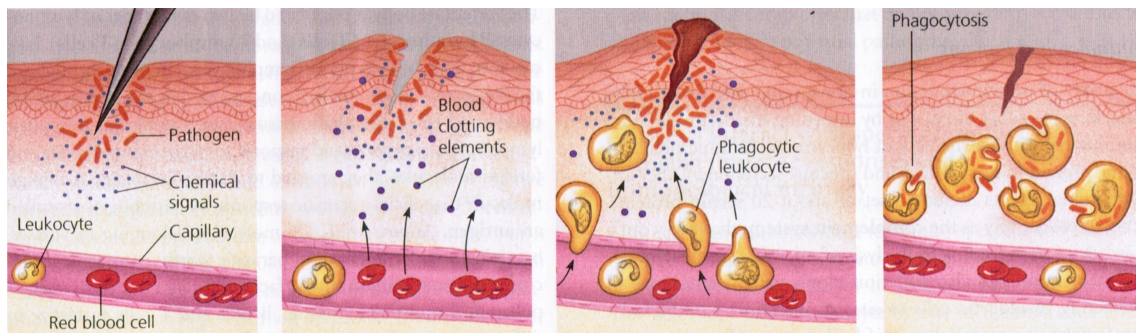


Figure 1.2: Processes occurring upon tissue damage. Chemical signals cause the nearby capillaries to dilate and become more permeable. Blood clotting elements can be delivered to the injured area and phagocytic cells consume pathogens together with cell debris: the tissue heals.^[10]

1.1.2 Tissue - Biomaterial Interface

However, the inflammation process can also be very critical if it happens because of injuries following surgical operations for implantation of a biomedical device meant to *improve* a patients health and condition. Generally, implantation of foreign material is accompanied by several host reactions such as inflammation, foreign body reaction, fibrosis and wound healing processes^[2,29,55]. The foreign body reaction is the end-stage response

of the inflammatory and wound healing process. First, there are blood-material interactions where soluble proteins adsorb on the biomaterial surface^[116] and a provisional matrix forms on and around the biomaterial. Acute and chronic inflammation can follow the adsorption of proteins. The extent of the inflammation depends on the extent of the injury and the site of implantation as well as on the biomaterial surface properties^[3]. The provisional matrix serves as a deposit of activating and inhibiting substances causing the implant to be either integrated, resorbed, or encapsulated. Both, resorption and encapsulation can be unwanted reactions, because the implant can become ineffective depending on the intended application.

1.1.3 First Approach: Non-Fouling Biomaterial Surfaces

Earlier efforts principally attempted to impede protein and cellular adhesion and with that, adverse reactions like inflammation, fibrosis, thrombosis and infection by creating *protein-resistant* surfaces or protein-resistant surface coatings for biomaterials^[104]. These so-called 'non-fouling' surfaces eliminate non-specific protein adsorption on biomaterials, preventing foreign body reactions.

Maroudas discovered in 1975 that cell attachment on highly water soluble polymers adsorbed on planar surfaces is quite weak due to the high steric exclusion volume of the polymers^[62] inspiring many researchers to define common features for non-adhesive, non-fouling surfaces. It was found that non-fouling surfaces are usually hydrophilic, not charged, and have hydrogen bond acceptors but no hydrogen bond donors^[110].

Non-fouling surfaces have then been created using many different techniques such as supported phospholipid bilayers^[25,60], polysaccharide chemistry^[22,61,64,77], functionalized alkanethiols^[11,54,78], and poly(ethylene glycol) chemistry^[36,110]. The most known approach among them uses poly(ethylene glycol) (PEG) to render the surface protein-resistant. The effect of PEG is based on two main features. First, its water solubility and, second, its entropic repulsion. Water molecules can strongly interact with PEG by hydrogen bonding when the PEG is in *gauche* conformation because in this conformation, the distance between oxygen atoms in a PEG chain is very similar to the distance between oxygen atoms in bulk water^[72].

1.1.4 Second Approach: Surface-Mediated Drug Delivery

due to advances in healthcare, for example in tissue engineering using scaffolds, the need for beneficial interaction between tissue and biomaterial has arisen.^[121] In this perspective, the cellular contact with artificial substrates can be desired to influence the cell behavior from the surface. 'Surface-mediated drug delivery' allows for sustained drug delivery to the local environment, mediated from a functionalized surface. The idea is, for example, to deliver drugs to cells growing on a patterned substrate enabling the temporal and spatial control of the drug release. This could be used to stimulate otherwise homogeneous cell cultures with different parameters at different positions. Drug releasing surfaces have already proven useful in diverse biomedical applications including the creation of drug-eluting stents^[17,18], the delivery of antibiotic and anti-inflammatory drugs, guided differentiation of stem cells, and transcutaneous delivery of vaccines and adjuvants.^[121] Another example is DNA transfection, because the elevated concentration of DNA maintained within the cellular micro-environment enhances transfection efficiency^[40-43,90]. However, the application of this concept for drug delivery in a general fashion is a relatively new approach^[121]. In order to use this approach more universally, a way to modify the properties of biomaterial surfaces is needed. The following section describes methods to chemically modify surfaces.

1.2 Functional Surface Modifications

Surfaces can be chemically modified using a variety of different methods. One of the most popular ways is to coat the surface with functional polymers. This can be done by different techniques such as Langmuir-Blodgett deposition^[99,120] or self-assembled monolayers (SAMs)^[15,73,74]. Another option is the layer-by-layer (LbL) technique^[13,14], whereas the polymers are sequentially added to the surface. The multilayer structure of LbL-deposited films allow for high loadings of biologically active agents compared to the SAM technique and it is much simpler and faster than the Langmuir-Blodgett technique^[122]. The LbL technique is used for a tremendous amount of different materials which will be discussed in detail in the following section.

1.2.1 Layer-by-Layer Deposition

LbL-assemblies can be based on several principles. Stockton et al.^[96] demonstrated the buildup of a LbL film with polyaniline and a variety of different nonionic water soluble polymers by **hydrogen bonding**. Shimazaki et al.^[95] built a multilayer based on **charge transfer** by employing poly[2-(9-carbazolyl)ethyl methacrylate] and poly[2-[(3,5-dinitrobenzoyl)oxy]ethyl methacrylate], both bearing nonionic pendant groups in the side chains, which have electron-donating character and electron-accepting character, respectively. Another principle for LbL formation is **covalent bonding**. Sun et al.^[98] fabricated highly stable covalently attached multilayer films by UV irradiation of ionic self-assembled multilayer films of diazo-resins and poly(sodium styrene sulfonate). Multilayer thin films composed of a positively charged protein and cationic polymer layers were prepared against their electrostatic force of repulsion, using the concept of **biological recognition** by depositing avidin and biotin-labeled polymers alternately and repeatedly^[4]. Kotov's analysis in the late nineties revealed that both ionic and **hydrophobic interactions** must be taken into account considering LbL multilayer formation^[49]. Another concept often employed for LbL formation is the use of oppositely charged species such as nanoparticles, polypeptides, nucleic acids and polyelectrolytes that are adsorbed on a surface and form a thin film based on electrostatic interactions. The LbL-assembly of **polyelectrolytes** is detailed in the following paragraph.

1.2.2 Polyelectrolyte Multilayers (PEMs)

PEMs adsorbed by the LbL technique, first introduced by Decher et al.^[13,14], have provided a new powerful tool to coat surfaces. Polyelectrolytes adsorb spontaneously onto oppositely charged substrates reversing the net charge (Figure 1.3). This overcompensation enables the subsequent adsorption of an oppositely charged polyelectrolyte. This technique has been extensively used among a variety of biomedical applications because of its ease of preparation, capability of incorporating high amounts of different types of biomolecules in the films, and robustness of the products under ambient and physiological conditions^[102,115]. Moreover, the thickness of the thin films can be controlled in the nanometer scale because the thickness of a single bilayer of polyelectrolyte is usually in the range of a few nanometers. PEMs can be used to coat almost any kind of charged surface using several deposition techniques such as dip coating^[13,14], spin coating^[44], spray coating^[86] and dewetting^[94]. The simplicity and variability of PEMs has made

them a popular tool in nanomedicine^[122]. For applications with cells, several aspects are important. The following four aspects are detailed below: the classification into weak and strong polyelectrolytes, the adhesion of cells on PEMs, the possibility to chemically cross-link the PEMs, and the knowledge about PEMs used for drug delivery.

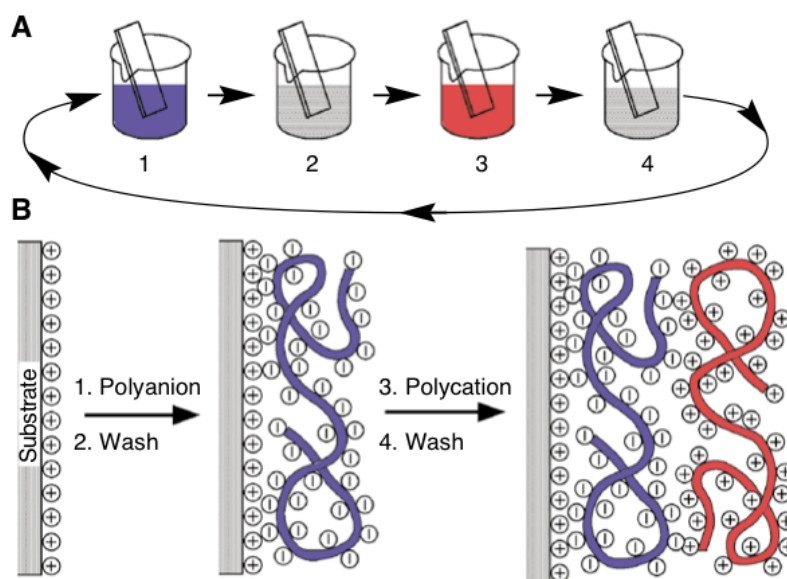


Figure 1.3: Layer-by-layer adsorption of polyanions and polycations onto slightly charged surfaces, introduced by Decher et al.^[13] is a popular and powerful tool to chemically modify surfaces.

Weak and Strong Polyelectrolytes Polyelectrolytes can generally be divided into two categories: strongly and weakly interacting polyelectrolytes, depending on their acid dissociation constant (pK_a). A high or low pK_a means that the polyelectrolytes are fully ionized at neutral pH, resulting in a strong electrostatic interaction between the oppositely charged chains. A medium pK_a value, however, means that the polyelectrolytes are in a less-ionized state at neutral pH resulting in weak interactions between the oppositely charged polymer chains. PEMs made of strong polyelectrolytes are usually stiff and flat, whereas PEMs created from weak polyelectrolyte couples result in hydrated, soft and undulating films. Films prepared with weak polyelectrolytes are, therefore, highly sensitive to the pH of the environment.

Cell adhesion on PEMs The interaction of cells with a large variety of polyelectrolytes and in particular with the terminating layer has been studied by several

groups^[83,107,108,111,117]. It was found that, depending on the type of cells, the film composition and the terminating layer of the films are important parameters for the adhesion, growth and function of the cells. Richert et al. have shown that the stiffness, seems to play the key role when it comes to adhesion and spreading of cells on a polyelectrolyte multilayer substrate^[81,82]. The stiffer the PEM, the more likely the cells adhere well and grow on the surface. Therefore, cross-linking is an important tool for modulation of the PEM stiffness and, consequently, of interactions between cells and PEM films.

Cross-Linking of PEMs PEM films can be chemically cross-linked leading to stiffening and considerable improvement of its resistance against pH and enzymatic degradation. The carboxyl groups of the polymer chains can be cross-linked with amine groups by carbodiimide chemistry using mild conditions (room temperature, salt containing medium). Thereby, covalent amide bonds are formed. Mixtures of N-Hydroxysulfosuccinimide sodium salt (s-NHS) and N-(3-Dimethylaminopropyl)-N'-ethylcarbodiimide hydrochloride (EDC) were used to cross-link PEMs made of PLL/HA. The stiffness of the film could be substantially increased when the EDC concentration was increased^[81,82,87]. EDC is a zero-length cross-linker, meaning that the reaction consists exclusively of the transformation of ionic into covalent bonds, without insertion of any additional molecules in the film^[5]. There are also other options to generate covalent bonds within PEMs, like the use of high temperature (130 °C) to induce amide or imide bonds, the photo-cross-linking of polyelectrolytes modified with photo-reactive groups, or the use of click chemistry^[6,85].

Drug Delivery and PEMs PEMs can be loaded with functional molecules. One option to achieve this is by direct incorporation, such that the functional molecule plays the role of the polyelectrolyte. Examples are DNA^[57], heparin^[51], protein^[56], viruses^[58] and many more^[53]. An important question for this approach is the integrity of the functional entities that needs to be confirmed prior to its release. Boulmedais et al. showed for example that the secondary structure of a film composed of polypeptides is the same as the peptide structure in solution^[7]. Another important issue is that the active molecule is not protected from the environment and can easily be accessed by enzymes or cells in the surrounding. Furthermore, it was important to find a method to increase the loading capacity within a PEM thin film. Another option to load PEMs with functional molecules is the incorporation of *carriers* into the PEMs that encapsulate the active agent. Popular carriers are polymer capsules, micelles and phospholipid vesicles^[38,46,47,68–70,86,97,112,113].

1.2.3 Phospholipid Vesicles as Nano-carriers

Liposomes are hollow capsules made of phospholipids, which naturally contain a hydrophobic tail and a hydrophilic head group. Figure 1.4 shows a schematic drawing of a) a phospholipid and b) a cross section through a liposome filled with a green dye. In aqueous solutions, above a certain concentration, these lipids self-assemble into lipid bilayer structures to avoid contact of the hydrophobic tails with the aqueous environment. Liposomes are very well suited carrier systems due to several advantages such as their simplicity of production, their low permeability for even small species, their biocompatibility and the versatility in the choice of substances to be incorporated^[92,115].

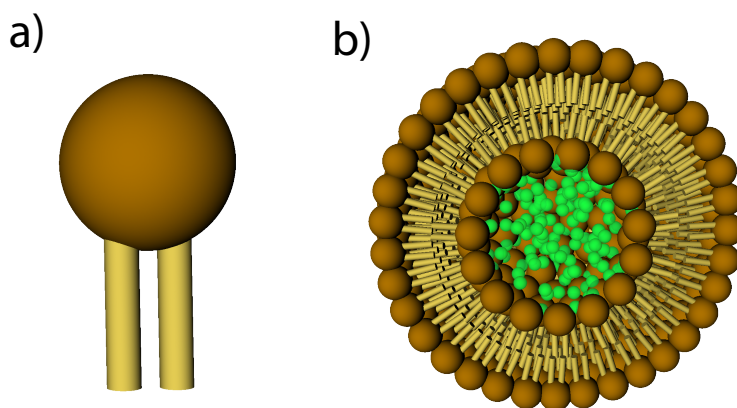


Figure 1.4: Schematic drawing of a) a phospholipid and b) a cross section through a liposome filled with a green dye.

Many groups incorporated such functional liposomes into the PEMs^[68–70,112,113] to increase the degree of loading of active factors within the coating. One issue for the incorporation of liposomes into PEMs is their stability, since liposomes have previously been reported to undergo spontaneous disruption upon adsorption onto PEMs^[68–70,86,112,113]. Michel et al. have demonstrated that negatively charged vesicles can be stabilized by polycation adsorption prior to deposition onto the PEM^[70]. Figure 1.5 schematizes the embedding of vesicles into a film consisting of PLL/HA. The vesicles fuse upon adsorption if they are not stabilized in advance.

1.2.4 Triggered Release from Liposomes

The active substance within the vesicle-PEM assembly can be released by destruction or opening of the vesicles within the PEM film. Various techniques have been reported to

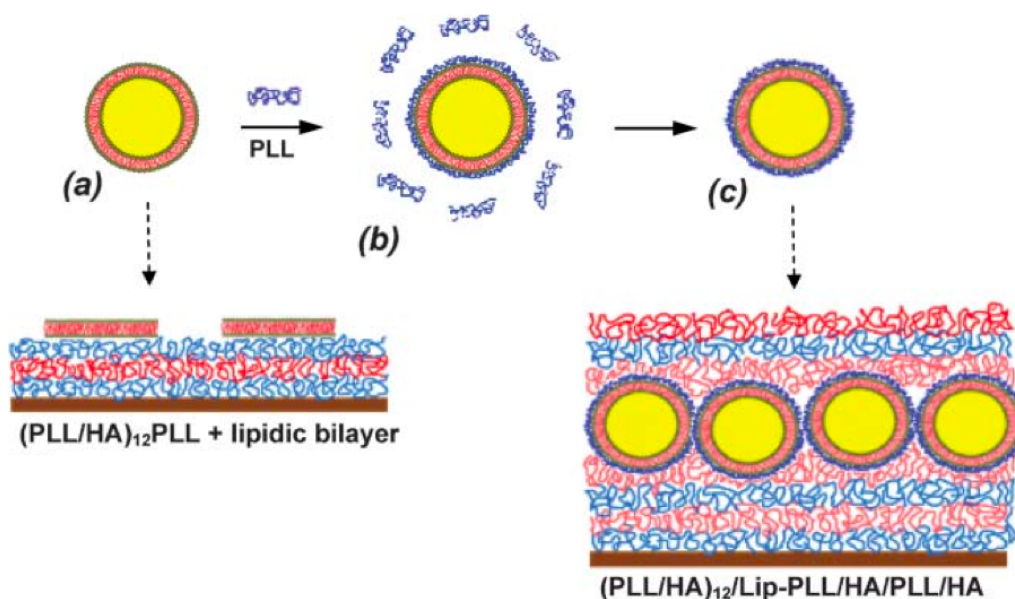


Figure 1.5: Embedding of vesicles (a) into a film consisting of PLL/HA. The vesicles fuse upon adsorption if they are not stabilized (b-c) in advance.^[112]

stimulate the release from liposomes. For example by increasing the **temperature** up to 45 °C which induced the release of an encapsulated dye from vesicles embedded in PEMs^[112,113]. A different option is **by light**, whereas a model compound was encapsulated in thermosensitive liposomes, which were then coated with gold to form plasmon-resonant shells with optical resonances. When exposed to 1064 nm laser light, these liposomes released their content in a spectrally-dependent manner.^[106] Another light-triggered example is using photo-polymerizable phospholipids. Exposure to UV (254 nm) radiation resulted in photo-polymerization of the lipid in these liposomes and the release of an encapsulated fluorescent dye^[119]. Ong et al. used **redox reactions** to trigger release from Q-DOPE liposomes upon their redox activation when the quinone headgroup possesses specific substituents. The key component of the triggerable, contents-releasing Q-DOPE liposomes is a 'trimethyl-locked' quinone redox switch attached to the N-terminus of DOPE lipids that undergoes a cleavage event upon two-electron reduction^[76]. Several groups^[48,88,89] showed the triggered release from liposomes by **ultrasound**, for example Kopeček et al. demonstrated the ultrasound-controlled drug delivery using echogenic liposomes using color Doppler ultrasound. Other methods are the use of **magnetic fields**, whereas low-frequency alternating magnetic field was applied to increase the permeability of 'magnetoliposomes' *i.e.* liposomes including magnetic nanoparticles^[75]. Volodkin et

al. used **near infrared light** to selectively release encapsulated dye from liposome-gold nanoparticles^[114]. Also **pH-triggered** release^[12,20,37,46] was demonstrated. One example is liposomes bearing a copolymer that were embedded in glucose oxidase (GOD)-immobilized alginate beads. The acidification induced by the enzymatic reaction would be responsible for the glucose-triggered release^[37]. Originally, pH-sensitive liposomes were designed in order to release their contents in response to acidic pH within the endosomal system while remaining stable in plasma. This improved the cytoplasmic delivery of various polar materials and macromolecules such as anti-tumor drugs, toxins, proteins and DNA^[109]. The pH-sensitivity is attributed to the protonation or deprotonation of the hydrophilic head groups of the phospholipids and, thereby, the induced shape change of the lipids. This results in either pore formation or rearrangement of the lipid bilayer, releasing the encapsulated content^[105]. Figure 1.6 shows the mechanism for negatively charged lipids. The lipids head size is decreased upon a decrease in pH, due to neutralization of the negative charge. The neutralization causes a decrease in electrostatic repulsion which causes rearrangements of the lipid bilayer of the liposome. Thereby, the encapsulated dye is liberated.

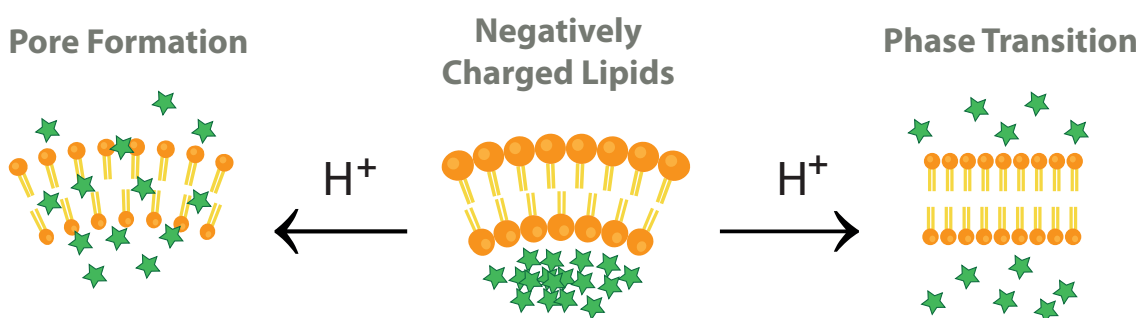


Figure 1.6: Schematical view of pH dependent shape changes of negatively charged lipids in lipid bilayers. H^+ stands for acidic environment. The lipids head size is decreased upon a decrease in pH, due to neutralization of the negative charge. The neutralization causes a decrease in electrostatic repulsion which causes rearrangements of the lipid bilayer of the liposome. Thereby, the encapsulated dye is liberated.

Electrochemically stimulated release, however, is an especially attractive release mechanism for *surface* based systems since it makes low-cost, spatially controlled release possible, using micro electrodes produced by standard semiconductor technology. Furthermore, an electrochemical trigger can be applied *locally* with minimal effect on surrounding biological tissue.

1.3 Research Status in the Laboratory of Biosensors and Bioelectronics at my Arrival

When I started my PhD, one research axis of our laboratory of Biosensors and Bioelectronics (LBB) was the development of a platform technology that allows for the electronically controlled, local delivery of drugs. This technology should not only have the potential to solve the encapsulation problems of implants because it is analogous to the concept of drug-eluting stents, but also be used for biomedical fundamental and applied research. In order to reach this goal the following specific aims were defined:

1. To develop a platform technology using the electronically controlled growth and dissolution of layer-by-layer (LbL) polyelectrolyte films for the controlled release of bioactive molecules (i.e. anti-inflammatory drugs or neurotransmitters).
2. To understand and model the mechanisms of the reversible, electrochemically induced stretching and expansion of LbL films with incorporated redox-active molecules and find the conditions for the highest proportional thickness change.
3. To develop novel, intelligent polymer films that can change their shape on the micron- and nano- scale under electrical control and explore their applications in biomedicine and biotechnology.

In the last years the laboratory had established a unique set of electrochemical (EC) instrumentations and the corresponding expertise (e.g. EC quartz crystal microbalance (EC-QCM), EC optical waveguide lightmode spectroscopy (EC-OWLS), EC atomic force microscopy (EC-AFM) and EC confocal laser scanning microscopy (EC-CLSM)) and initiated various basic research projects as well as applications that relied on the use of electrical currents and potentials to control the behavior of biomolecules and cells at surfaces^[23,32].

The laboratory had not only experience with electrochemical methods, but also with the combination of EC and PEMs. It was, for example, found that PEMs could be reversibly swelled and contracted by electrochemistry^[30]. Furthermore, preliminary results obtained by EC-OWLS and EC-AFM indicated the possibility to remove or destroy vesicles immobilized by DNA-hybridization on a surface.

In addition, the laboratory participated in the Germaine de Stael program collaborating with the Institute Charles Sadron, Strasbourg, who are leading experts in the area of polyelectrolyte multilayer (PEM) films. Through this collaboration they had contact to a large number of scientists with long term experience in this field and, for example, just demonstrated together the feasibility of the EC-controlled buildup and dissolution of PLL/Heparin films (Figure 1.7).

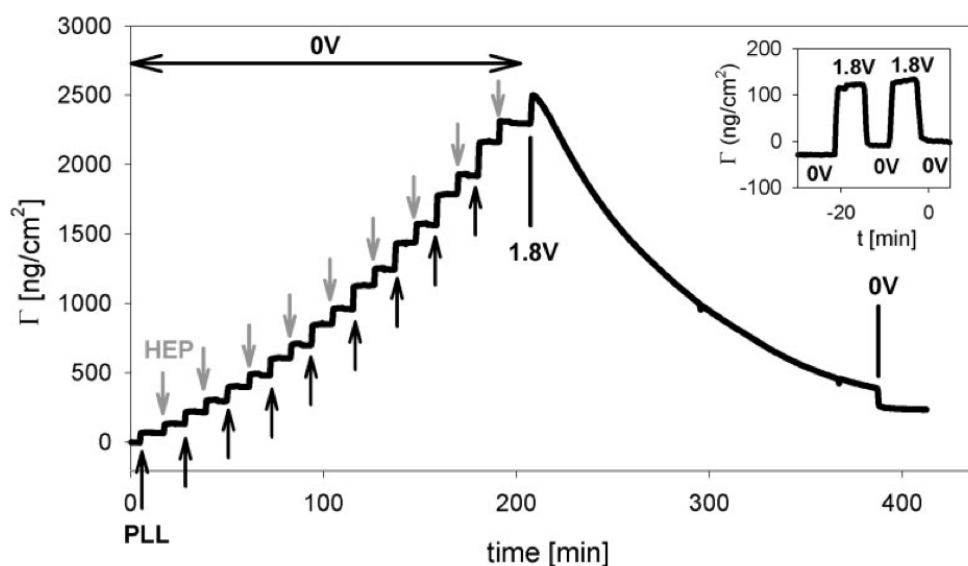


Figure 1.7: EC-OWLS curve of PLL/Heparin deposition and dissolution. Vertical bars represent the application of electric potentials of 1.8 and 0 V. The inset shows the evolution of the adsorbed mass, induced on the bare substrate, as a function of time when the electric potential was switched between 0 and 1.8 V.^[8]

Coming from a material science background with experience in applications of biological materials and surface sciences, my interest focused on the engineering of the interface between living and inorganic materials. Therefore, the first goal of controlled release from substances embedded in a functional surface coating was most appealing to me.

1.4 Scope of the Thesis

Surface-mediated drug delivery holds great potential to influence the cell behavior on the surface of a biomaterial and allows for sustained drug delivery. The main goal of this project was to design and create a platform that could be used for surface-mediated drug delivery. More precisely, to fabricate a functional surface coating consisting of a polyelectrolyte multilayer matrix and therein embedded liposomes. The liposomes contain a

model-drug which is delivered to cells growing on top of it by an electrochemical (EC) stimulus (see Figure 1.8).

Thus, it was necessary to get a fundamental understanding of the effect of the application of an electrochemical potential onto the direct environment, such as the aqueous solution, the polyelectrolyte multilayers, the liposomes, and the cells. The proposed project was roughly divided into four milestones.

1. Stable incorporation of liposomes in the PEM (Section 4.2.2).
2. Proof of principle: EC-triggered release from liposomes in PEMs (Section 4.3).
3. Optimization of the platform in terms of control and loading capacity (Chapters 5 and 6).
4. Modification of the platform for cell compatibility and EC-triggered release to the cells (Chapter 7).

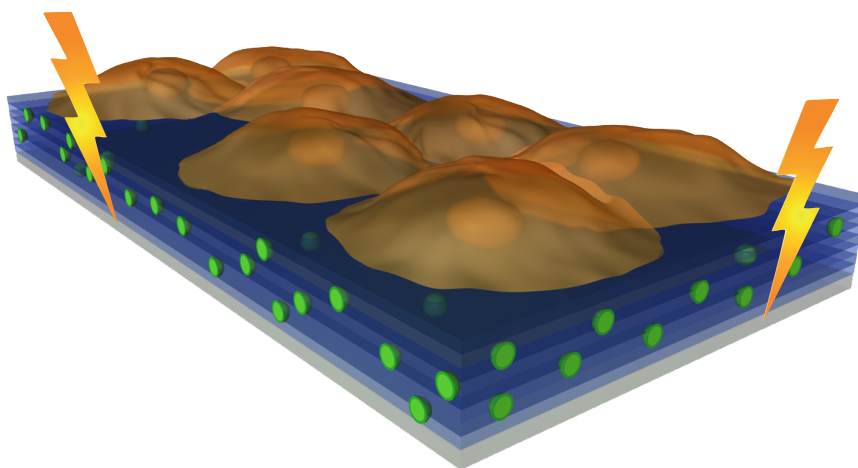


Figure 1.8: Overview of the envisioned platform. The blue structure represents the PEM matrix and the green containers are the vesicles that encapsulate a model-drug. On top of the platform cells are growing. The flashes symbolize the application of an electrochemical stimulus.

First experiments in collaboration with other LBB-PhD students showed that the substrate in combination with the PEM couple plays an important role for the morphology. We found that weakly interacting polyelectrolytes form droplets of different sizes depending on the substrates' dielectric permittivity, whereas strongly interacting polyelectrolytes form a continuous film with only a few bilayers independent of the substrates physical

properties (Section 3.1). We, furthermore, found that weak and hydrated polyelectrolyte couples dissolve upon an EC-trigger whereas strong polyelectrolyte systems can only dissolve if they are a few tens of nanometers thick, if they are thicker, they can delaminate from the surface (Section 3.2.1). We could then also demonstrate, that the EC-stability of a PEM film made of (PLL/DNA)₆ could be changed by the application a potential during the buildup of the film (Section 3.2.2). These findings served as an essential basis for the results in Chapters 4 - 7.

1. Stable incorporation of liposomes in the PEM

Many groups reported the spontaneous and immediate rupture of vesicles upon adsorption onto PEMs. Therefore, vesicles were usually stabilized prior to adsorption^[68–70,86,112,113]. Thus, to embed vesicles into the PEM without rupture was the first issue to be addressed. It turned out that the adsorption of 100 wt% negatively charged vesicles onto PLL-containing PEMs resulted in a stable adsorption of vesicles. This was attributed to the mobility of the positively charged PLL chains which migrated up to the liposomes, compensated their negative charges and caused the liposomes to remain in their spherical shape (Section 4.2.2). This means that a proof of principle to embed vesicles in PEMs *without* extra stabilization could be achieved.

2. Proof of principle: EC-triggered release from liposomes in PEMs

The basic principle of EC-triggered release is that a pH-gradient is created by applying a current to the substrate in aqueous solution. It is known that the application of a galvanostatic current at large enough voltages (1.5 V in our setup) induces electrolysis of water, creating a pH gradient extending a few hundred nanometers from the substrate. The magnitude of the pH gradient depends on the applied current. The principle is shown in Figure 2.6. The thereby induced changes in the pH close to the substrate can trigger the release from pH-sensitive vesicles.

The first findings in Chapter 3 served as the basis for the experiments and results in Chapter 4, which describes the search for the different parts in the platform that needed to fulfill several requirements: Sections 4.2.1, 4.2.2 and 4.2.3 describe the selection of the pH-insensitive uPEM made of (PLL/PSS)₉PLL, the pH-sensitive vesicles made of 100wt% DOPS and the cPEM made of (PLL/PGA)₂ that does not harm the vesicle integrity underneath. Section 4.3 shows the proof of principle that the dye could be released

from the vesicles by means of a current application without removing the vesicles from the surface.

3. Optimization of the Platform in Terms of Control and Loading Capacity

For an optimal surface-mediated drug delivery system, we wanted to control not only the release but more parameters such as the location, material, and release kinetics of the substance that will be delivered. Therefore, this part of the thesis focused on the patterning of the platform and the tailorability of the release by current variation. In Section 5.2 we demonstrate the local control over the dye release by employing two different patterning strategies. This was done by covering the continuous working electrode with a patterned insulator (SU-8) on one side and by dividing the working electrode mechanically into separate electrodes on the other side. This led to high parallelization and an increase in reproducibility of the experiments. Section 5.3 demonstrates the temporal control over the release by applying different current densities. After being able to control the location and kinetics of the release, we aimed at further increasing the loading capacity of the platform. We found that vesicles could be spontaneously adsorbed in a multilayer-fashion due to the stabilizing effect of the migrating PLL chains (Chapter 6). This enabled us to increase the loading capacity up to 17 times.

4. Modification of the Platform for Cell Compatibility and EC-Triggered Release to the Cells

Finally, we could proceed to the delivery of the dye to living cells, introducing several new constraints for the used platform. First, we needed to find a cPEM that resisted the current application and allowed for cell adhesion. A cPEM made of cross-linked $(\text{PLL}/\text{HA})_{12}\text{PLL-g-PEG-RGD}$ was selected after systematic investigations of possible candidates (Section 7.2). Then, a dye that was only released from the vesicles upon an EC-trigger, but spontaneously stained the cells after the release was required. After analyzing several dyes, we found that calcein was most suited for the delivery to cells (Section 7.3). We could show that calcein is indeed delivered to the *inside* of the cells after the application of a current for 3 minutes (Section 7.4) without affecting the cell viability.

To summarize, in this thesis we demonstrated the design, development and fabrication of a functional surface coating for drug delivery. We succeeded in triggering the

release of a dye from vesicles embedded in a PEM by the application of an EC-stimulus. The dye was released and taken up by cells growing on top of the coating.

All result chapters have the same structure. First, I briefly explain the goal of the chapter and describe its challenges and difficulties. These Sections are called 'Challenges, Strategies & Encountered Problems'. The idea there is to show also the process of obtaining the results and the often rocky road to the final success. Then, I present the results that were obtained and published.

2.1 Materials

For all experiments, the same principal system was used. As sketched in Figure 2.1 an indium tin oxide substrate was coated with a PEM underneath the vesicles (uPEM), on which vesicles were adsorbed. The vesicles were then covered by a covering PEM (cPEM).

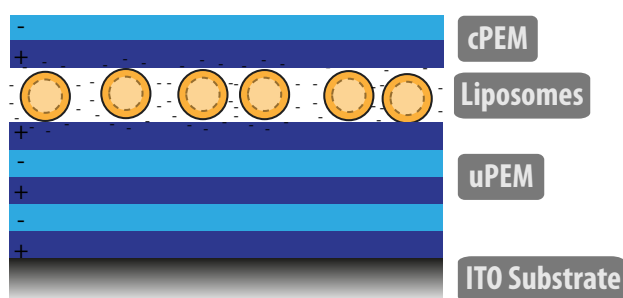


Figure 2.1: Schematic drawing of the used system and the names of the different parts.

2.1.1 Sodium Chloride Solution

All experiments were carried out in 150 mM NaCl dissolved in ultrapure water (resistivity = 18.2 M Ω /cm, Milli-Q gradient A 10 system, Millipore Corporation) if not noted differently. No buffer was used to avoid buffering the electrochemically generated pH-gradient (pH 5-6 at rest *i.e.* $V_{appl} = 0$ V).

2.1.2 Substrates/Working Electrodes

All experiments were performed on indium tin oxide (ITO) coated glass, produced by MicroVacuum (Hungary). For AFM and CLSM experiments, squared samples of $2.3 \times 2.3 \text{ cm}^2$ with a thickness of approximately $300 \mu\text{m}$ glass coated with approximately 50 nm ITO were used. For the QCM experiments, quartz glass crystals were coated with approximately 200 nm ITO.

2.1.3 Polyelectrolytes

The following polyelectrolytes were used.

- PLL: Poly-L-lysine hydrobromide, MW = 24'000, pKa \sim 11, (Sigma Aldrich P7890)
- PLL-FITC: Poly-L-lysine hydrobromide labeled with fluorescein isothiocyanate (FITC), 0.003-0.01 mol FITC per mol lysine monomer, MW = 15'000-30'000 (Sigma Aldrich, P3543)
- PSS: poly(sodium 4-styrene sulfonate), MW = 70'000, pKa \sim 1 (Sigma Aldrich 24,305)
- PGA: Poly-L-glutamic-acid sodium salt, MW = 15'000 – 50'000, pKa \sim 4 (Sigma Aldrich P4761)
- PAH: Poly(allylamine hydrochloride), MW = 58'000, pKa \sim 9 (Sigma Aldrich 283223)
- HA: Sodium hyaluronate, MW = 360 kDa, pKa \sim 2-3 (Lifecore)
- PLL-g-PEG-RGD: PLL (20 kDa) grafted with polyethylene glycol (PEG, 2 kDa) and PEG- Arginine-Glycine-Aspartic acid (RGD, 3.4 kDa), g = 3.0 to 4.0 (Lys units /PEG chains) RGD functionalized PEG of 6-15% (SuSoS AG)

The chemical formulas of the used polyelectrolytes are given in Figure 2.2.

All polyelectrolytes were dissolved in 150 mM NaCl solution at a concentration of 0.5 mg/ml. The notation (PLL/PSS)_n means n layer pairs of the polyelectrolyte couple PLL and PSS. The PEM directly on the substrate is denoted as underlying PEM or short uPEM. The PEM covering the vesicles is denoted cPEM (see Figure 2.1).

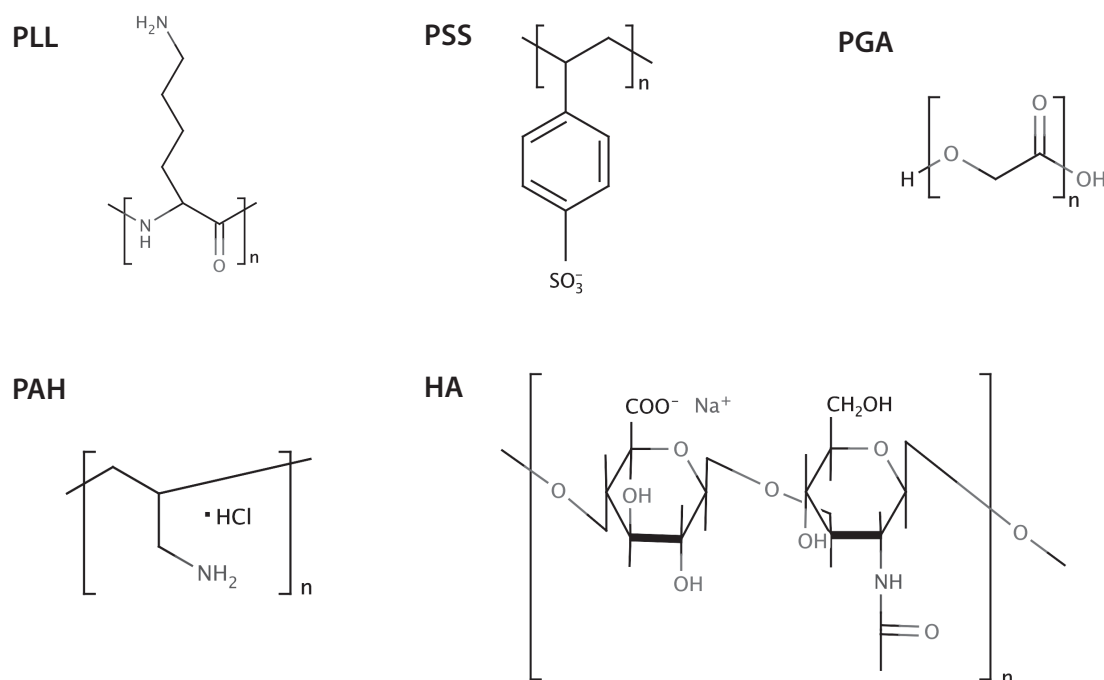


Figure 2.2: Chemical formulas of the used polyelectrolytes

2.1.4 Lipids

The lipids below were used for the experiments where the pH-sensitivity of vesicles was tested (Section 4.2.2). DOPS and DOPS combined with NBD-POPC were used for all other experiments.

- POPC: 1-palmitoyl-2-oleoyl-sn-glycero-3-phosphocholine (AVANTI polar lipids)
- CHEMS: Cholesteryl hemisuccinate (Tris-salt, Sigma)
- DOPE: 1,2-dioleoyl-sn-glycero-3-phosphoethanolamine (AVANTI polar lipids)
- DOPS: 1,2-Dioleoyl-sn-Glycero-3-(Phospho-L-serine) (Sodium Salt, AVANTI polar Lipids)
- NBD-POPC: fluorescently labeled 1-Oleoyl-2-[12-[(7-nitro-2-1,3-benzoxadiazol-4-yl)amino]lauroyl]-sn-Glycero-3-Phosphocholine (AVANTI Polar lipids).

All of the lipids were dissolved in chloroform and stored at -20°C until use. Chemical formulas are given in Figure 2.3.

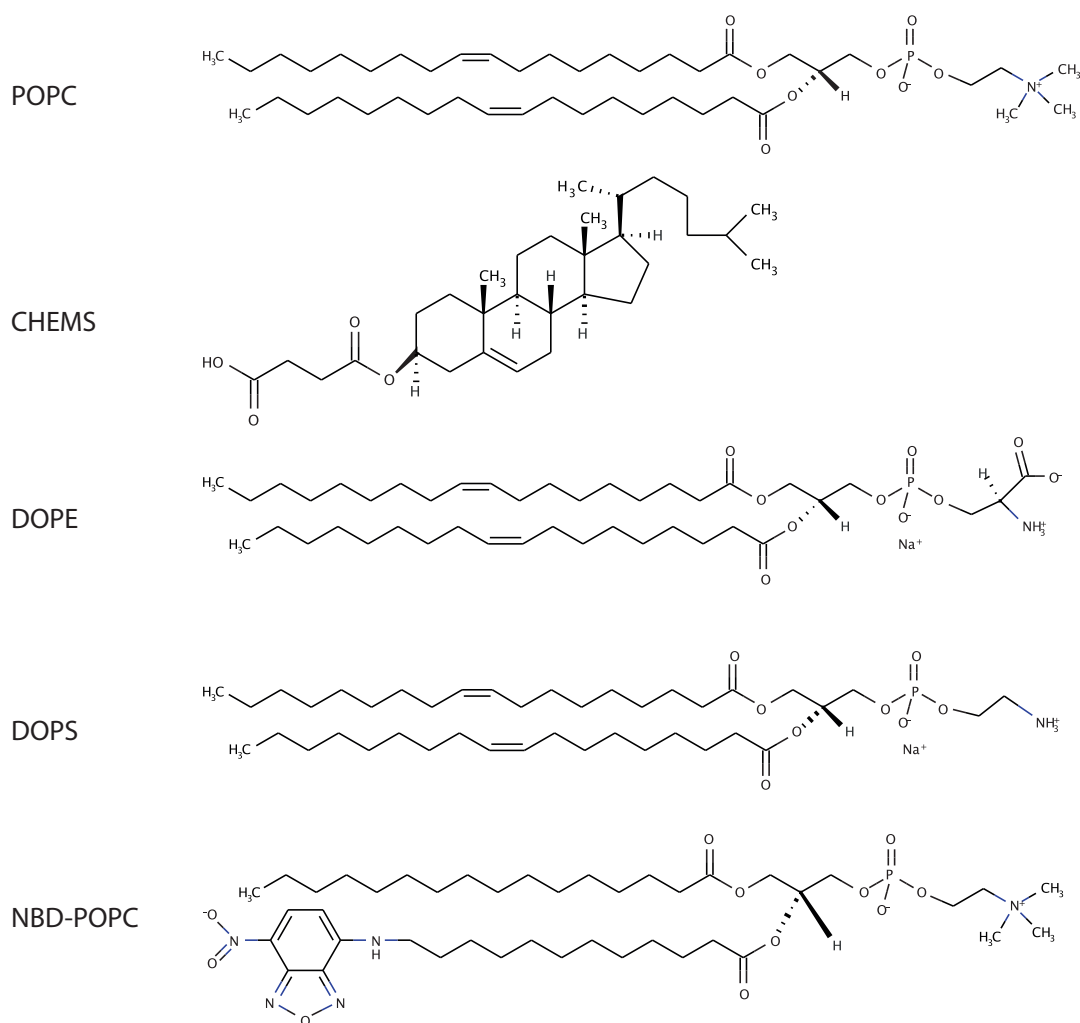


Figure 2.3: Chemical formulas of the used lipids.

2.1.5 Cells and Cell Additives

Cells C2C12 mouse myoblasts were purchased from American Type Culture Collection (LGC Standards, Molsheim, France). The cells were maintained at 37 °C, 7 % CO₂ atmosphere in growth medium (GM) consisting of Dulbecco's modified eagle's media (DMEM, Invitrogen, Switzerland) supplemented with 20 % fetal bovine serum (FBS, Invitrogen, Switzerland).

Sample Preparation The prepared samples were rinsed with 400 μ l and sterilized by UV light for 30 min. After the sterilization the GM was replaced with fresh GM and they were stored in the incubator at 37 °C for at least 10 min to heat them. For seeding the cells

onto the cPEM, adherent cells were trypsinized for 10 min in the incubator at 37 °C, and then GM was added to inactivate trypsin. Cells were counted with a Countess[®] Automated Cell Counter (Invitrogen, Switzerland) before seeding at 40'000 cells/cm² on the substrates. The samples were then incubated at 37 °C, 7 % CO₂ atmosphere in growth medium for at least 3 h. Subsequently, the GM was exchanged by 150 mM NaCl and rinsed once before applying electrochemical stimuli.

Cell Viability The cell viability was evaluated using the dead stain ethidium homodimer-1 (Invitrogen) 2 mM in DMSO/H₂O 1:4 (v/v). The cells were first washed with PBS once and then incubated with the dead staining solution (2 μl Ethidium homodimer-1 (2 mM) in 1 ml PBS) for 30 min and then imaged by CLSM (Excitation: 514 nm, filter: 488/514 nm and a cutoff at 515 nm).

Dyes For the cell experiments a variety of dyes was tested. CellTrackerTM green 5-chloromethylfluorescein diacetate (CMFDA) MW = 464.8581, (Invitrogen C2925), Qtracker[®] 605 Cell Labeling Kit (Invitrogen, Q25001MP), cholera toxin subunit B (recombinant), Alexa Fluor[®] 488 conjugate (Invitrogen C-22841) and calcein disodium salt (Fluka, 21030, MW = 666.50). For the experiments where cells were grown directly on the SU-8 pattern (Section 5.1), the cells were stained by CellTrackerTM green and fixed with paraformaldehyde for 30 min prior to imaging.

2.2 Methods

2.2.1 Substrate Cleaning

The substrates were cleaned in a step-wise manner. Firstly, by ultrasonication (Elna Transsonic Digital S, Iswork, Singapore) Isopropanol (puriss., Sigma Aldrich) and ultrapure water for 10 min in each subsequent solvent. The samples were rinsed with ultrapure water after every cleaning step. Then, they were dried with a nitrogen flow. Finally, they underwent UV/Ozone cleaning (Uvo Cleaner 42-220, Jelight Company, USA) for 30 min prior to spraying. After use, they were cleaned with a cotton stick that was soaked into sodium dodecyl sulfate (SDS, 2 wt%) and then rinsed with ultrapure water. The samples were reused as long as the resistance remained below 7 kΩ for the results in Chapters 5 and 7. The resistance was not controlled for the results in Chapters 4 and 6.

2.2.2 Patterning

Two different patterning methods were used. One, where parts of the ITO are covered by an insulating layer and one where the ITO is separated into individually addressable electrodes.

SU-8 Patterning

The patterning method was adapted from Guillaume-Gentil et al.^[33]. The negative photoresist SU-8 was spin coated onto the ITO at 1600 rpm during 40 s. The coated substrates were then soft-baked at 65 °C (ramped at 2 °C/min) for 10 min and then at 95 °C (ramped at 2 °C/min) for 30 min before cooling down to room temperature. Once the resist has dried, the sample was covered with a mask and exposed to UV light for 15 s. Then, a second soft baking step was added at 65 °C (ramped at 2 °C/min) for 1 min followed by a second temperature step at 95 °C (ramped at 2 °C/min) for 1 min. The substrates were then developed in PGMEA for 4 min. They were rinsed afterwards in isopropanol and dried by a N₂ flow. Finally, the patterned substrates were baked at 135 °C for 2 h.

4-Electrode substrates

A wafer saw was used to cut a cross-shape (2 μm deep, 40 μm wide lines) across the ITO layer on glass, resulting in one sample with 4 equally sized, electrically well separated electrodes on top of it that were individually addressable.

2.2.3 Vesicle Preparation and Adsorption

Three different kinds of vesicles were used: membrane-, cargo- and non-labeled vesicles.

1. Membrane-labeled vesicles consisting of 98 wt% DOPS and 2 wt% NBD-POPC. 5 mg of the lipids were dried under a constant flow of nitrogen for 30 min and then rehydrated in 150 mM NaCl.
2. Cargo-labeled vesicles consisting of 100 wt% DOPS were used and 5 mg of the lipids were dried and rehydrated in 50 mM calcein.

3. Non-labeled vesicles consisting of 100 wt% POPC, 100 wt% CHEMS, a mixture of CHEMS and DOPE, and DOPS were prepared the same way as cargo-labeled ones, but rehydrated in 150 mM NaCl instead of calcein.

The rehydrated lipid suspensions were each extruded through a double-stacked polystyrene membrane with a pore size of 200 nm. The extruded vesicles were diluted to a concentration of 0.5 mg/ml and stored in the fridge for maximum 30 days before use. The liposomes were characterized at 20 °C with a salt concentration of 150 mM NaCl at pH 5.5 (no buffer used) with respect to their hydrodynamic radius by dynamic light scattering (170 ± 33 nm) and ζ -potential (-45 mV) (Zetasizer, Malvern Instruments, United Kingdom). For the cargo-labeled vesicles the hydrodynamic radius did not change even after 6 months of vesicle storage.

The vesicles were always adsorbed for 30 min. After the adsorption of vesicles, the substrate was extensively rinsed ($> 7 \times 400 \mu\text{l}$ for membrane-labeled or non-labeled and $> 21 \times 400 \mu\text{l}$ for cargo-labeled vesicles).

2.2.4 Deposition of PEMs onto the Substrates

All uPEMs were deposited by spraying onto the substrates. The cPEM (PLL/PGA)₂ was always added by pipetting, where the polyelectrolyte was adsorbed for 5 min, followed by a rinsing step with 150 mM NaCl for 2 min. The cPEM for the cell experiments (PLL/HA)₁₂PLL-g-PEG-RGD was sprayed onto the adsorbed vesicles.

The spraying process was adapted from Izquierdo et al.^[39] and has been automated in our laboratory by a home-built spraying robot (Figure 2.4).

The custom made program first wets the substrate with 150 mM NaCl solution for 5 s. After a pause of 5 s the PLL solution (0.5 mg/ml) was sprayed for 5 s. After a pause of 15 s the substrate was rinsed with buffer or 150 mM NaCl solution for 5 s. After another 5 s break, the PSS solution (0.5 mg/ml) was sprayed for 5 s, followed by 15 s pause and rinsing of the substrate with buffer or 150 mM NaCl solution for 5 s. This procedure was repeated as many times as needed (n) in order to obtain a (PLL/PSS)_n-PLL multilayer. The PEM coated samples were stored at 4 °C in 150 mM NaCl solution for maximal 4 weeks until use.

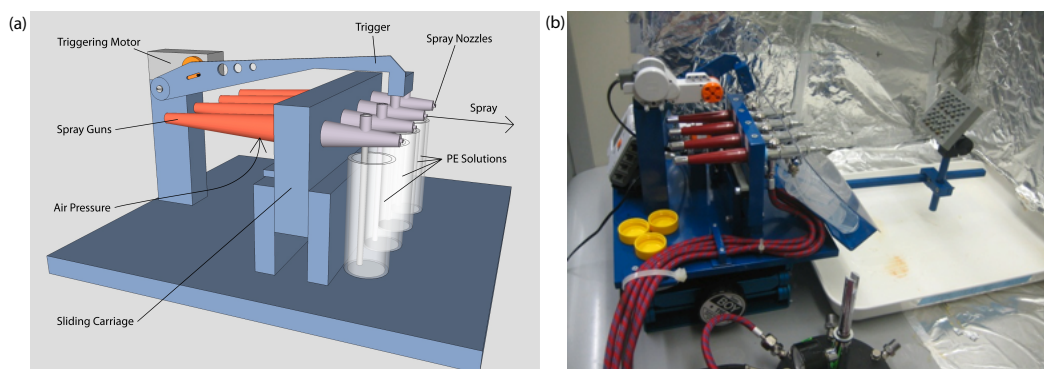


Figure 2.4: (a) a scheme and (b) a photo of the spraying robot that was used to spray all uPEMs and the cPEM for the cell-experiments.

2.2.5 Cross-linking

N-Hydroxysulfosuccinimide sodium salt (s-NHS) and N-(3-dimethylaminopropyl)-N'-ethylcarbodiimide hydrochloride (EDC) were purchased from Sigma Aldrich (Switzerland) and used at final concentrations of 400 mM EDC and 100 mM NHS in ultrapure water. Before use, pH was adjusted to pH 6 with 0.5 M NaOH to avoid harming the pH-sensitive vesicles underneath. ITO electrodes covered with the platform consisting of (PLL/PSS)₉PLL-vesicles-(PLL/HA)₁₂ PLL-g-PEG-RGD were incubated overnight for 12-16 h at 4 °C in the EDC/s-NHS solution, and rinsed 3 times with 150 mM NaCl.

2.2.6 (Electrochemical) Flow-cells

For all (EC-)CLSM and (EC-)AFM experiments the same flow-cell was used (Figure 2.5). The Teflon cell was provided with a silver wire anodized in a chloride containing solution to get an Ag/AgCl reference electrode, and with a platinum wire as counter electrode. A copper spring established the electrical contact with the ITO surface acting as working electrode. All given potentials are referred to Ag/AgCl.

2.2.7 Electrochemistry (EC)

All electrochemical experiments were carried out in the three-electrode flowcell shown in Figure 2.5. The flowcell was connected to an AMEL potentiostat/galvanostat (model 2053, AMEL electrochemistry, Italy). For the EC-QCM measurements a home-built, three-electrode, electrochemistry flow cell was used^[30]. Figure 2.6 shows a schematic

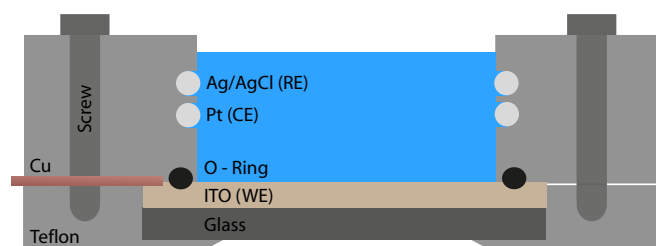


Figure 2.5: Scheme of the standard flowcell used to perform all (EC-)CLSM and (EC-)AFM experiments.

representation of the current-induced pH-gradient. The water is reduced upon the current application, which leads to the creation of H_3O^+ -ions decreasing the pH of the aqueous solution.

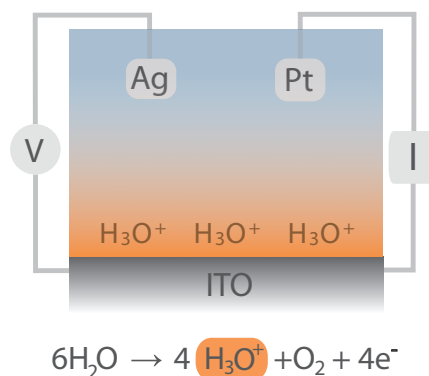


Figure 2.6: Schematic representation of the generation of a pH-gradient upon the application of a current to the ITO substrate. Reduction of water leads to the creation of H_3O^+ -ions decreasing the pH of the aqueous solution.

2.2.8 (EC-) Atomic Force Microscopy ((EC)-AFM)

A Nanowizard I BioAFM (JPK Instruments, Berlin, Germany) and Mikromasch CSC38/noAl cantilevers (R 0.04 N/m) were used, both in contact and intermittent contact modes. The samples were mounted in the custom-made electrochemical flowcell, described in 2.2.6. The ITO coated substrate was sprayed with $(\text{PLL}/\text{PSS})_n$ -PLL, kept in 150 mM NaCl and gently scratched with the tip of a screw driver to determine the thickness of the films. Then, the vesicles were added for 30 minutes and the flowcell was rinsed for 7 times with 400 μl NaCl (150 mM). Subsequently an extra layer of $(\text{PLL}/\text{PGA})_2$ was added in order to facilitate the imaging of the vesicles. After that, the sample was again gently scratched with the tip of a screw driver, in order to measure the film thickness after

vesicle adsorption. The images were always taken across an area with a scratch in order to use the scratch as the baseline for the volume evaluation. Image processing was performed using the open source software Gwyddion (Petr Klapetek & David Necas, Czech Republic). Processed images were exported as ASCII files for further calculation in MatLab. To determine the volumes of the PEM films on a defined area, the height-matrix over the area was integrated using MatLab^[31].

2.2.9 (EC-) Confocal Laser Scanning Microscopy ((EC-CLSM))

CLSM observations were carried out on a Zeiss LSM 510 microscope. NBD and calcein were detected after excitation at 488 nm with 4 % laser power, cutoff dichroic mirror 490 nm, and emission band pass filter 505 – 530 nm (green). The uPEM covered samples were mounted after quick rinsing with ultrapure water (Resistivity = 18.2 M Ω /cm) and drying with nitrogen. For the patterning and kinetic experiments we worked as follows: After the cPEM (PLL/PGA)₂ was added by pipetting, a galvanostatic current (10, 20, or 50 μ A/cm²) was applied. Then, a time series was started where an image was taken every 5 min for the slow release at 10 μ A/cm². For the fast release an image was taken every minute. For both cargo- and membrane-labeled vesicles each experiment was repeated 3 times and each time the difference between the fluorescent area and the bleached area was then calculated and normalized. The average of these values was then plotted against the time of the current application. The error bars are the standard deviation of the 3 experiments.

For the cell experiments, the whole setup was prepared one day in advance and the next day the cells were seeded onto the substrates and let in the incubator for 3 h. Then, the sample was brought to the microscope and a reference spot was bleached (approx. 20 min). Then, a current of 50 μ A/cm² was applied for 3 min and a fluorescent as well as a transmitted image was taken every minute. After that, the dead stain was added to the cells for at least 20 min. Subsequently, the sample was rinsed and the cell viability was assessed by taking 3 images per sample and calculating the percentage of living cells compared to dead ones.

2.2.10 (EC-) Quartz Crystal Microbalance ((EC)-QCM)

The QCM measurements were carried out with a QCM system from Q-Sense (Sweden), described in detail in^[84]. Briefly, QCM measures the changes in the resonance frequency (Δf) of a quartz crystal when material is adsorbed onto it. The quartz crystal was excited at its fundamental frequency (about 5 MHz) and at the third, fifth, and seventh overtones (n). A decrease in $\Delta f/n$ is, to a first approximation, linearly related (Sauerbrey equation^[35]) to an increase of the mass coupled to the oscillating crystal. Importantly, in the case of liposomes, the measured mass increase includes water coupled to the film inside the liposomes. The ITO coated surface of the quartz crystal sensor was the working electrode whereas the Ag/AgCl reference and the platinum counter electrodes were situated on the upper side of the flow cell. The QCM crystals have to be mounted in dry state. Therefore, shortly before mounting into the EC-QCM flow cell, the uPEM-covered quartz crystal was rinsed with ultrapure water and dried with nitrogen followed by rehydration in 150 mM NaCl solution within a few minutes. This procedure assured that no salt crystals formed upon drying the samples. The vesicle solution (0.5 mg/ml) was then injected and incubated for 30 min. After that, the flow cell was rinsed with 150 mM NaCl solution. Two additional layer pairs of (PLL/PGA) were then injected as described in^[32]. A galvanostatic current of $5 \mu\text{A}/\text{cm}^2$ (approximately 1.5 V) was then applied for different durations of time.

Morphology of Polyelectrolyte Multilayers and their Electrochemical Dissolution

Parts of this chapter were published in three publications:

O. Guillaume-Gentil, R. Zahn, S. Lindhoud, N. Graf, J. Vörös and T. Zambelli; From Nanodroplets to Continuous Films: How the Morphology of Polyelectrolyte Multilayers Depends on the Dielectric Permittivity and the Surface Charge of the Supporting Substrate, *Soft Matter*, 7:3861-3871, 2011

O. Guillaume-Gentil, N. Graf, F. Boulmedais, P. Schaaf, J. Vörös, and T. Zambelli; Global and Local View on the Electrochemically Induced Degradation of Polyelectrolyte Multilayers: from Dissolution to Delamination, *Soft Matter*, 6:4246-4254, 2010

L. Diéguez, N. Darwish, N. Graf, J. Vörös, T. Zambelli; Electrochemically Controlled Deposition and Dissolution of PLL/DNA Multilayers, *Soft Matter*, 5:2415-2421, 2009

In the beginning of my thesis I participated to selected projects under the responsibility of other PhD students focusing mainly on the electrochemically induced dissolution of PEMs. The obtained results served as the basis for many important details of the present work. I worked mostly in AFM investigations and sample preparation, establishing a good basic knowledge of the processes and instruments involved in PEM research.

Initially, the dissolution process of the PEM films was planned to be followed by *in-situ* AFM. These investigations revealed the surprising fact that the PEMs did not always form continuous layers but sometimes also formed droplets on the used substrates. This led to a systematic study about how the morphology of PEMs was affected when different PEM couples were deposited on different substrates^[35].

3.1 PEM Morphology vs. Substrate

We investigated the influence of the supporting substrate on the PEM growth and its morphology. We chose two different polyelectrolyte systems: (PAH/PSS) and (PLL/HA). The physicochemical properties of these two systems have been intensively studied, since they serve as model systems for two different kinds of PEM classes. (PAH/PSS) multilayers grow linearly and form multilayers with low water and counterion content. (PLL/HA) multilayers represent the class of exponentially growing multilayers that are typically highly hydrated and show a high counterion content.

We used atomic force microscopy (AFM) to study the two systems on four commonly used substrates: glass, indium tin oxide (ITO), gold, and mica. Glass slides are used as standard substrate in PEM research, yet different techniques may require substrate of different nature. Substrates covered with ITO are used for measurements combining optical and electrochemical techniques (e.g. EC-OWLS), while gold-coated quartz crystals are commonly used for QCM experiments. Mica is widely used as a standard substrate for AFM measurements because of its mono-crystalline structure.

We found that the surface coverage of the assembly and its topography were dependent on the dielectric permittivity of the substrate and the strength of the electrostatic interactions between polyanions and polycations: for (PAH/PSS), a strongly interacting polyelectrolyte couple, no dependency of the surface morphology on the physical properties of the underlying substrate was observed. In contrast, the weakly interacting pair (PLL/HA) formed rapidly continuous, flat layers on substrates of low dielectric permittivity and inhomogeneous droplet-films on substrates of high dielectric permittivity (Figure 3.1).

The reasons for the different observed morphologies were supposed to be as follows. Polyelectrolytes induce image charges in the surface. The sign and magnitude of these charges vary depending on the dielectric permittivity of the substrate. These image charges change the interactions between the polyelectrolytes and thereby their dewetting behavior and surface morphology. For substrates with a low dielectric permittivity (e.g. ITO), the presence of image charges increases the electrostatic repulsion between the polyelectrolyte chains or complexes. This results in high surface coverage of the PEM and continuous films already at low deposition numbers. For substrates with a high dielectric permittivity (e.g. gold), the image charges effectively lower the electrostatic repulsion within the polyelectrolyte chains or complexes. This increased monomer-monomer in-

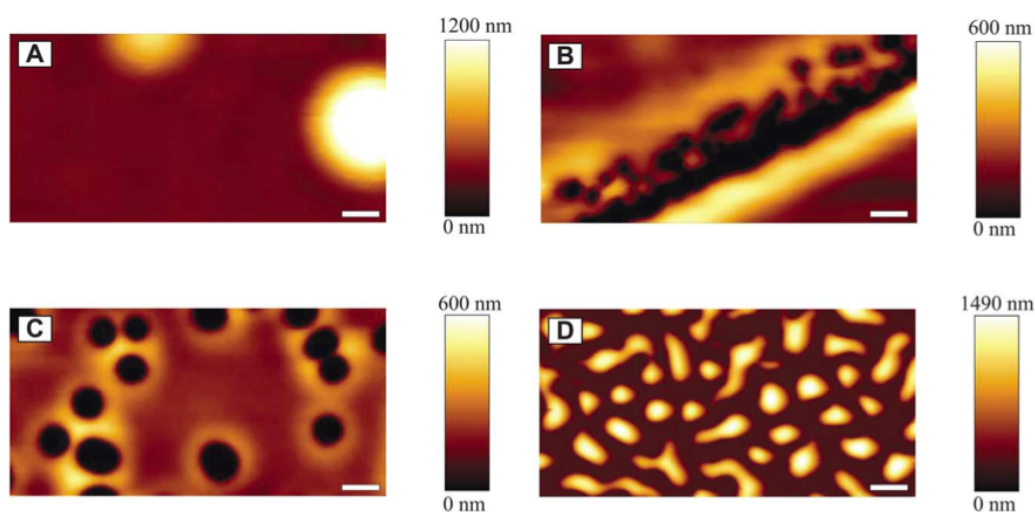


Figure 3.1: Topographical AFM images of (PLL/HA)₂₄ films deposited on ITO (A), glass (B), mica (C) and gold (D). All four images are $100 \times 50 \mu\text{m}^2$, scale bars are $5 \mu\text{m}$ [35]

teraction results in a collective dewetting of the polymer film from the surface and the formation of droplets on the surface. For PEMs with strong electrostatic interactions (PAH/PSS) this kind of dewetting process is kinetically frozen. Accordingly, continuous (PAH/PSS) films of similar morphology were formed on all different substrates used in this study.

For (PLL/HA), we compared the amount of adsorbed polymeric material on the surface to the *surface charge* of the different substrates in use, and found that for higher surface charge more material is adsorbed on the surface. The morphology of the multi-layer seems not to be influenced by the surface charge. This was shown by comparing (PLL/HA) multi-layers on gold substrates with and without a precursor layer of PEI. The surface coverage and the surface morphology (droplet films) were identical for the two systems, but the high surface charge of the initial PEI layer resulted in significantly more material adsorbed on the surface.

3.2 Electrochemically Induced PEM Dissolution

For biomedical applications focused on the controlled release of drugs *directly* embedded in the LbL films, the dissolution of the LbL film is the intriguing point to be investigated because the release actually corresponds with the dissolution of the film. Therefore, two studies were performed. In the first one we aimed at a deeper understanding of the

EC-induced dissolution and delamination of the PEMs, depending on their composition. The second study was to investigate the influence on the stability of PEMs towards EC-dissolution by the application of a potential during the PEM buildup.

All experiments were carried out with EC-OWLS and EC-AFM both with flow-cells modified to be operated in electrochemical conditions with a physiological HEPES buffer. OWLS waveguides and AFM samples were covered with ITO deposited according to the same procedure for an unambiguous results comparison. The ITO surface acted as the working electrode of a three-electrodes cell, while potentials were applied with respect of an Ag/AgCl wire (reference electrode) and the EC current was collected by a platinum wire (counter electrode).

3.2.1 Dissolution vs. Delamination

We intended to understand why the electrochemical stimulus induced the dissolution of certain PEM couples and the delamination of others^[34]. We assessed the influence of an applied electric potential on different polyelectrolyte systems, combining global and local investigation techniques. The widely studied PEMs (PLL/HA) and (PAH/PSS) were selected as model systems. PLL and HA are natural and weak polyelectrolytes often used for biomedical applications. (PLL/HA) assemblies are known to be highly hydrated, blended structures in which both polyelectrolytes can inter-diffuse. On the other hand, (PAH/PSS) multilayers with the strong polyanionic component form compact and highly organized films in which the polyelectrolytes are not mobile. We worked in potentiostatic mode at 1.9 V.

We found that weak and highly hydrated (PLL/HA) assemblies with thicknesses up to several hundreds of nanometer continuously dissolved upon electrochemical trigger. We assumed that almost all the primary amine groups on the PLL chains (pKa of ~ 9) are already protonated, i.e. positively charged, at pH 7.4; consequently, the pH decrease upon electrochemical treatment would not significantly affect the polycation charges. Contrastingly, a pH decrease would strongly affect the polyanion charges: while fully ionized at pH 7.4, the carboxylic acid groups of hyaluronic acid (pKa of ~ 3) get protonated at lower pHs, neutralizing negative charges on the HA chains.

Consequently, two simultaneous phenomena occurred at acidic pH. On one hand, counter-anions (e.g. Cl^- , OH^-) migrated into the assembly to maintain its charge neutrality, as the neutralization of the hyaluronic acid chains resulted in an excess of posi-

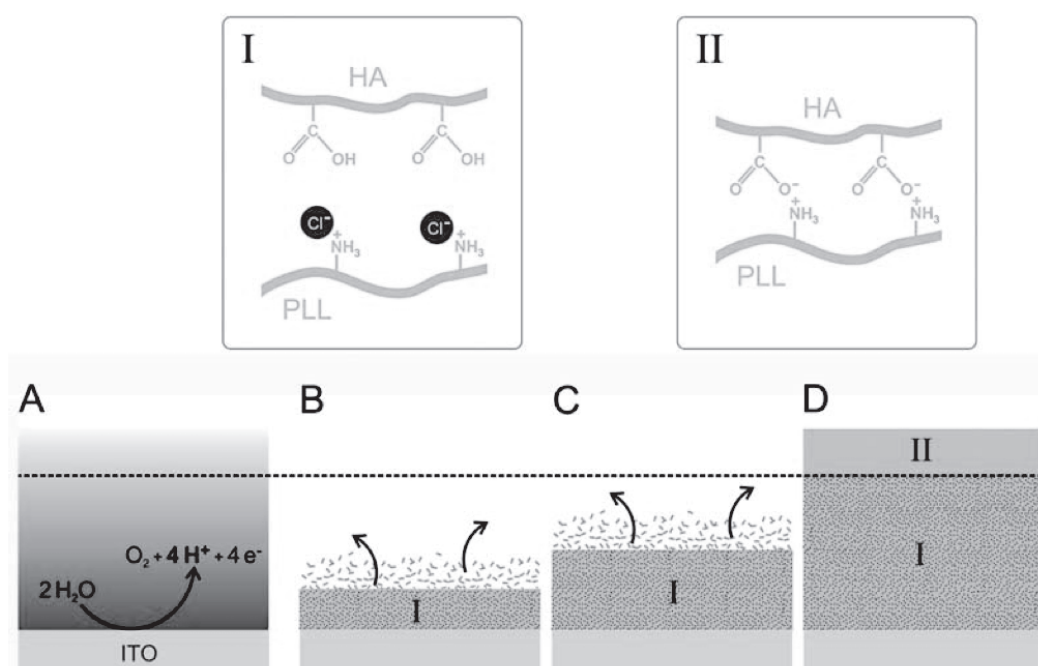


Figure 3.2: Electrochemically induced dissolution of (PLL/HA) multilayers. (A) The application of small oxidative voltages induces water electrolysis. Consequently, a gradient of protons extending from the electrode surface is established. In the area where a sufficiently low pH is reached (I), the carboxylic groups on HA chains get protonated, counter-anions migrate in to compensate for the residual excess of positive charges, and the electrostatic interactions between the polycations and polyanions are weakened. If the (PLL/HA) film is completely confined in this area, i.e. for (PLL/HA)₁₂ (B) and (PLL/HA)₂₄ (C), the neutralized polyelectrolytes can be released into the bulk solution, hence the gradual film dissolution. (D) For thicker films such as (PLL/HA)₅₀, the pH change in the upper part of the film is not sufficient to induce the neutralization of the HA negative charges. As a consequence, the film is capped by unaffected polyelectrolyte layers (II) which prevent the release of polyelectrolytes into the bulk solution.^[34]

tive charges within the multilayer. On the other hand, through the neutralization of the polyanions chains, the electrostatic interactions between the polyanion and polycation chains were weakened, and free polyelectrolytes could be released into the bulk solution, at least from the outermost layers of the film (Figure 3.2 A-C). In addition, both PLL and HA could diffuse within the assembly, which might have accelerated the whole process. This mechanism was in accordance with the results of the dissolution of (PLL/HA) films up to a thickness of ~ 350 nm. For the case of thicker (PLL/HA) films, where no morphological changes were detected, it was considered that the outermost part of the film is above a critical distance from the electrode, where the pH was no more sufficiently low to induce the disruption of ionic bounds (Figure 3.2 A, D). Polyelectrolytes neutralized near the surface of the electrode would most probably deprotonate while diffusing through the unaffected pH zone and re-form ionic bounds to other polyelectrolyte chains. As such no polyelectrolyte could be released into the bulk solution.

Stronger and more compact films, on the other hand, dissolved only if their thickness was of a few tens of nanometers, whereas thicker films delaminated from the electrode. We assumed the same mechanism for (PAH/PSS) assemblies as described above. The water electrolysis generated a gradient of protons extending from the working electrode. Similarly to PLL, PAH has primary amine groups with a pKa value around 8.6 and as such, most of these amine groups are already charged at pH 7.4. Conversely, the pH decrease will significantly affect the amount of negative charges on the polyanion chains. While the carboxylic groups of HA chains have a pKa around 3, the pKa of sulfonate groups on the PSS chains is around 1, meaning that a higher concentration of protons is required to destabilize (PAH/PSS) films compared to (PLL/HA) films. This explains why we indeed observed a very slow dissolution of 30 nm thick (PAH/PSS) coatings and no dissolution for thicker films, while (PLL/HA) films up to 350 nm thickness rapidly dissolved.

In the case of (PAH/PSS) films with thicknesses of 65 nm and above, the electrochemical treatment induced the formation of bumps that grew, coalesced and finally led to the complete detachment of the film. A recent report describing the dissolution of (PLL/HA) assemblies above a critical ionic strength showed the formation of cavities within the multilayers at high ionic strength^[71]. The authors proposed that these cavities are filled with free polyelectrolyte chains and their counter-ions, inducing extra osmotic pressure that leads to the growth of these cavities. A similar process could be envisaged in the case of delaminating (PAH/PSS) films. Indeed, the sulfonate groups of PSS were neutralized within the first bottom layers of the film but the molecules could not diffuse out due to the intact tight PEM layer above. As such, chloride counter-ions diffused in, to compensate for the excess positive charges of PAH. The increased counter-anion concentration might have led to an extra osmotic pressure and the formation of cavities in the assembly, localized at the electrode surface. The size of these voids would grow during the electrochemical treatment as more and more polyelectrolyte chains would get neutralized, leading to the coalescence of the voids and finally to the detachment of the polyelectrolyte film. Another hypothesis involves the formation of gases at the electrode surface. Indeed, oxygen is produced in parallel to protons through water electrolysis, and chloride ions present in the vicinity of the electrode might also be oxidized to form Cl₂. It is then possible that these gases produced at the working electrode during the electrochemical treatment accumulated under the polyelectrolyte film and participated in the formation of the bumps. The fact that no formation of bumps was observed in the case of thinner dissolving films further supported both hypotheses.

Finally, the proposed mechanism was confirmed through the results obtained by combining both polyelectrolyte systems. (PLL/HA) structures within the first 350 nm above the working electrode dissolved when deposited on a 25 nm thick PAH/PSS film or directly onto the electrode, while they did not dissolve when separated from the electrode by a PAH/PSS film of 65 nm. As expected, the (PLL/HA) structures deposited on the thin, dissolving PAH/PSS film dissolved faster than the (PAH/PSS). Considering that the dissolution process is mainly based on polyanion protonation, this experiment also showed that more protons were produced at the electrode surface than captured in the thin (25 nm) (PAH/PSS) film. However, thicker (65 nm) PAH/ PSS film seem to completely consume the proton produced, thus the (PLL/HA) adlayer remained unaffected.

3.2.2 Influencing the Stability for PEM Dissolution

We then tried to obtain a deeper insight into the phenomena accompanying the application of a bias to an electrode and the consequently induced dissolution of an LbL film deposited on it. As test system we chose an LbL film composed of PLL, a biodegradable polycation, and DNA as possible candidate for future biological applications (e.g. transfection).

We found that (PLL/DNA)₆ films fabricated at 0 V were stable in physiological buffer (pH 7.4) and that applying a potential above 1.8 V induced only a partial and slow dissolution. Figure 3.3A shows the evolution of the adsorbed mass measured by EC-OWLS as a function of time during the fabrication and subsequent dissolution of six bilayers of PLL and DNA (PLL/ DNA)₆. The deposition was carried out at 0 V. The fabrication curve was characterized by the typical 'stairway' course where every step corresponded to the injection of a polyelectrolyte. The obtained film was stable, meaning that the adsorbed mass remained constant in the buffer solution once the fabrication was terminated. By applying a bias of $V_{diss} = 1.9$ V, the mass underwent a rapid increase and then a slow decrease. The rapid increase of the mass upon applying a voltage was due to the accumulation of ions at the ITO/buffer interface (i.e. the formation of a Stern layer) affecting the refractive index. The slow decrease was related to the dissolution of the film. The time evolution of the dissolution at 1.9 V could be fitted to an exponential decay curve with a time constant τ of 44 min and a mass percentage of remaining film of approximately 50%. This indicated that the dissolution of the film indeed occurs but it was slow and only partial.

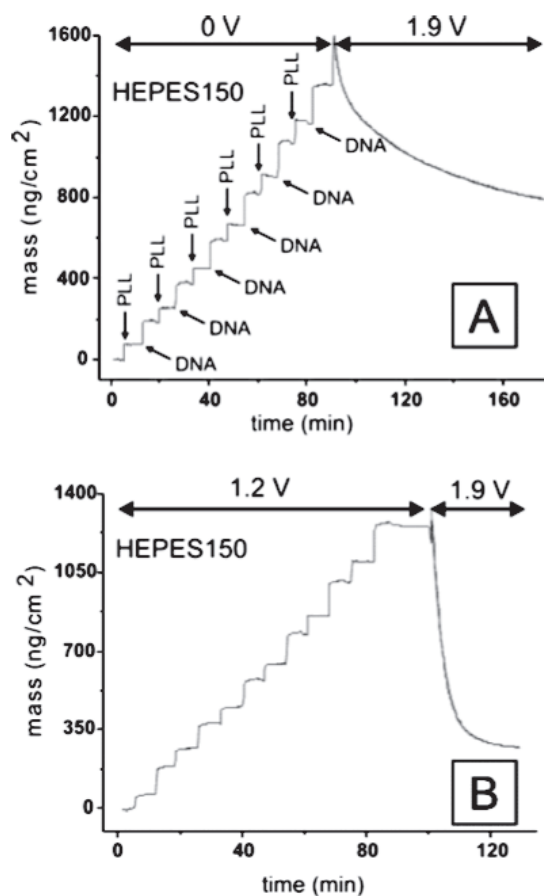


Figure 3.3: Adsorbed mass measured by EC-OWLS during the build-up and 1.9 V induced dissolution of multilayers. The influence of the bias during the build-up is shown. (PLL/DNA)₆: (A) 0 V, 150 mM; (B) 1.2 V, 150 mM.^[16]

On the contrary, the dissolution was much more effective and quicker if a potential was applied already *during* the deposition of the film. Figure 3.3B shows the evolution of the adsorbed mass measured by EC-OWLS as a function of time during the fabrication and subsequent dissolution of (PLL/DNA)₆ where a bias of $V_{dep} = 1.2$ V was applied during the buildup. While the mass of the film after deposition was unaffected by the bias, a striking difference appeared for the dissolution: for the case of a bias of 1.2 V was applied during the film deposition the dissolution could be fitted with a much smaller time constant (5 instead of 44 min) and a much smaller mass percentage of remaining film (20% versus 50%). Applying a bias during the fabrication, thus, makes the LbL film less stable meaning that the dissolution process is accelerated.

To explain the different stability with respect to EC-dissolution, the following mechanism was proposed. At the cathode, not only protons are produced but also Cl₂, which

promptly reacted with water producing HClO. HClO is known to react with the amines of the lysine side chains forming monochloramine. Chloramines decompose to nitrogen-centered radicals or carbonyl groups. Since carbonyl can cross-link with free amine groups via Schiff base formation, amine side groups can intra- or inter-molecularly cross-link and, therefore, lose their charge, diminishing their ability to electrostatically interact with the polyanions. This means that the electrostatic overcompensation during the film deposition was altered by the presence of an applied potential leading to a weaker PEM assembly.

3.3 Chapter Conclusion

We showed that the physical properties of the supporting substrate have a strong influence on the architecture of PEMs. This was not considered in previous studies which investigated the effect of various chemical and physical parameters on the properties of polyelectrolyte multilayers. Additionally, we found that weakly interacting polyelectrolyte couples dissolve upon an EC-trigger, whereas strongly interacting ones either remain on the surface or delaminate from it, depending on the film thickness. We also showed that the stability towards EC-dissolution could be decreased by applying a potential during the buildup process.

These findings were very important for the following results of my thesis. The knowledge about the dissolution of certain PEMs under certain circumstances, for example, as well as the fact that PEMs establish different morphologies on different substrates was crucial for the choice of the uPEM and cPEM in my system (Chapter 4).

Electrochemically Stimulated Release from Liposomes Embedded in a Polyelectrolyte Multilayer

Parts of this chapter were published in N. Graf, F. Albertini, T. Petit, E. Reimhult, J. Vörös, T. Zambelli; Electrochemically Stimulated Release from Liposomes Embedded in a Polyelectrolyte Multilayer, *Advanced Functional Materials*, 21:1666-1672, 2011

In this chapter, we describe the basic system in which the advantages of PEM coatings with high loading of liposomes, containing a model drug, are combined with externally controlled release. The PEM was deposited on an ITO electrode wherein lipid vesicles filled with a fluorescent dye were embedded. The use of vesicles with a strong negative charge and the choice of a PEM matrix with a polycation as topmost layer enabled the generation of stable liposomes in the PEM. Furthermore, the triggered release from the embedded liposomes could efficiently be induced as a consequence of the electrochemically induced local pH change in the vicinity of the electrode.

4.1 Challenges, Strategies & Encountered Problems

The main challenge for the proof of principle was to find the appropriate materials fulfilling all the requirements for the buildup and the triggered release. Since the system was rather complex, the properties of one material depended on other materials in contact with it. The first point was to find an appropriate substrate for the upcoming experiments. The substrate needed to be conductive and it should be possible to use the same substrate for different techniques, since we previously found that the morphology of PEMs is different on different substrates 3.1. Therefore, we decided to work with ITO which is conductive

and transparent, enabling not only the electrochemical stimulation but also the analysis by means of the inverted microscope in our laboratory. The next point was to find an underlying PEM (uPEM) that was homogeneous (i.e. covering the entire substrate) already within a few bilayers to make the process of the platform buildup fast and cost-effective. Subsection 4.2.1 discusses the different PEM couples that were evaluated. After that, we needed to find vesicles that are pH-sensitive in the range of pH we could generate by the application of a current. The use of the semi-conducting ITO as a substrate forced us to apply positive potentials and currents, because the ITO breaks (i.e. converts to metal) when negative potentials are applied. Positive currents result in an acidic pH close to the surface (Figure 2.6). Thus, pH-sensitive vesicles for acidic pH were desired. Another requirement was the stable adsorption of the liposomes on the uPEM. Many groups reported the spontaneous rupture of vesicles upon adsorption onto PEMs. Therefore, vesicles were usually stabilized prior to adsorption^[68–70,86,112,113]. Subsection 4.2.2 discusses the choice of the lipids for the vesicle formation and the adsorption of the vesicles onto the uPEM. The last material that had to be found was the covering PEM (cPEM). The cPEM was meant to protect the vesicles from the environment. Therefore, it was important that the cPEM did not affect the integrity of the vesicles underneath. Subsection 4.2.3 shows the investigation of different cPEMs.

The strategies and encountered problems are detailed in each paragraph.

4.2 The Components of the System

The designed platform can be schematized in three layers: the underlying PEM (uPEM), the vesicles, and the covering PEM (cPEM) (Figure 4.1).

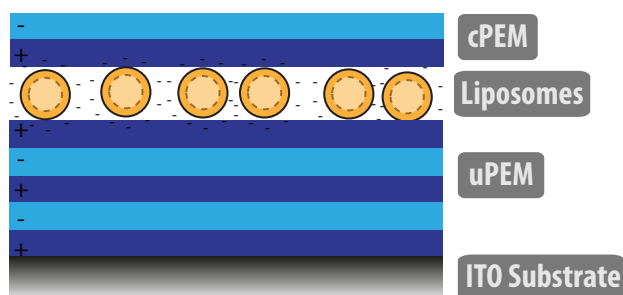


Figure 4.1: Schematic representation of the different components in the platform.

4.2.1 Underlying PEM (uPEM)

The uPEM acted as the scaffold where the liposomes were immobilized and was then addressed by the electrochemical stimulus. From previous experiments it was known, that not all PEM couples formed a continuous film on ITO (Section 3.1). To make use of the current-based pH gradient generation for the release from pH-sensitive vesicles, the polyelectrolyte couple for the uPEM needed to; 1) be thick enough to form a continuous film on the substrate to prevent direct contact of the vesicles with the electrode but thin enough to permit the H^+ -ions to reach the vesicles and allow for the buildup in a reasonable time; 2) must not dissolve upon the application of a current and the corresponding change to acidic pH.

Three different uPEM couples were analyzed by AFM: $(PLL/PGA)_9$, $(PLL/HA)_9$, and $(PLL/PSS)_9PLL$. The image was taken across an artificially induced scratch (Figure 4.2). The morphology images revealed that $(PLL/PGA)_9$ and $(PLL/PSS)_9PLL$ both formed a continuous film with 9 bilayers whereas $(PLL/HA)_9$ formed single droplets on the surface. Therefore, PLL/HA was excluded from further investigations. The thickness of the other two couples was derived from cross sections, being approximately 50 and 40 nm respectively.

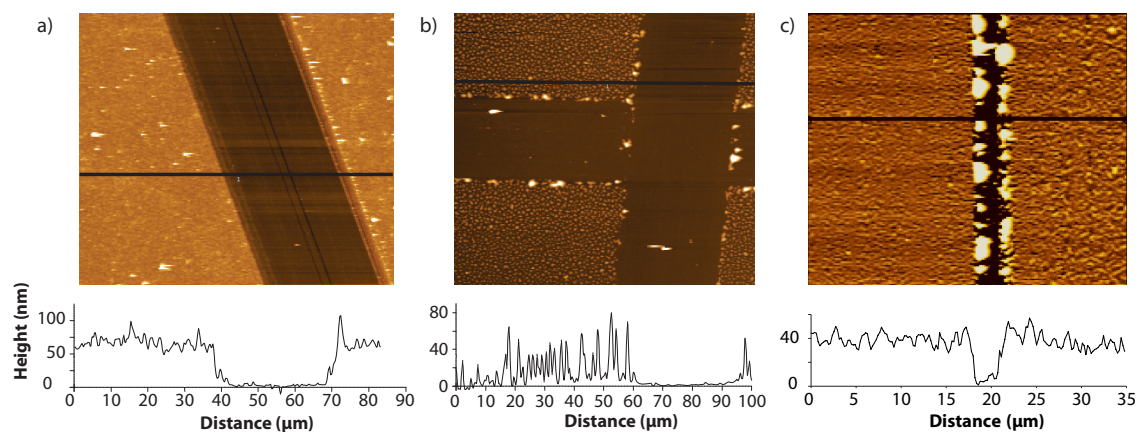


Figure 4.2: AFM images and cross sections of the different uPEM couples that were analyzed. All images were taken across an artificially induced scratch. a) $(PLL/PGA)_9$, b) $(PLL/HA)_9$, c) $(PLL/PSS)_9PLL$. The width of the images is a) 90, b) 100 and c) 35 μm .

Since we were planning to adsorb negatively charged vesicles onto the uPEM, all the following experiments were performed with the topmost layer being cationic. $(PLL/PSS)_9PLL$ and $(PLL/PGA)_9PLL$ were sprayed onto QCM crystals and then exposed to different saline solutions with pH ranging from pH 7 to pH 1.5 (Figure 4.3). The frequency curve for $(PLL/PSS)_9PLL$ remained stable and increased only slightly (≈ 7 Hz)

down to a pH of 1.5. The long vertical lines in the curve were associated with the injection of the solution. This indicates that (PLL/PSS)₉PLL was not much affected by low pH. (PLL/PGA)₉PLL on the other hand, showed a substantial frequency shift of approximately 300 Hz after the insertion of pH 3.5, indicating that the PEM film dissolved upon this pH change. The further injection of pH 1 did not change the frequency anymore. This was in agreement with previous investigations whereas weakly interacting polyelectrolytes were more sensitive to pH changes due to the higher pK_a value of the polyanion compared to the pK_a value of polyanions in strongly interacting couples (Section 3.2.1).

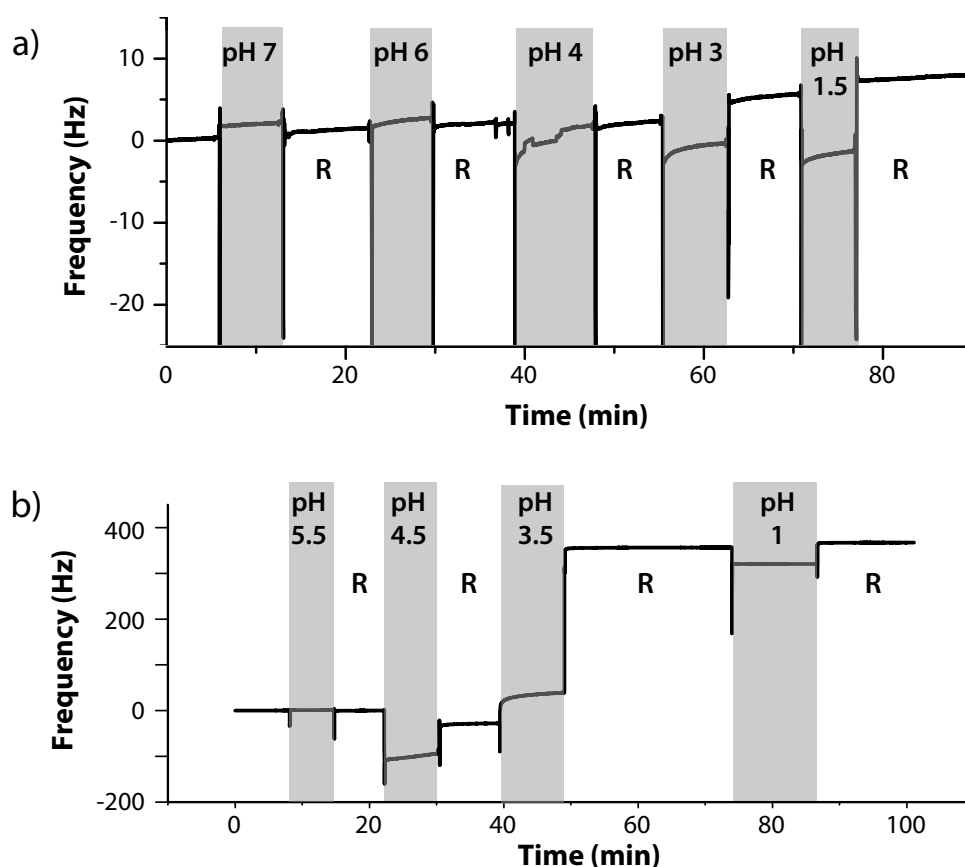


Figure 4.3: QCM measurements of a) (PLL/PSS)₉PLL and b) (PLL/PGA)₉PLL exposed to different pH solutions. The long vertical lines in the curve were associated with the injection of the solution. R: corresponds to a rinsing step with 150 mM NaCl.

Then, (PLL/PSS)₉-PLL films were sprayed on EC-QCM crystals covered with ITO and a current density of 5 $\mu\text{A}/\text{cm}^2$ was applied. The increase in frequency was determined to be 2.6% of the shift for a complete (PLL/PSS)₉-PLL film (Figure 4.4). Based on calculations for free H⁺-ions in a non-buffered aqueous solution^[24], this current density induced a pH of approximately 4.5, 50 nm away from the electrode substrate, i.e., a com-

parable distance to the measured thickness of the uPEM. However, the actual pH in our system could even be lower than 4.5, since the H^+ -ions cannot move completely freely away from the electrode, trapped by the uPEM that can act as a barrier for the diffusion of monovalent ions like protons^[50].

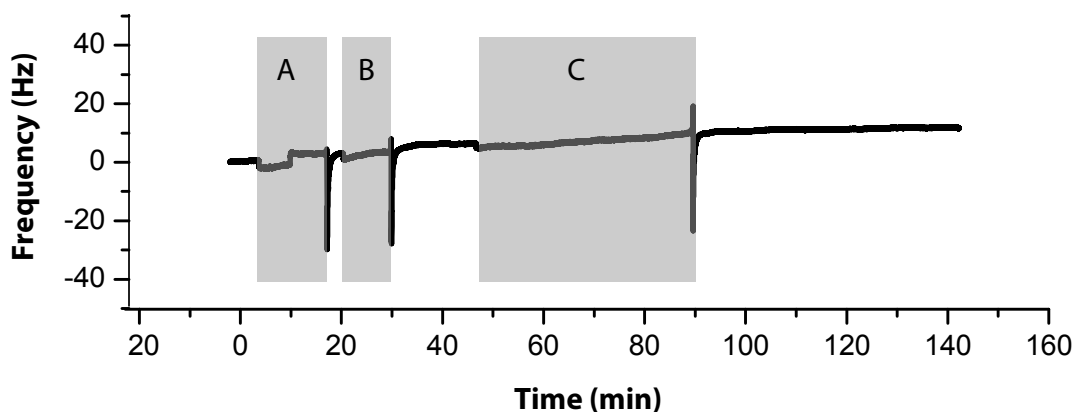


Figure 4.4: A current of $5 \mu A/cm^2$ was applied to $(PLL/PSS)_9PLL$ for different time periods (A-C). The QCM signal remained constant, indicating that uPEM remained intact for current applications in the applied range.

4.2.2 Liposomes

The liposomes needed to satisfy two requirements: 1) their lipid composition should render them sensitive to the pH gradient caused by the application of the current at the electrode and 2) the liposomes should be immobilized as intact non-leaking vesicles on the uPEM, in order to avoid premature release of their content.

Several lipid compositions were evaluated for their pH-sensitivity. The QCM-results are summarized in Figure 4.5. Both POPC and DOPS showed a pH-sensitivity in the range of pH 3 in agreement with the literature: MacDonald et al.^[59] reported an apparent pKa of 4.6 to 3.7 for DOPS lipids depending on the NaCl ionic strength. The pKa of an acid/base group defines the pH where 50% of the groups are protonated and 50% are deprotonated. Thus, if the pH is lowered to below the pKa of the acid/base groups of a lipid, its protonation will change and with that its headgroup dimensions. If this change in shape occurs for a large number of lipids in a liposome the intrinsic curvature of the membrane will change, which is expected to lead to membrane destabilization causing release of its content and even rupture of the liposome^[105]. This meant that both the lipids DOPS and POPC could be used for the liposomes in our system. However, POPC

lipids are not charged whereas DOPS lipids are negatively charged. We suspected that it was easier to incorporate charged liposomes into a film whose assembly was based on electrostatic interactions. We, therefore, decided to continue the experiments with DOPS-liposomes.

Lipid Composition	Acidic pH	Basic pH
POPC on Au	3	Not tested
CHEMS on Au	No change	11
DOPS on PLL on Au	3	11
CHEMS/DOPE (4:6) on PLL on Au	1.5	11

Figure 4.5: Table showing the threshold pH values upon which the different liposomes were disrupted. The values were obtained by QCM.

To investigate whether the vesicles desorb from the surface or only release their content, cargo- as well as membrane-labeled DOPS vesicles were deposited on a positively charged monolayer of PLL on ITO and exposed to different pH solutions. CLSM images of the cargo-labeled (Figure 4.6 a) and the membrane-labeled vesicles (Figure 4.6 b) were taken after exposure to different pH solutions from pH 7.4 - pH 1.5. The cargo was released upon exposure to a critical pH between pH 4.5 and pH 3.5 or lower (Figure 4.6 a). These findings showed that DOPS vesicles did not rupture upon adsorption to the PLL monolayer. The vesicles were only destabilized and consequently released their content when they were exposed to a solution of pH < 4.5. From the stable fluorescence of the membrane-labeled liposomes at all pH values (Figure 4.6b), it can be concluded that the lipids remained on the surface even after release of the cargo. No fluorescent recovery after photobleaching (FRAP) was observed for the membrane-labeled vesicles, indicating that the vesicles remain at least partly intact when the pH is lowered.

After confirming that the 200 nm DOPS vesicles can release encapsulated molecules upon a pH decrease below 4.5, the vesicles were adsorbed onto the uPEM (PLL/PSS)₉-PLL. The adsorption of the vesicles and the addition of the cPEM were followed by EC-QCM (4.7). The EC-QCM resonance frequency decreased continuously during the 30 min of vesicle adsorption indicating that no spontaneous rupture occurred (Figure 4.7, B).

This is a remarkable observation for our PEM system since liposomes have previously been reported to undergo spontaneous disruption upon adsorption onto PEMs^[68-70,86,112,113]. One explanation for the adsorption of intact vesicles could be that

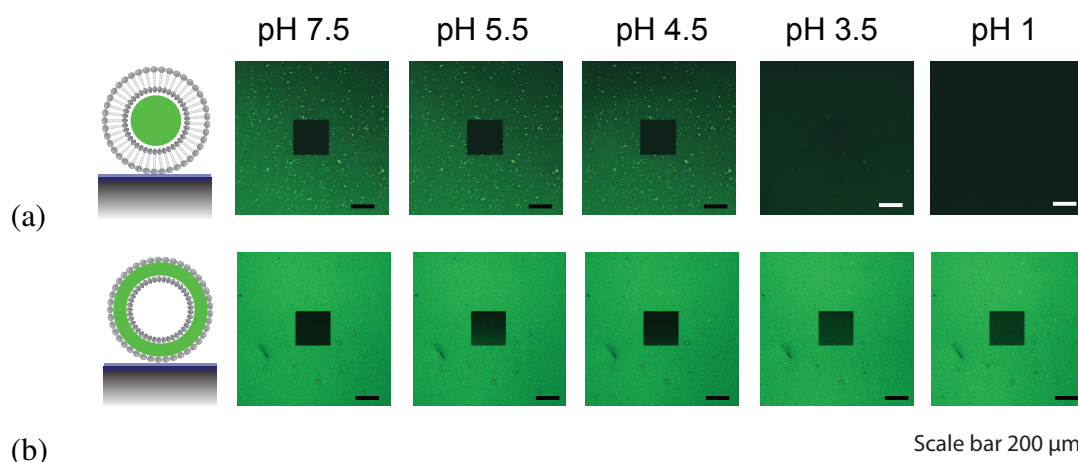


Figure 4.6: CLSM investigations of the pH effect on DOPS vesicles. CLSM images were recorded on the same system, i.e. DOPS vesicles on a monolayer of PLL. The black square is a bleached spot to show the back- ground intensity. Images were taken at the change from pH 7.5 to 1 of cargo-labeled and membrane-labeled vesicles. The cargo-label disappears upon the pH change while the membrane remains intact, showing that the vesicles do not desorb but rupture.

the negative charges of the lipids are compensated upon adsorption, possibly by diffusion of the polycation PLL from the uPEM to cover the entire liposome membrane. Tezcaner et al.^[103] have shown that the PEM couple PLL/PSS grows exponentially. Such exponentially growing multilayers were first described by Elbert et al.^[19] and then further investigated on the polyelectrolyte couple (PLL/HA)^[52,79] According to these investigations, PLL can diffuse through the multi-layer film and, therefore, each time when HA is adsorbed to the film, not only the PLL deposited as the uppermost layer but also PLL diffusing through the film can compensate the adsorbing HA. Thereby, more HA (and therefore also more PLL) can be adsorbed with each bilayer. We propose that the same mechanism might explain why the vesicles do not need to be stabilized prior to adsorption as previously suggested^[68–70,86,112,113]. As soon as a vesicle adsorbs on the surface, PLL diffuses onto it and compensates for the negative charges of the lipids.

To strengthen the assumption that the mobility of the PLL chains plays a key role in the intact adsorption of the DOPS vesicles, reference experiments where vesicles were adsorbed to a linearly growing uPEM consisting of (PAH/PSS)₉PAH were performed (Figure 4.8). After the deposition of membrane-labeled DOPS vesicles a defined region was photobleached. After 24 minutes the fluorescence in the bleached area has almost completely recovered, showing that the vesicles do indeed form a lipid bilayer upon adsorption onto a linearly growing PEM without mobile PLL.

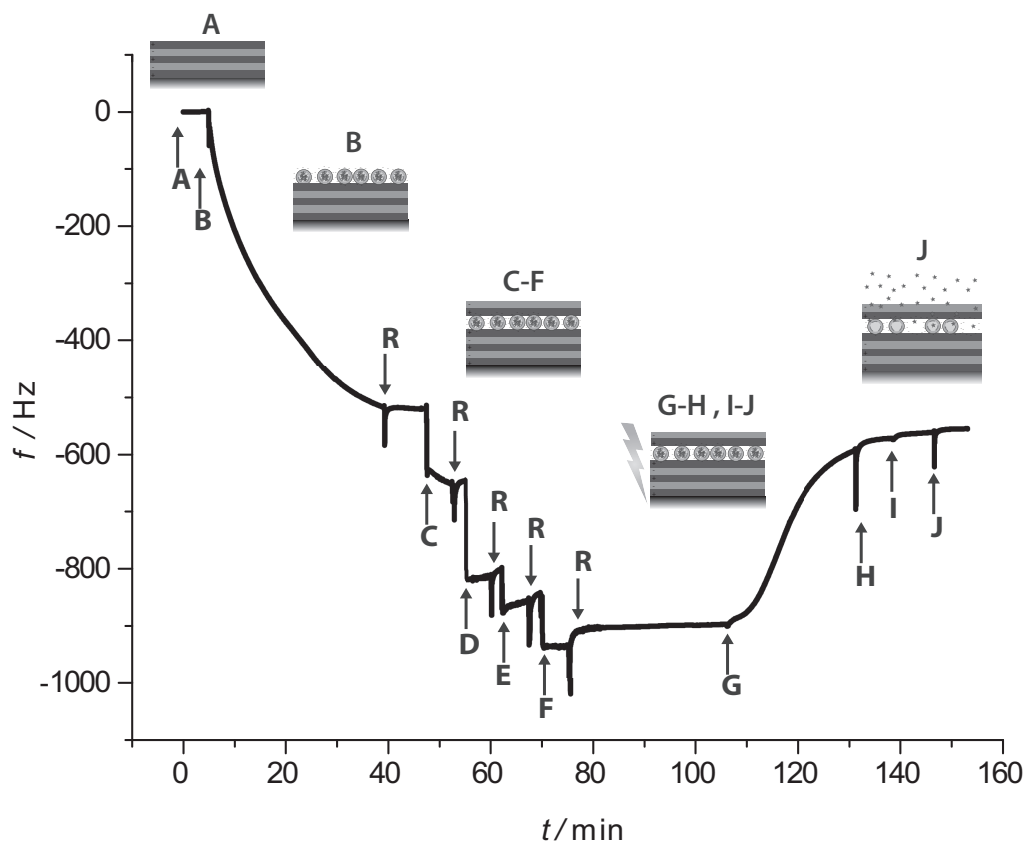


Figure 4.7: QCM graph of the different steps of the platform build-up and the application of a current to release the entrapped dye from the vesicles. A) Pre-sprayed uPEM (PLL/PSS)₉-PLL matrix on an ITO coated quartz crystal. B) Adsorption of DOPS vesicles. C-F) Adsorption of two additional layer pairs of (PLL/PGA). F-G) 25 min of waiting to show the stability of the system. G-H): Application of $20.5 \mu\text{A}/\text{cm}^2$ for 25 min inducing an increase in the frequency interpreted as mass loss due to conformational changes in the liposome layer which coincides with the release of the dye from the vesicles. H) Rinsing and I-J) further application of $5 \mu\text{A}/\text{cm}^2$ for 5 min and rinsing. R) Rinsing.

Recently, Khan et al.^[45] have shown that the formation of lipid bilayers upon the adsorption of liposomes onto a TiO_2 is largely influenced by the asymmetric distribution of the neutral phosphatidyl choline (PC) and the negatively charged phosphatidyl serine (PS) lipids. The PS lipids segregate from the PC lipids within the liposomes and migrate to the positively charged surface, thereby inducing the lipid bilayer formation. Since our system contains almost only DOPS lipids, no segregation occurs and instead, the PLL migrates up to the liposomes. Thereby, the spherical shape of the liposome becomes less deformed with a smaller contact area to the underlying uPEM than it would have without the charge compensation. The decreased membrane curvature and pinning of lipids to the substrate reduces the driving force for vesicle rupture^[45,91] This might also be an explanation as to why, in previous publications, liposomes that were combined with exponentially growing

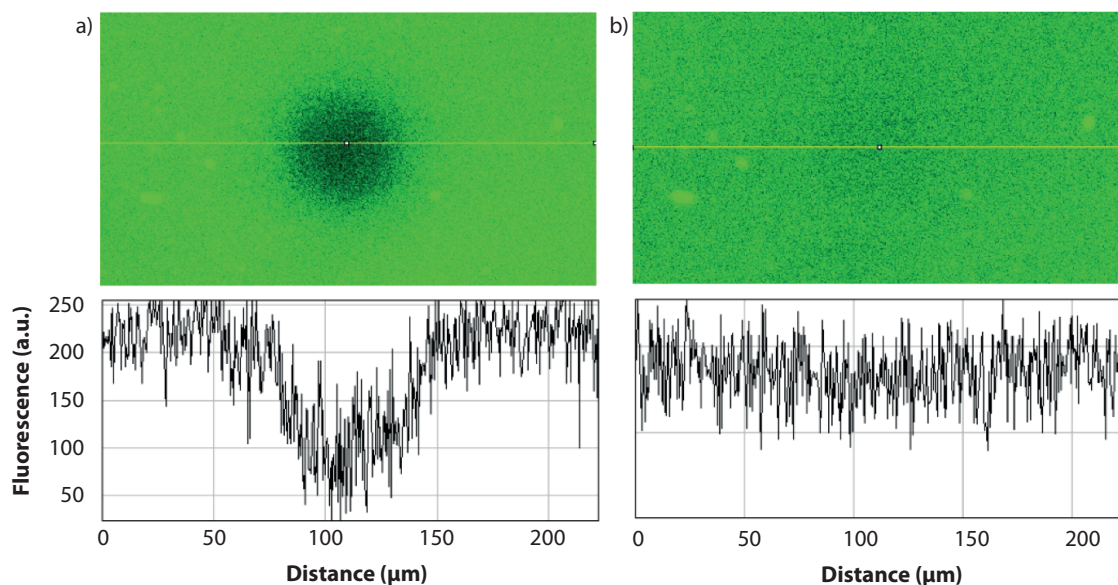


Figure 4.8: FRAP images of membrane-labeled DOPS vesicles adsorbing onto a $(\text{PAH/PSS})_9\text{PAH}$ film. a) Immediately after adsorption. b) After 24 minutes. The recovery of the fluorescence after 24 minutes shows that the vesicles formed a lipid bilayer upon adsorption.

PEMs still needed stabilization prior to adsorption to prevent their spontaneous rupture. Such vesicles contained only 5-10 wt% of negatively charged lipids, whereas the liposomes used in this work consisted to 98-100 wt% DOPS lipids. Finally, we noticed that the absolute frequency shift of approximately 520 Hz after 30 min of liposome adsorption is substantially higher than the 220-350 Hz commonly found in the literature for a randomly adsorbed monolayer of liposomes of similar size^[80] Together with the fact that the vesicles remain intact upon adsorption, this suggests that more than a monolayer of vesicles adsorbs onto the $(\text{PLL/PSS})_9\text{-PLL}$ coated substrate mediated by PLL diffusing onto the negatively charged membrane. This hypothesis was further investigated in Chapter 6.

4.2.3 Covering PEM (cPEM)

In order to protect the liposome layer and create a defined surface that could be readily modified to favor e.g., cell attachment, additional polyelectrolyte layers were added to cover the liposomes. To find the optimal polyelectrolyte couple, both $(\text{PLL/PSS})_2$ and $(\text{PLL/PGA})_2$ were considered as cPEM. For $(\text{PLL/PSS})_2$ it was found that the frequency signal upon deposition of the second polyelectrolyte increased immediately after the decrease, indicating mass loss and possible vesicle rupture (Figure 4.9).

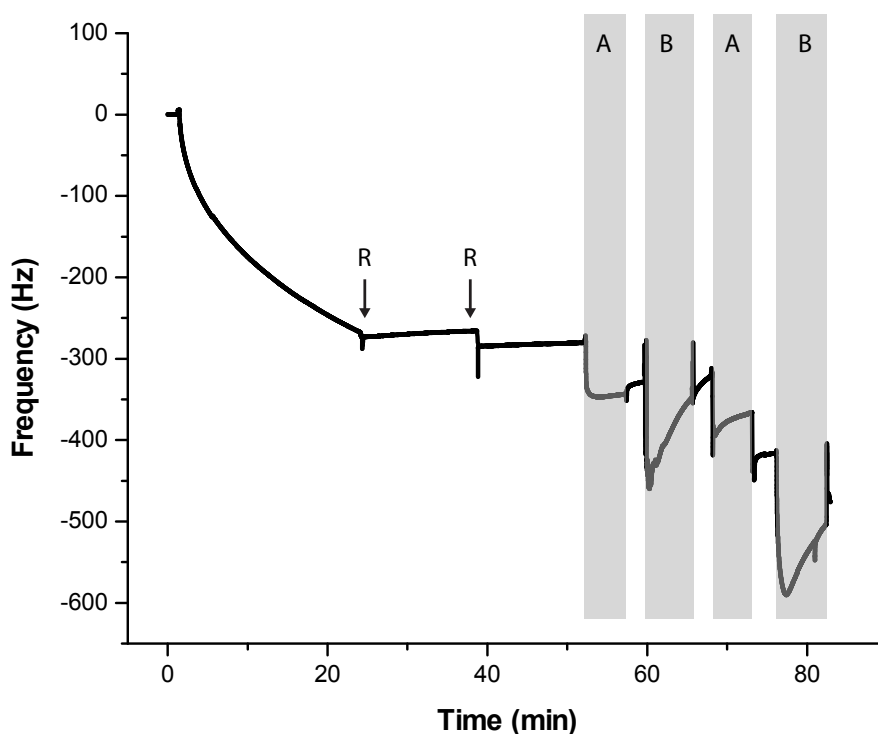


Figure 4.9: QCM curve of vesicles adsorbed onto presprayed gold crystals with $(\text{PLL}/\text{PSS})_9\text{PLL}$. After the vesicles were adsorbed, the flowcell was rinsed twice (R) and then PLL (A) and PSS (B) were sequentially injected.

On the contrary, it could be observed that during the adsorption of $(\text{PLL}/\text{PGA})_2$, the frequency decreased (mass increased) in the expected step-wise manner for addition of polyelectrolyte layers without distortion of the liposome layer (Figure 4.7, C-F). After rinsing, Δf remained constant, indicating that the $(\text{PLL}/\text{PGA})_2$ covered liposome containing multilayer structure was stable. One explanation as to why $(\text{PLL}/\text{PSS})_2$ did not result in the expected mass increase in the QCM might be that the electrostatic interaction of the strong polyelectrolyte couple $(\text{PLL}/\text{PSS})_2$ with the underlying vesicles and the uPEM results in compression and possible rupture of the vesicles, whereas $(\text{PLL}/\text{PGA})_2$ is a much weaker polyelectrolyte couple and might, therefore, not interact so strongly with the underlying vesicles and the uPEM.

The addition of the cPEM was also followed by CLSM and was found not to significantly alter the fluorescence of the underlying vesicles (Figure 4.10).

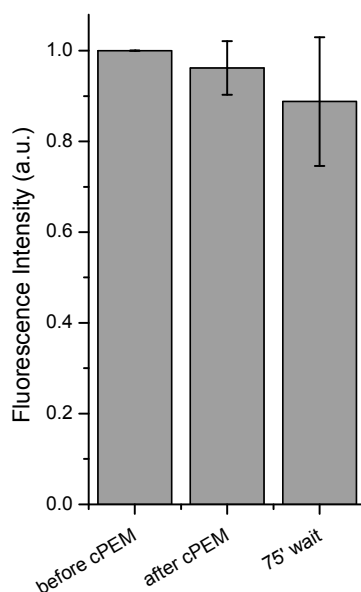


Figure 4.10: Change in fluorescent intensity of cargo-labeled vesicles upon adsorption of the cPEM (PLL/PGA)₂ and 75 minutes waiting. Upon cPEM addition the intensity of the dye remains almost unchanged, showing that the cPEM does not significantly alter the vesicle shape and stability. After 75 minutes the intensity decreased slightly to approximately 90% of its original value indicating a slight leakage of the vesicles.

4.3 EC-Triggered Release from the Platform

25 min after the completed assembly of the uPEM/liposome/cPEM film a galvanostatic current of $5 \mu\text{A}/\text{cm}^2$ was applied for 25 min. After stopping the applied current and rinsing the flow cell, the EC-QCM frequency increased by 300 Hz (Figure 4.7, G-H), i.e., a large fraction of the multilayer mass was released. This increase corresponds to approximately 60% of the original decrease in Δf caused by the adsorption of the vesicles. In situ EC-CLSM was used to determine whether the galvanostatic current induced loss of mass was due to rupture of the vesicles with simultaneous release of the encapsulated water and dye volume, as was the case for the controls for pure pH change performed on PLL-adsorbed liposomes described above, or to desorption of liposomes from the PEM matrix. The evolution of the difference between the fluorescent area and the reference spot for the completely assembled platform with cargo and membrane labeled vesicles upon electrochemical stimulus was thus followed by EC-CLSM (Figure 4.11).

75 min after the completed assembly of the platform, a galvanostatic current of $5 \mu\text{A}/\text{cm}^2$ was applied for 75 min, inducing a decrease in the intensity of the cargo dye (displayed in red) to approximately 0% of its original value, while the membrane dye

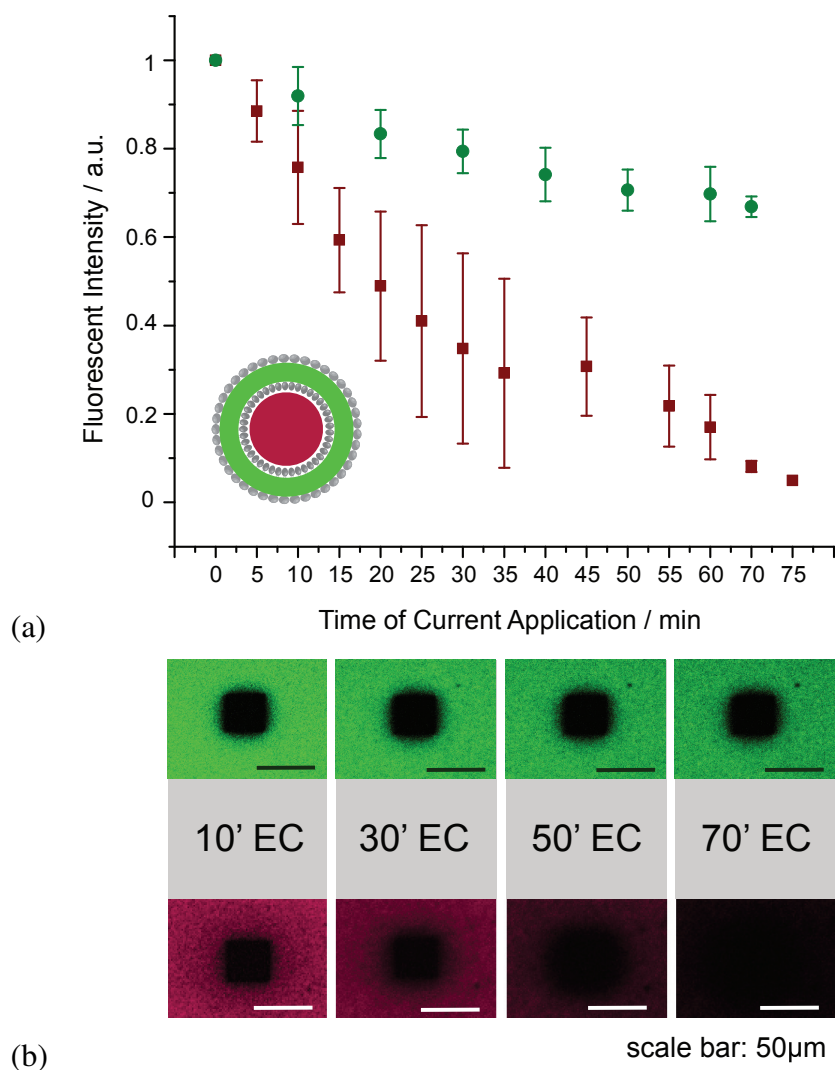


Figure 4.11: a) Change in fluorescence intensity of membrane and cargo labeled liposomes embedded in a PEM matrix upon the application of $5 \mu\text{A}/\text{cm}^2$. After 75 min, approximately all cargo dye (displayed in red) has disappeared, while 75% of the membrane-dye (displayed in green) remained on the substrate. This indicates that most of the content could be released from the vesicles without liposome desorption. b) Details of the fluorescent images after 10, 30, 50, and 70 min of current application. It can be seen that the cargo-dye disappears with current application while the fluorescent intensity of the membrane dye remains high.

(displayed in green) only decreased to 75% of its original value. These EC-CLSM observations demonstrate that the cargo can indeed be released from approximately 75% of the vesicles without desorption since a loss through desorption would be accompanied by a decrease of the membrane and cargo dye signals at the same rate. Moreover, it shows that the negatively charged calcein does not seem to remain in the PEM by electrostatic interaction with the PLL after the release. This might be because the negative charges of the DOPS lipids which were most probably compensated by migrating PLL chains (see Subsection 4.2.2), occupy most of the 'free' positive charges of the PLL. It is likely that the vesicles in close proximity of the working electrode release their content faster than the ones further away from it. This is because the the H^+ -ions generated at the working electrode are diffusing away from the flowcell. This means that the pH is gradually increasing with the distance to the electrode. However, Figure 4.11 shows that after the application of a current for 75 min, almost 100% of the initial fluorescent intensity of the cargo-labeled vesicles was released, indicating that, after 75 min, the z-distribution of the vesicles in the PEM no longer exerts an effect on cargo-release. The fractional release of lipid material indicated by the loss in membrane fluorescence in Figure 4.11 could be due to either intact liposome desorption or to loss of lipid membrane fragments desorbing as aggregates with the PLL. A mechanism for the former could be desorption of vesicles only weakly bound by electrostatic interaction due to the change in pH reducing the liposome charge. Together with the QCM data and the absence of fluorescent recovery after photobleaching (FRAP) for the membrane-labeled vesicles, this indicates that a fraction of the vesicles in the PEM might desorb during the application of the current while the majority only release their content and possibly form pores. However, we cannot exclude the possibility that some of the cPEM is desorbing during the release as well.

4.4 Chapter Conclusion

In this chapter we demonstrated the fabrication of a platform for electrochemically triggered release from vesicles stably embedded in a surface-based matrix. The platform consists of a working electrode as a substrate, a PEM matrix, and pH sensitive liposomes with an aqueous interior containing the compound to be released. The liposomes are directly integrated in the spray-coated PEM matrix through adsorption without additional stabilization. Our results indicate that, in analogy with exponentially growing PEMs, PLL diffuses at the interface uPEM-liposomes. DOPS liposomes being negatively charged,

the polycation PLL encapsulates the liposome membrane stabilizing them and, thereby allowing them to: 1) attain a less distorted shape and 2) probably adsorb in more than a monolayer, increasing the loading capacity of the system. The layer of vesicles was further stabilized by an additional PEM layer (cPEM); selection of the appropriate PEM couple of (PLL/PGA) provided a suitable interface for eventual future cell attachment. We furthermore demonstrated that the application of a galvanostatic current as planned and hoped led to release of the entrapped, water soluble cargo dye from the pH-sensitive vesicles, while the underlying PEM remained intact. The results strongly support the assumption that the EC stimulus creates a locally confined low pH extending from the working electrode which leads to destabilization and rupture of the vesicular assembly due to protonation of the PS head groups of the lipids.

Platform Optimization for Temporal and Spatial Release Control

Parts of this chapter were published in N. Graf, A. Tanno, A. Dochter, N. Rothfuchs, J. Vörös, T. Zambelli; Electrochemically Driven Delivery to Cells from Vesicles Embedded in a Polyelectrolyte Multilayer, *Soft Matter*, DOI: 10.1039/c2sm07272f

After demonstrating the proof of principle of releasing dye from PEM-embedded vesicles by the application of a galvanostatic current in the previous Chapter. This Chapter introduces how to tailor the release in terms of place and time to get one step closer to a controllable surface-mediated drug delivery system.

5.1 Challenges, Strategies & Encountered Problems

To trigger the release locally, the substrate needed to be patterned. We suggested two different methods for patterning (Section 5.2). The first idea was to add an insulator onto continuous ITO samples and patterned it by standard photolithography. The level of our clean-room facility determined the resolution of the pattern to be approximately 20 μm . To know about the feasibility of the creation of a *local* pH gradient, we took an existing lithography mask with circular and rectangular holes. This enabled also for the comparison of the pH distribution on sharp and curved edges. Once we approximated the lateral spreading of the pH on the surface, the continuous ITO substrate could be exchanged by a substrate with several individually addressable ITO electrodes. This then allowed for the parallel monitoring of different parameters and increased the reliability of the experiments since it became possible to directly compare the obtained fluorescence intensity to

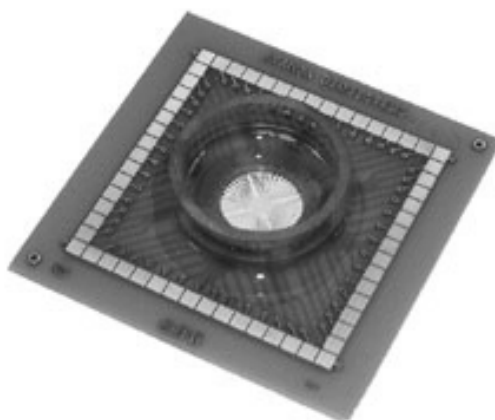


Figure 5.1: Micro electrode array (MEA) for electrochemistry. A glass ring is attached to the chip to allow for experiments in aqueous solutions.

the original intensity on the same sample with the same settings. Therefore, we ordered micro electrode arrays (MEA) with 60 separate ITO electrodes. Unfortunately, these MEAs were conceived to be used in aqueous solutions and had, therefore, a glass ring attached to it (Figure 5.1). This ring made it impossible to spray the substrate. Another issue was that these chips are usually completely coated with an insulator having holes only in correspondence of the tip of the micro electrodes. It turned out that spraying and vesicle adsorption in these holes of $46\ \mu\text{m}$ diameter was difficult. The holes were not always covered by PEM and even when they were covered, they were not homogeneously covered. Therefore, chips without ring and without covering insulator were ordered and an adequate ring was fixed onto the chip by superglue after spraying. Since the chips were then without insulator, the total amount of ITO surface in contact to the solution was not a priori known and was then calculated by stitching images from the microscope. The connection to the potentiostat was then established by an array of pins contacting the golden squares at the end of the micro electrodes (Figure 5.1). In order to achieve a three-electrode configuration, a chloridized silver wire immersed into the solution above the chip was used as reference electrode. However, it was not possible to use the potentiostat in galvanostatic mode since it was actually designed for recording of small potentials, nor could we apply the small currents needed for such a small surface area. Consequently, we looked for a simpler way to obtain separately addressable ITO electrodes. The second idea was to simply cut the continuous ITO layer on the glass samples by a wafer saw, resulting in a sample with four individually addressable electrodes that could be prepared and analyzed in the flowcell as the samples before.

To investigate the release speed versus the applied current, the appropriate current window had to be found. It turned out that this window was between 5 and 30 $\mu\text{A}/\text{cm}^2$, being rather small (Section 5.3). Everything above 30 $\mu\text{A}/\text{cm}^2$ turned black immediately whereas currents below 5 $\mu\text{A}/\text{cm}^2$ did not induce any loss in fluorescent intensity. This was because the pH gradient can only be generated if the hydrolysis of water occurs. The hydrolysis takes place above a potential of 1.5 V in the used three-electrode setup, while currents below 5 $\mu\text{A}/\text{cm}^2$ were obtained by a potential below 1.5 V.

Once able to investigate different parameters on one sample and to tune the speed of the release, even more parameters could be simultaneously considered, by being able to place differently loaded vesicles on different areas on the sample. The easiest way to do so, would be to place empty vesicles and load them selectively afterwards. That was why we were interested to know if the release from the vesicles could eventually be reversible, such that by applying a current in a highly saturated dye solution, resulted in dye diffusing into the vesicles (i.e. refilling). Section 5.4 discusses the issues encountered when we tried to approach this goal.

5.2 Spatially Controlled Release

5.2.1 Adding Patterned Insulator

In order to demonstrate the possibility of releasing the dye locally and to approximate the lateral spreading of the pH gradient, we added an insulator onto continuous ITO samples and patterned it by standard photo lithography. Figure 5.2 shows a confocal laser scanning microscopy image of such a sample before (a) and after 50 min (b) of an electrochemical stimulus application of 50 $\mu\text{A}/\text{cm}^2$. Underneath the confocal images, a scheme of the setup is displayed. The release of the dye happened only in the areas with direct ITO contact, whereas the rest of the area remained green. The borders of the black areas are very distinct, indicating that more than 90 % of the release happened in the regions with direct ITO contact. However, one can see a slightly shaded area around these regions, indicating that the pH gradient was slowly diffusing across the borders of the insulator.

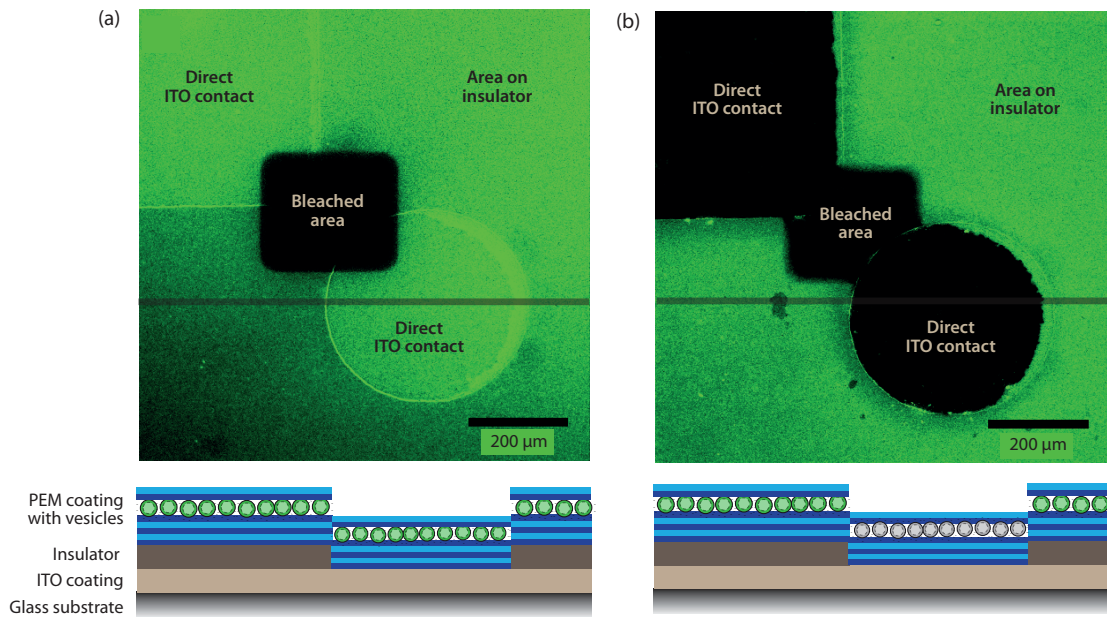


Figure 5.2: $(\text{PLL/PSS})_9\text{PLL}$ -vesicles- $(\text{PLL/PGA})_2$ built up on an ITO sample covered with a patterned insulator of $2\ \mu\text{m}$ thickness. The rectangular and the circular shape are the areas that are in direct contact with the ITO whereas the rest is on the insulator. The black rectangular in the middle is a bleached spot to adjust the microscope settings and to serve as a reference. (a) Before application of a current. (b) After applying the current. The images underneath are schematic drawings of the setup.

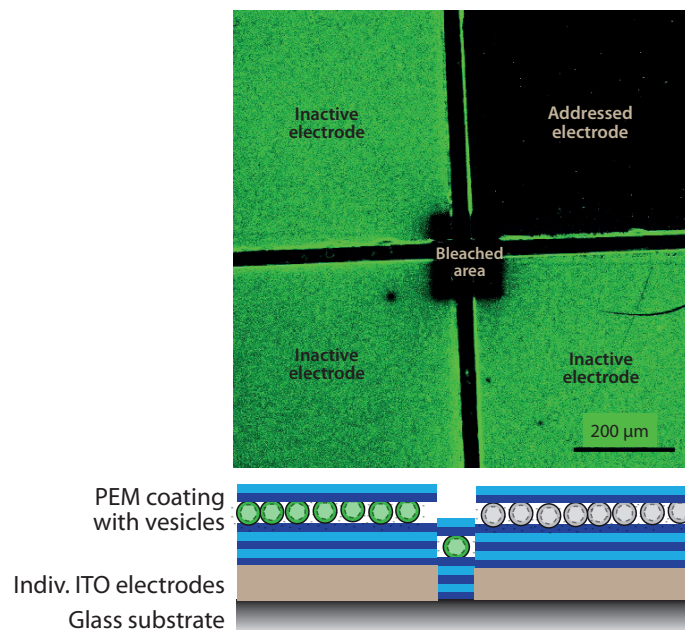


Figure 5.3: A 4-electrode substrate after the application of a current on the upper right electrode. The image below shows a schematic drawing of the setup.

5.2.2 Separate ITO Electrode

Based on these findings, we decided to prepare samples where the ITO electrodes are separated by a gap of $40\ \mu\text{m}$ to ensure, the release is only triggered on the addressed electrode. Figure 5.3 shows an example of a 4-electrode sample after a current of $40\ \mu\text{A}/\text{cm}^2$ in the upper right corner was applied for 15 min. Below the image, a scheme of the setup is displayed. The upper right corner is completely black, whereas the other corners remained green and were apparently not affected by pH gradient generated by the applied current. This shows, that it is possible to localize the release and to perform three experiments on one sample (leaving one corner untreated for reference purposes) increasing the reproducibility of the experiments. The thin residual green line around the upper right corner can be attributed to the vertical wall of the cut while the rest of the cross appears dark because it is out of focus.

5.3 Temporally Controlled Release

Such a 4-electrode sample was then used to measure release kinetics in a highly reproducible and efficient way. Figure 5.4 shows release curves of membrane- and cargo-labeled vesicles upon the application of different current densities. The fluorescent intensity of the membrane-labeled vesicles remained very high (87%), showing that the membrane remains mostly on the sample during a current application of $40\ \mu\text{A}/\text{cm}^2$ for 22 min. The cargo-labeled samples on the other hand, showed a clear decrease in fluorescent intensity with the speed depending on the applied current density. However, there is a threshold current density between 10 and $15\ \mu\text{A}/\text{cm}^2$, suggesting that at $10\ \mu\text{A}/\text{cm}^2$ the minimal pH needed to release the dye might not always be reached whereas above $15\ \mu\text{A}/\text{cm}^2$ the minimal pH is completely reached. For higher currents, the pH gradient most probably spread further away from the substrate, resulting in more and faster release from the vesicles. This demonstrates that it is possible to control the speed of the release from the vesicles by variation of the applied current density.

5.4 Refilling Vesicles

A question after the successful release of the dye from the vesicles, was *how* the dye was released or, more specifically, if the vesicles remain *intact* after the release. A combined

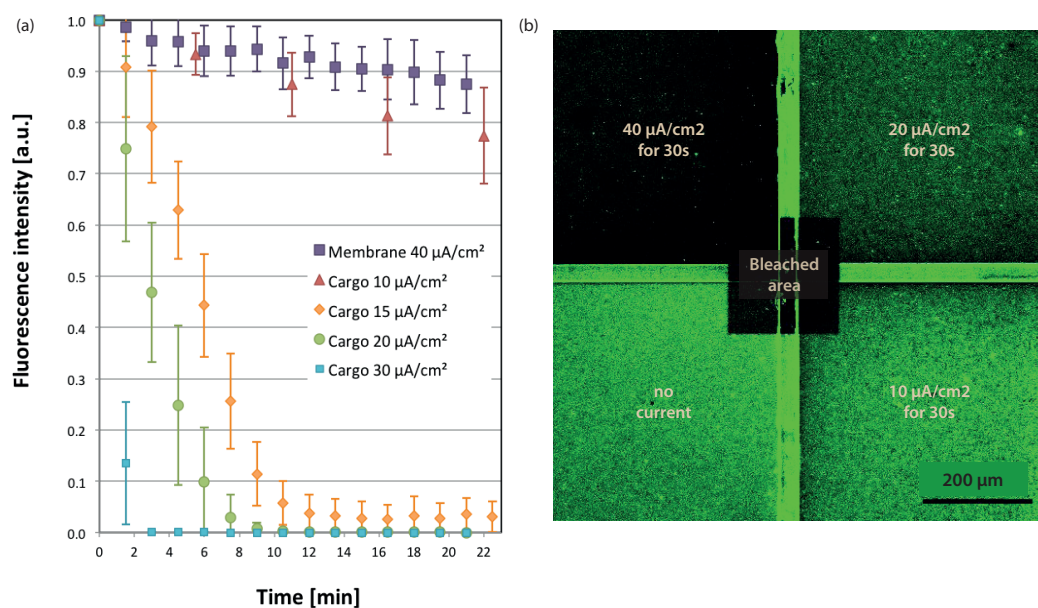


Figure 5.4: (a) Release kinetics for different currents over time. The higher the applied current, the faster the dye release. It seems that the needed current threshold for release is between 10 and 15 $\mu\text{A}/\text{cm}^2$. (b) Visualization of the different release speeds on a 4-electrode sample where different current densities were applied for 30 seconds.

AFM-CLSM experiment was carried out. The AFM was mounted onto the CLSM and cargo-labeled vesicles were embedded between an uPEM of $(\text{PLL}/\text{PSS})_9\text{PLL}$ and a cPEM of $(\text{PLL}/\text{PGA})_2$. Then, a fluorescent image was taken to confirm the integrity of the vesicles. Subsequently, a region was scanned by AFM (Figure 5.5a) and the tip was removed from the surface only by approximately 10 μm to enable us to re-find the scanned area again after the EC application. After the EC stimulus of 50 $\mu\text{A}/\text{cm}^2$ for 50 min another fluorescent image was taken, to confirm that the vesicles released their cargo. Then, the area was scanned again by AFM (Figure 5.5b). The majority of the vesicles seemed to remain intact, however, the overall morphology had changed. Instead of a regular distribution of small islands, some larger islands appeared during the EC application as if the vesicles aggregated or fused to larger capsules.

This experiment confirmed the earlier reported indication that the vesicles might remain intact after the EC-stimulus (see Section 4.3). The finding that the vesicles seem to remain intact, led to the hypothesis of a release process by reversible pore formation. If this was really the case, one should not only be able to release dye *from* vesicles but also to fill dye *into* vesicles by the application of a current and, moreover, to release and refill dye in cycles (Figure 5.6).

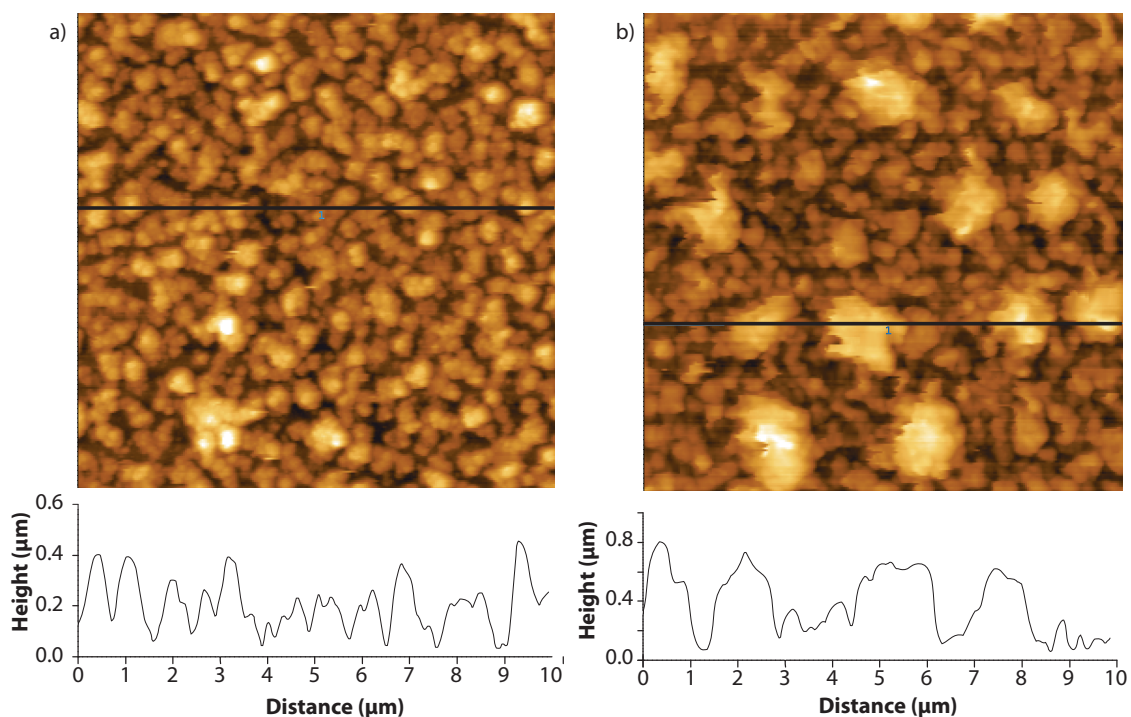


Figure 5.5: AFM images before and after the application of the EC stimulus. The images were taken at the same spot. The majority of the vesicles seem to remain intact, however, the overall morphology has changed. It seems, as if the vesicles aggregated upon the EC stimulus.

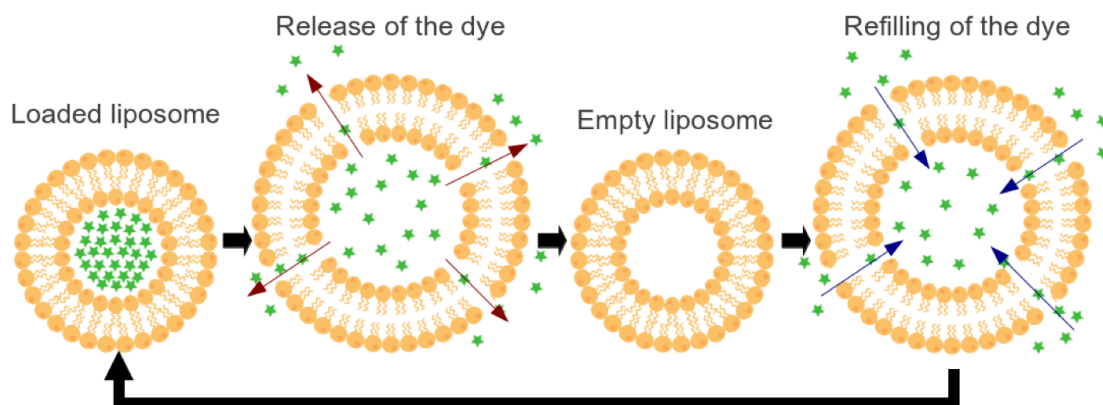


Figure 5.6: Schematic drawing of a possible cycle for the release and refill of vesicles by the application of a current.

To investigate this hypothesis, we first performed a CLSM experiment where cargo-labeled vesicles were embedded between an uPEM of $(\text{PLL}/\text{PSS})_9\text{PLL}$ and a cPEM of $(\text{PLL}/\text{PGA})_2$. The dye was then liberated by applying an electrochemical stimulus of $50 \mu\text{A}/\text{cm}^2$ for 21 min. The release was recorded by CLSM taking a picture every 1.5 min. After the fluorescent image appeared black, the supernatant was exchanged by a concen-

trated solution of calcein (50 mM). Then, another EC stimulus of $50 \mu\text{A}/\text{cm}^2$ was applied for 30 min. After that, the ITO substrate was unmounted from the flowcell and immersed sequentially into 4 beakers filled with 250 ml of 150 mM NaCl to rinse away the calcein in solution. Subsequently, the sample was mounted again into the flowcell and again $50 \mu\text{A}/\text{cm}^2$ were applied for 21 min, taking an image every 1.5 min. Figure 5.7 shows an overview of the obtained results. A reappearance of fluorescent intensity was observed after the re-application of an EC-stimulus with a supernatant of concentrated calcein. Moreover, the sample was bleachable again and the fluorescence was lost when the EC-stimulus was re-applied again. It appeared as if the refilling of the vesicles worked and the reloaded vesicles could be emptied again. However, the fluorescence intensities of the first and second release cannot be compared directly since the settings on the microscope were changed. It is possible that the reappeared fluorescence was a consequence of the fact that the liposomes were not entirely emptied in the first release, which was not visible due to the settings on the microscope or that the negatively charged calcein bounded to the polycation in the PEM. Moreover, the reproducibility of these results was very poor.

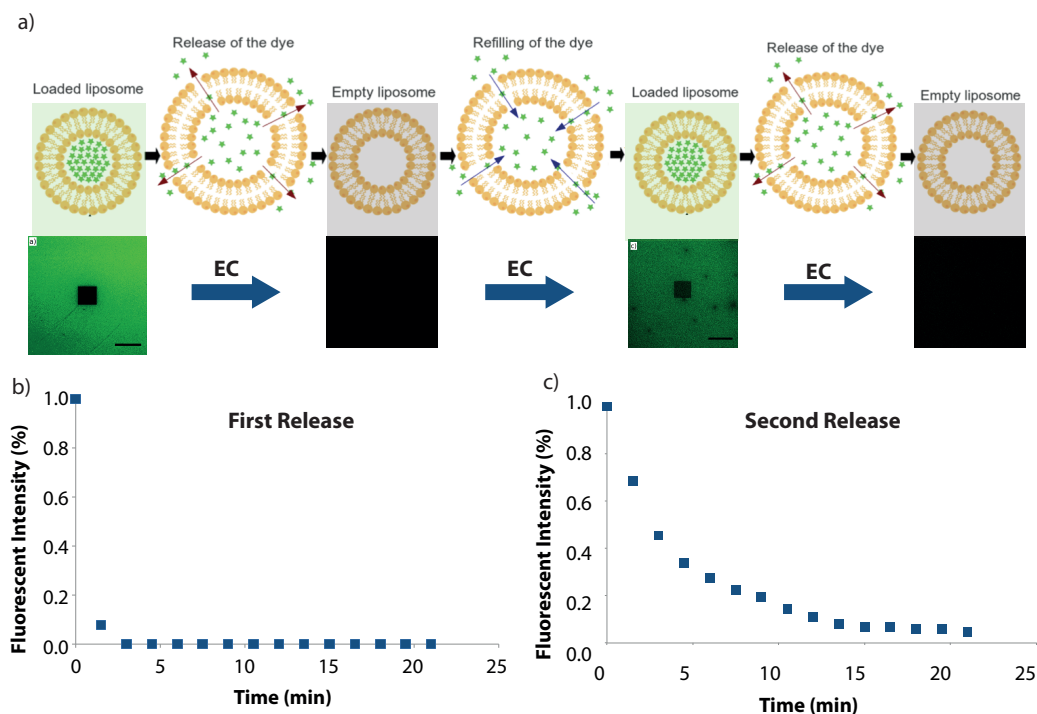


Figure 5.7: Overview of the obtained results for the first refill experiment. a) Schemes and CLSM images of the different stages of the release-refill-cycle. b) Fluorescent intensity decrease upon the application of $50 \mu\text{A}/\text{cm}^2$ for 21 min to the initially loaded platform. c) Fluorescent intensity decrease upon the application of $50 \mu\text{A}/\text{cm}^2$ for 21 min to the 'reloaded' platform.

For these reasons a *systematic* study of the possibility to refill the liposomes was carried out. For that purpose a set of new investigation parameters were defined. So far we always worked galvanostatically to ensure a constant pH gradient generation. However, when the supernatant was exchanged from NaCl to concentrated calcein, the normal currents resulted in potentials of 0.8-1.1 V. This was most probably due to the addressability of calcein by electrochemistry. We supposed that the charged calcein contributed to the electrochemical current so that the EC current used for the release was achieved at lower potentials. Therefore, the hydrolysis of water and, thereby, the pH gradient generation could not take place. Hence, it was decided to work *potentiostatically* at 1.5 V instead of galvanostatically as a first attempt. Secondly, reference experiments had been planned where only uPEMs were exposed to concentrated calcein solution and the EC-stimulus. Thirdly, we decided to work with empty vesicles and investigated only the *filling* process. This would save time and eliminate the possibility that a re-occurrence of fluorescent signal is due to dye left in the vesicles from the first release.

Figure 5.8 shows the result of the reference experiment, where a constant potential of 1.5 V was applied to *one* of the four ITO electrodes that were all covered by the uPEM exposed to 5 mM calcein for 30 min. After this experiment, the sample was bleached. Only in the corner where a current was applied, the area of the bleach spot became darker. All corners appear slightly green, since the gain had to be very high in order to see such small changes. We concluded that a small amount of fluorescent dye was taken up by the uPEM. This could be correlated to the high concentration of calcein, or because the positively charged PLL chains are not occupied by compensating the charges of the negative liposomes (Chapter 4.3) since no liposomes were adsorbed in this experiment. However, there might be a chance that if also empty liposomes are adsorbed onto the uPEM they take up a *larger* amount of calcein than the uPEM *alone* and, therefore, the dye taken up by the uPEM could be neglected.

An experiment was designed where the amount of calcein taken up by the uPEM and the amount of calcein taken up by liposomes could be compared directly. In a first step, the uPEM was deposited onto a 4-electrode substrate. The uPEM was then exposed to a 5 mM calcein solution while to the *two top* of the four electrodes 1.5 V were applied. After a rinsing step, unlabeled liposomes were deposited. Then the sample was again exposed to 5 mM calcein solution while applying 1.5 V to *two right* electrodes. In this way the electrode that was earlier connected and the one that was not yet connected were addressed in this step. The fourth electrode served as reference. It was expected, that the reference does not show fluorescence and remains black. It was possible that the exposed

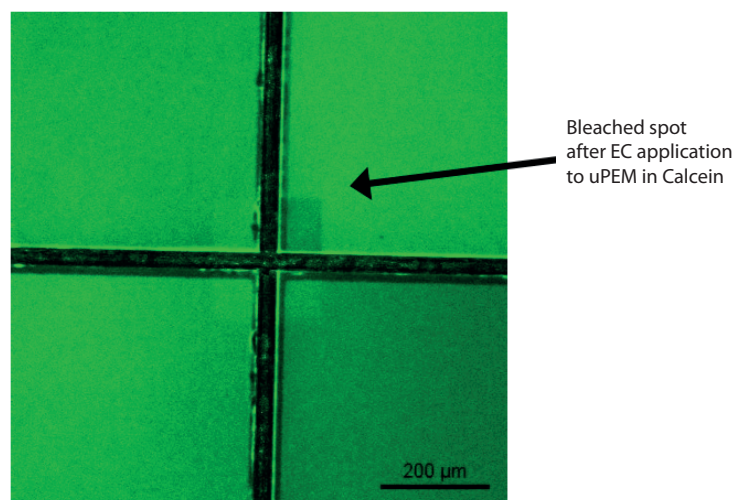


Figure 5.8: Reference experiment exposing one corner of the electrode covered by uPEM to concentrated calcein solution while applying 1.5 V to top right electrode for 30 min.

uPEM gained some fluorescence but we assumed that only a minor amount. Furthermore, it was expected, to see a distinct difference in fluorescence between the electrode where only the uPEM was exposed to the calcein solution and the electrode where the unlabeled liposomes were exposed to the calcein solution, since the liposomes are hoped to take up much more fluorescent dye than the uPEM. The electrode where both the uPEM and the unlabeled liposomes were exposed to calcein with 1.5 V was expected to have the highest fluorescence intensity and represented an overlap of the two other fluorescent intensities. Figure 5.9 a shows a sketch of the expected result and 5.9 b the obtained result.

It can be seen, that the obtained result did not coincide with the expected result. There was no difference in fluorescence between the four electrodes. From these observations it could be concluded, that refilling of the liposomes was not successful. A possible explanation might be that calcein is twofold negatively charged. The lipids that build up the liposome are also negatively charged and it was therefore conceivable that they electrostatically repel the calcein dye and do not allow the calcein to pass through the lipid bilayer. It is possible that the refill could still be feasible if other parameters were chosen. However, several constraints make it difficult to find the appropriate candidate. The dye should not be negatively charged, not addressable by EC below 1.5 V, not diffuse spontaneously across lipid bilayers and be compatible with the generated pore size which is still unknown yet.

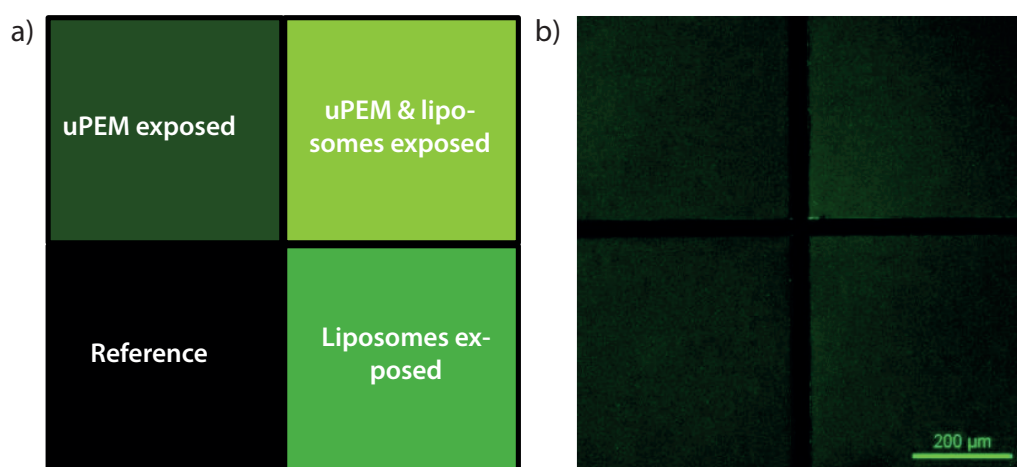


Figure 5.9: a) Sketch of expected CLSM image, top left electrode represents fluorescent intensity of refill of the uPEM, top right electrode both refill of uPEM and refill of unlabeled liposomes and bottom right electrode refill of unlabeled liposomes. b) Obtained CLSM image.

5.5 Chapter Conclusion

In this chapter we demonstrated that optimizations in the platform lead to a controllable functional surface coating. Firstly, we showed that a separation distance of $40\ \mu\text{m}$ between ITO coatings on a surface is enough to apply the current to individual ITO electrodes and release the content of the vesicles only within the area of the addressed electrode underneath. Furthermore, it was shown that by varying the applied current, the release rate can be tuned. A galvanostatic current of $30\ \mu\text{A}/\text{cm}^2$ set free the dye within less than 2 minutes, whereas 80 % of the dye was still not released after 22 min when applying $10\ \mu\text{A}/\text{cm}^2$. Finally, it was found that refilling the liposomes with calcein was not possible for the presented system.

Increasing the Loading Capacity of the Platform by Spontaneous Vesicle-Multilayer Formation

Parts of this chapter were published in N. Graf, E. Thomasson, A. Tanno, J. Vörös, T. Zambelli; Spontaneous Formation of a Vesicle Multilayer on Top of an Exponentially Growing Polyelectrolyte Multilayer Mediated by Diffusing Poly- L-lysine, *Journal of Physical Chemistry B*, 115:12386-12391, 2011

To improve the functional surface coating, we looked for a way to increase the loading capacity of active factors in the coating. One option to increase the loading capacity of a liposome-based release system is to immobilize the vesicles on the surface not only in a two dimensional layer but in a three dimensional fashion.

6.1 Challenges, Strategies & Encountered Problems

Based on the finding that PLL is diffusing within the PEM and, thereby, stabilizing adsorbing vesicles (Chapter 4), we assumed that there must be a direct correlation between the amount of available PLL in the underlying PEM (uPEM) and the amount of adsorbing vesicles. Therefore, DOPS-vesicles were adsorbed on different amounts of PLL/PSS bilayers.

Nevertheless, we quickly realized that a possible vesicle-multilayer is in a size-range which was difficult to access. On one hand, the method needed to provide a high resolution to resolve differences in vesicle adsorption for different amount of uPEMs, and on the other hand, the method needed to be sensitive within a wide size-range because one layer of vesicles is approximately 200 nm thick, so a vesicle-multilayer would be in the

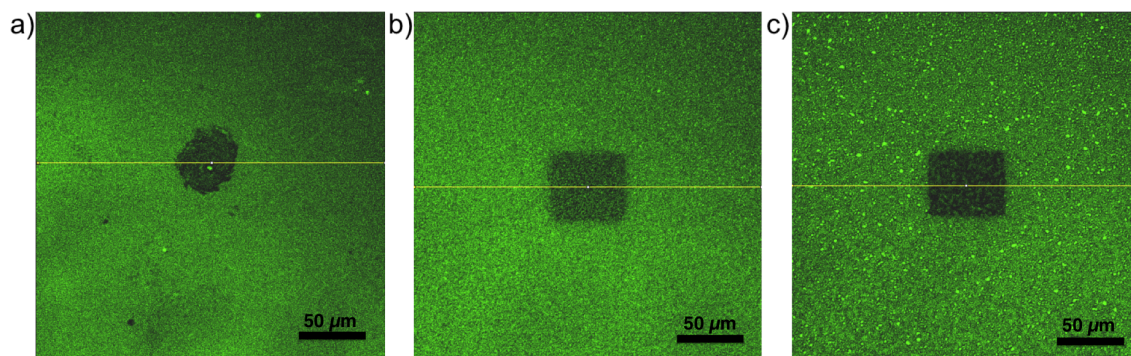


Figure 6.1: CLSM images of membrane-labeled vesicles adsorbed onto a) 9.5, b) 20.5, and c) 50.5 uPEMs made of (PLL/PSS). The images have been taken with the same settings. No significant difference between the fluorescent intensity was found. However, the images appear more 'grained' with more uPEMs.

micrometer range. Techniques like optical waveguide light mode spectroscopy (OWLS) or total internal reflection fluorescence (TIRF) are very sensitive to small changes in adsorption on a surface. However, they rely on changes in an evanescent electromagnetic field that decays exponentially from the surface and, thus, allow only for observations that are less than 200 nm away from the surface.

The **absorption** of light by fluorophores is known to be proportional to the concentration of fluorophores in the sample (Lambert-Beer's law). Thus, we should be able to see differences for different amounts of labeled vesicles. Unfortunately, the variation on different positions on the sample were much larger than among samples with different amounts of vesicles. We suspected two reasons for that. First, the used flowcell was not closed, but with an open water surface which might have resulted in small water movements, affecting the absorption measurements. Second, the wavelength range of the instrument was from 500 - 700 nm, which is slightly above the absorption maximum of our fluorophores at 488 nm, causing the signal to noise ratio to be very low and, thereby, increasing the variation between different measurements.

Also the fluorescent **emission** of fluorescent dye is proportional to its amount. Therefore, we adsorbed membrane-labeled vesicles to different amounts of (PLL/PSS)-uPEMs: 9.5, 20.5, and 50.5 uPEMs (Figure 6.1). All images were taken with the same settings. No significant difference between the fluorescent intensity was found. We believe that the differences lay within the focal plane whose thickness is determined by the pinhole. However, the images appear more 'grained' with more uPEMs, indicating a change in the micro-environment on the surface.

The next technique we tried was the z-stack function of the confocal laser scanning microscopy (CLSM) to get a direct proof of the PLL migrating in the vesicle multilayer. The resolution of the z-stack was approximately $2\ \mu\text{m}$ with the used setup. Fluorescent PLL was used to fabricate the $(\text{PLL}/\text{PSS})_{100}$ film, and the subsequent vesicle adsorption was monitored by CLSM. If the PLL migrated up to the vesicles, the fluorescent PLL should spread over a larger thickness than before vesicle adsorption. For the parameters of our setup, the fluorescent signal of the PLL/PSS film before vesicle adsorption is not an ideal step function, but already spread over $4\text{--}8\ \mu\text{m}$ (data not shown), a much bigger value than the actual thickness for 100.5 bilayers derived by AFM ($1.2\ \mu\text{m}$), impeding every further quantitative investigation of the PLL migration. Much thicker uPEM ($> 8\ \mu\text{m}$, approx. 800 uPEMs) would be needed for the CLSM, which could not any more studied by AFM and QCM, which were the two techniques that enabled us to study the system successfully for uPEMs up to 50.5 bilayers.

6.2 Amount of Vesicle Adsorption vs. uPEM Thickness

The first point we investigated was a possible correlation between the amount of underlying polyelectrolyte multilayers (uPEMs) and the amount of adsorbing vesicles onto it. We analyzed this hypothesis by AFM and QCM.

6.2.1 AFM Investigations

Four substrates were prepared with different uPEMs made of 0.5, 9.5, 20.5 and 50.5 bilayers. The samples were then imaged by means of AFM before and after addition of the vesicles onto the uPEMs. The vesicles were let adsorb for a defined time of 30 min to assure the same conditions for all the samples. Images and profiles across a scratch of the bare PLL/PSS films revealed the following thicknesses: $< 1\ \text{nm}$ (0.5 uPEM), $55\ \text{nm}$ (9.5 uPEM), $270\ \text{nm}$ (20.5 uPEM) and $580\ \text{nm}$ (50.5 uPEM). AFM images and cross sections of the adsorption of vesicles on the uPEMs for 30 min are displayed in Figure 6.2. Two situations were selected: Vesicles adsorbed on top of a single layer of PLL (a), and on 50.5 bilayers (b). A lot of material and many peaks and valleys could be observed for vesicles adsorbed onto 50.5 uPEMs, whereas the cross section for vesicles adsorbed onto 0.5 uPEMs looks much more regular and smoother. The liposomes appeared intact in both cases.

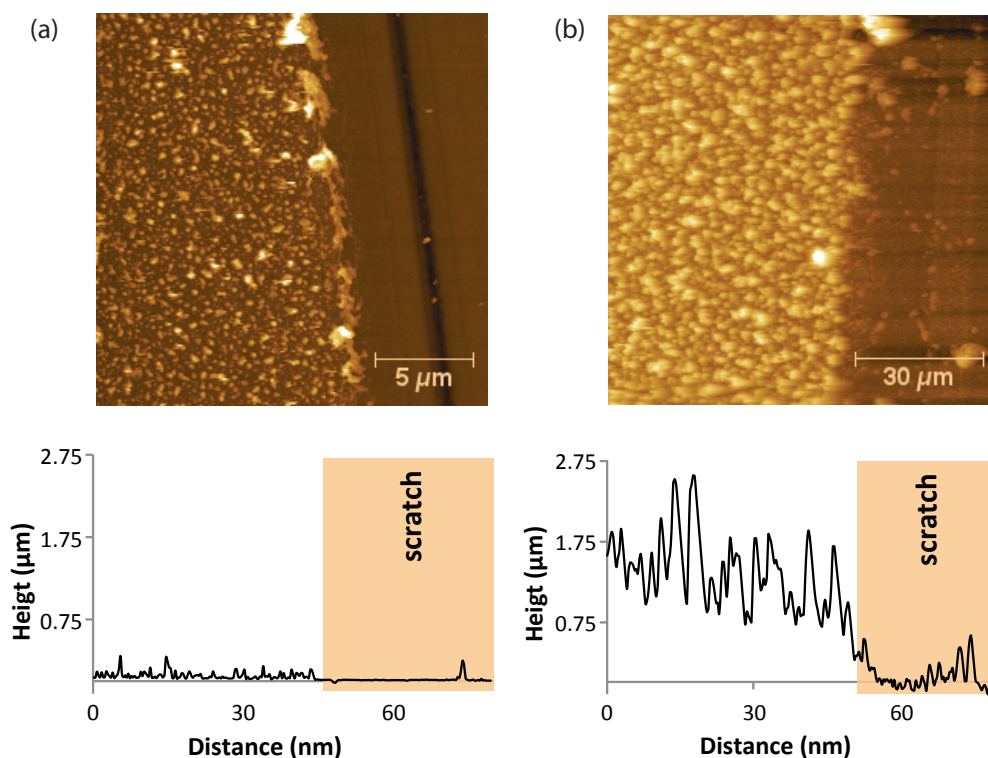


Figure 6.2: AFM images of the topography across an artificially induced scratch, of vesicles adsorbed onto 0.5 (a) and 50.5 (b) uPEMs. Note that for better visualization, a zoom-in of the image for vesicles on 0.5 uPEMs is displayed.

To quantify the vesicle adsorption on the uPEMs, the volume of an $20 \times 20 \mu\text{m}^2$ area was calculated for each AFM sample before and after the vesicle addition (Figure 6.3). On a single PLL layer, whose volume is considered to be negligibly small, the volume of the adsorbing vesicles was approximately $21 \mu\text{m}^3$. The volume for vesicles adsorption onto 9.5, 20.5 and 50.5 uPEMs was found to be 115, 230 and $365 \mu\text{m}^3$, respectively. Subtracting the volume of the uPEM results in an additional difference (ΔV) for the vesicle adsorption of 90, 120 and $130 \mu\text{m}^3$. The increase in ΔV with increasing uPEMs suggests that there seems to be a correlation between the amount of adsorbing vesicles and uPEM thickness. In order to evaluate the efficiency of the spontaneous multilayer formation the volume of the adsorbed vesicles for different uPEMs was compared to the volume of a monolayer of vesicles on 0.5 uPEMs. The ratios were found to be 1, 4, 5.5 and 6, respectively (Figure 6.3 b). This means, that the loading capacity of the system was increased by a factor of 6 simply by increasing the amount of uPEMs.

However, there seems to be a plateau in vesicle adsorption for uPEMs thicker than 20.5 (Figure 6.3 b). Since the AFM experiments were carried out at a fixed adsorption

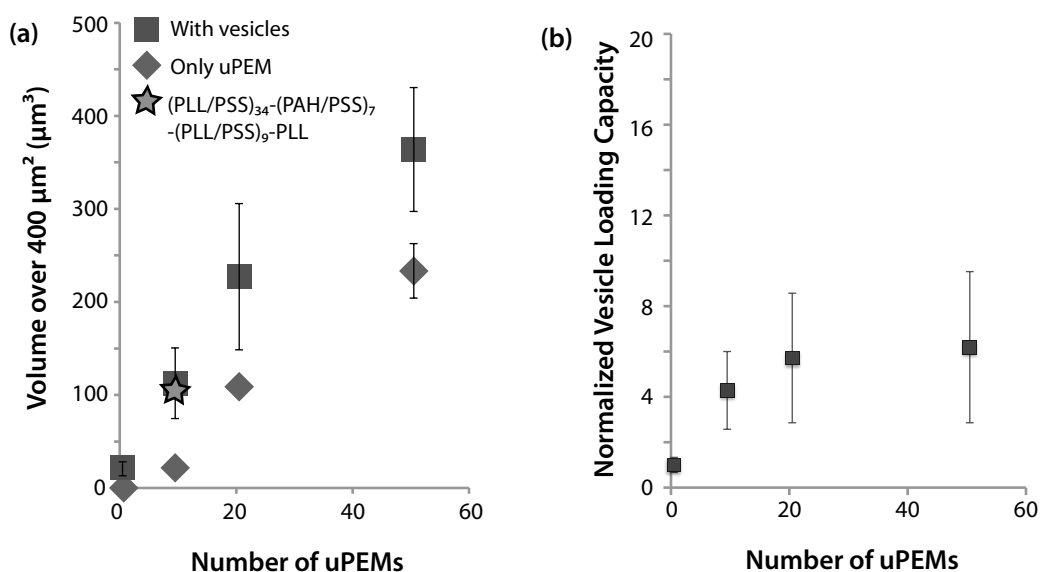


Figure 6.3: a) Volumes derived from $20 \times 20 \mu\text{m}^2$ AFM images of vesicles adsorbed onto 0.5, 9.5, 20.5 and 50.5 uPEMs. The green star displays the amount of vesicle adsorption onto an uPEM made of (PLL/PSS)₃₄-(PAH/PSS)₇-(PLL/PSS)₉-PLL (Section 6.3). b) Enhancement of vesicle loading capacity of PEM coated substrates normalized to direct binding on a PLL monolayer.

time, we checked whether the loading capacity can be even further increased if the vesicles were left on the surface for longer times. The results are shown in the following Section.

6.2.2 QCM Investigations

The QCM technique allows to follow the adsorption processes in situ. Therefore, another experiment was performed by means of QCM. Vesicles adsorption onto different uPEM with thicknesses of 0.5, 3.5, 9.5 and 20.5 was studied over time. The vesicles were adsorbed until a saturation in frequency shift was established but for a minimum time of 30 min.

Indeed, the trend from the AFM experiments could be confirmed. A bigger frequency shift was observed if the same vesicles were adsorbed to higher amounts of uPEMs for 30 min. However, at 30 min the vesicle adsorption onto 20.5 uPEMs did not saturate yet. It can actually be noticed that the time for saturation after vesicle adsorption was increasing from 5 min for 0.5 uPEMs, to 10 min for 3.5 uPEMs, to 20 min for 9.5 uPEMs, to more than 2 h and 40 min for 20.5 uPEM (Figure 6.4 a and b).

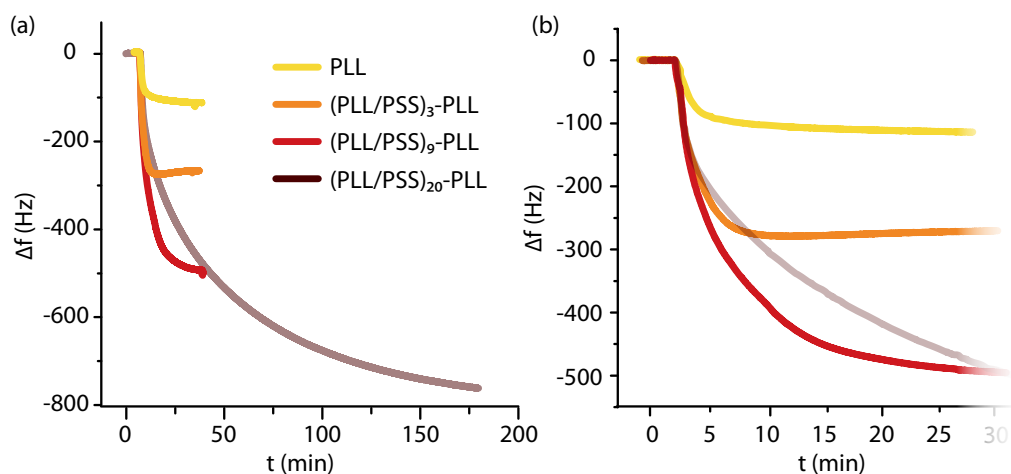


Figure 6.4: a) QCM data of vesicles adsorbing onto 0.5, 3.5, 9.5 and 20.5 uPEMs. b) Zoom-in to the first 25 min, to see the time needed for saturation for vesicles adsorbing onto 0.5, 3.5 and 9.5 uPEMs. The thicker the uPEM underneath, the higher was the saturation frequency. Moreover, saturation time also increased with an increasing amount of uPEMs.

The frequency shift after saturation was found to be around 100 Hz for 0.5 uPEMs and approximately 280 Hz, 500, 750 Hz and 2000 Hz for 3.5, 9.5, 20.5 and 50.5 uPEMs (data for 50.5 in Figure 6) leading to ratios of 1, 2.3, 4, 6.5 and 17 (Figure 6.5).

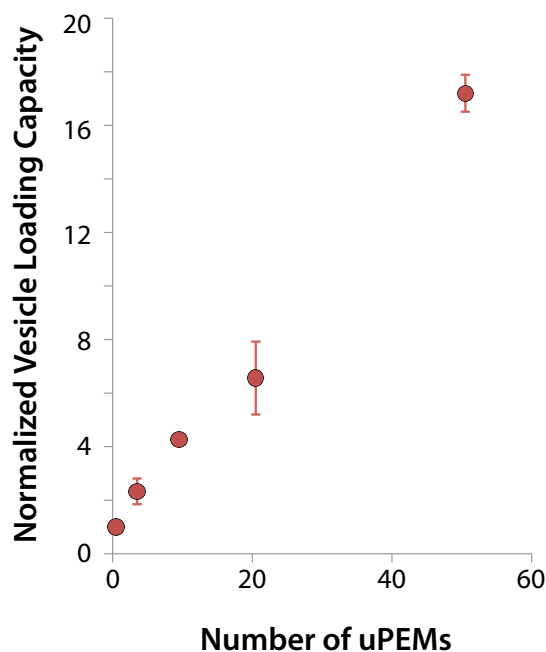


Figure 6.5: Ratios of normalized vesicle adsorption versus the amount of uPEMs. If the adsorption time is long enough one can get an up to 17-fold increase in loading capacity. The 50.5 point is derived from the QCM curve in Figure 6.7. while the other data point are from Figure 6.4.

This means, in comparison to the adsorbing vesicles in one layer, we have an up to 17-fold increase in loading capacity of our system within 6 h simply by adjusting the underlying amount of (PLL/PSS) couples. Other multilayer vesicle constructs show an up to 6-fold increase of the loading capacity compared to a single layer, by sequential adsorption of liposomes and linkers within 6 to 8 h^[9,27,28]. The ratios for 9.5 and 20.5 uPEMs are in a comparable range for the AFM and the QCM measurements (Figure 6.3 b and 6.5). It can be seen, that for 50.5 bilayers the ratio is much higher for the QCM. This is because the vesicles in the AFM experiment were only adsorbed for 30 min, whereas in the QCM they were adsorbed for more than 6 h. If one looks at the value after 30 min in the QCM data (Figure 6.4 b) one sees that the frequency shift for the adsorption is approximately 500 Hz, leading to a ratio of 5 for 20.5 uPEMs, close to the one obtained by AFM (5.5).

6.3 Adding a PEM-Barrier for the PLL

The AFM and QCM data indicated that there are multilayers of intact vesicles on the uPEMs. Because of its stabilization role as described in Michel et al.^[68] we assumed that PLL abundance is the crucial factor for the creation of spontaneous vesicle multilayers. Multilayers consisting of PLL and PSS are exponentially growing^[103]. This means, that PLL is able to diffuse in the highly hydrated film as it was demonstrated for the PLL/HA system^[79]. Normally vesicles deform when they adsorb to an oppositely charged surface because of electrostatic interactions between the lipids and the surface. We believe that upon vesicle adsorption the positively charged PLL chains migrate up to the negatively charged vesicles^[26] and allow new arriving vesicles to stick on the PLL-vesicle complexes (Figure 6.6).

This would also explain the increasing saturation time for vesicle adsorption onto thicker uPEMs. Since the uPEM, as well as the vesicle layer on top of the uPEM, becomes thicker, the diffusion distance of PLL to the newly arriving vesicles is significantly growing.

The confirmation of the suggested role of PLL in increasing the loading capacity of vesicles was assessed with QCM: the same vesicles were adsorbed onto 50.5 (PLL/PSS) uPEMs and another 50.5 layered uPEM which was made of (PLL/PSS)₄₃-(PAH/PSS)₇-PLL instead. This combination of PEMs was chosen since the intermediate (PAH/PSS) layer is known to hinder the diffusion of PLL acting as a barrier for it^[71,79,82,118].

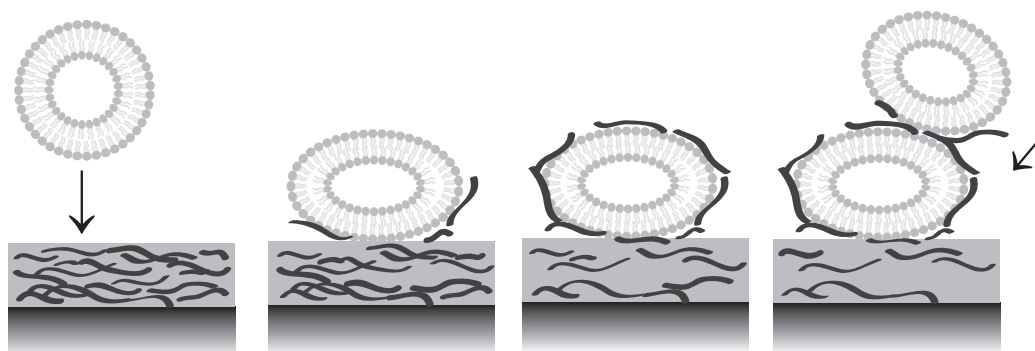


Figure 6.6: Illustration of the PLL migration to stabilize the vesicles upon adsorption. PLL is able to diffuse up to the vesicle and stabilize it by compensation of the negative charges. This allows the vesicles to remain in a less distorted shape than without stabilization. Then more PLL can migrate up along the vesicles and overcompensate their negative charges. Newly arriving vesicles can then again attach to the now slightly positively charged vesicles.

If the increase in vesicle adsorption was due to PLL diffusion, amount of adsorbed vesicles would be similar to the increase for 0.5 uPEMs, since the amount of PLL that can diffuse is the same in both cases. Figure 6.7 shows the adsorption curves for vesicles adsorbed onto a 'normal' 50.5 uPEM made of (PLL/PSS) and onto the 50.5 uPEM with the 'barrier'. The saturation value for vesicles adsorbed onto (PLL/PSS)₄₃-(PAH/PSS)₇-PLL was approximately 200 Hz. This is in the range of the value for 0.5 to 3.5 uPEMs (115 and 270 Hz). The value for vesicles adsorbed onto the 'normal 50.5 uPEM' was around 2000 Hz after approximately 6 h.

This shows that the PLL diffusion is indeed crucial for the formation of spontaneous vesicle multilayers. The thicker the uPEM, the larger is the 'reservoir' for PLL that can diffuse and migrate and, thereby, allow newly arriving vesicles to remain bound to the surface. This finding was further confirmed by a similar experiment carried out by AFM, putting the PSS/PAH barrier at a different position in the PEM. The adsorbed amount of vesicles on (PLL/PSS)₃₄-(PAH/PSS)₇-(PLL/PSS)₉-PLL was 102 μm^3 (derived from Figure 6.8 a) being very close to the 112 μm^3 on (PLL/PSS)₉-PLL (Figure 6.3 a).

The remaining open question is the correlation between the kinetics of the multilayer formation with the PLL diffusion. Three simultaneous processes lead to the multilayer formation: a) PLL diffusion in the PLL/PSS film, b) sticking of the vesicles from the solution to the PLL top layer, and c) PLL diffusion in the vesicle multilayer. The amount of PLL in the vesicle multilayer should be measured as function of time to determine the rate of each process. Yet, the QCM technique does not allow to extract the amount of PLL acting as a 'glue' in the vesicle multilayer and the amount of attached vesicles

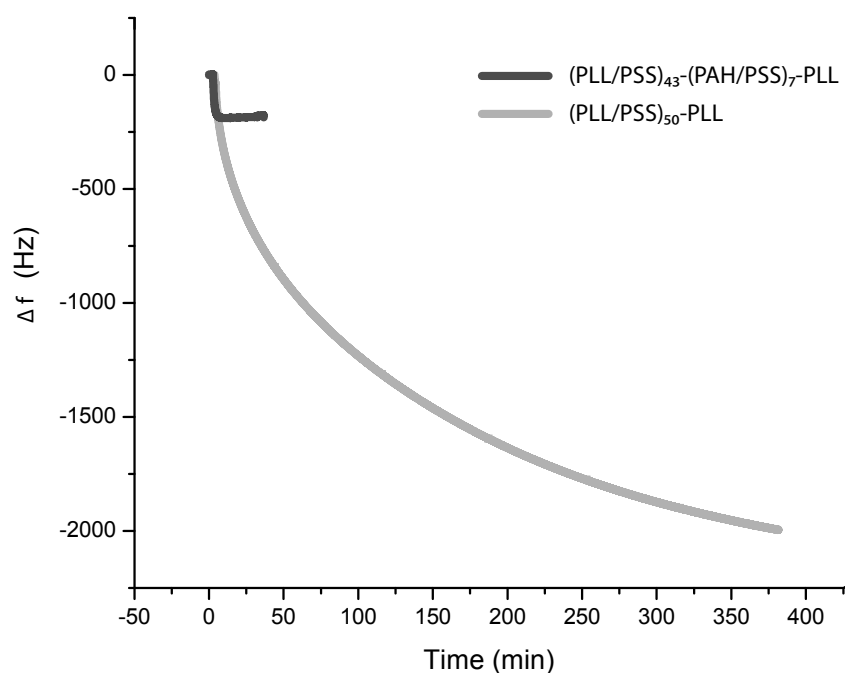


Figure 6.7: QCM curves for vesicle adsorption onto "normal" 50.5 uPEM made of (PLL/PSS) and onto the "barrier" 50.5 uPEM made of (PLL/PSS)₄₃-(PAH/PSS)₇-PLL. This shows that the PLL diffusion is indeed crucial for the formation of spontaneous vesicle multilayers. The thicker the uPEM, the larger is the "reservoir" for PLL that can diffuse and migrate and, thereby, allow newly arriving vesicles to stick to the surface.

from the total adsorbed mass, while the CLSM z-stack has not the sufficient z resolution to follow the PLL diffusion.

6.4 Chapter Conclusion

We were able to obtain 'spontaneous 3D-vesicle constructs' on top of a PLL-containing PEM with an up to 6-fold increase in loading capacity within 30 min and 17-fold after 6 h. We showed that the amount of adsorbed vesicles is dependent on diffusion distance and availability of PLL in the underlying PEM layers.

This is, to our knowledge, the first time that the construction of a vesicle multilayer with different thicknesses could be steered only by the composition and thickness of the underlying PEM film. These findings might be relevant for surface-based drug delivery applications where the loading capacity is a key factor.

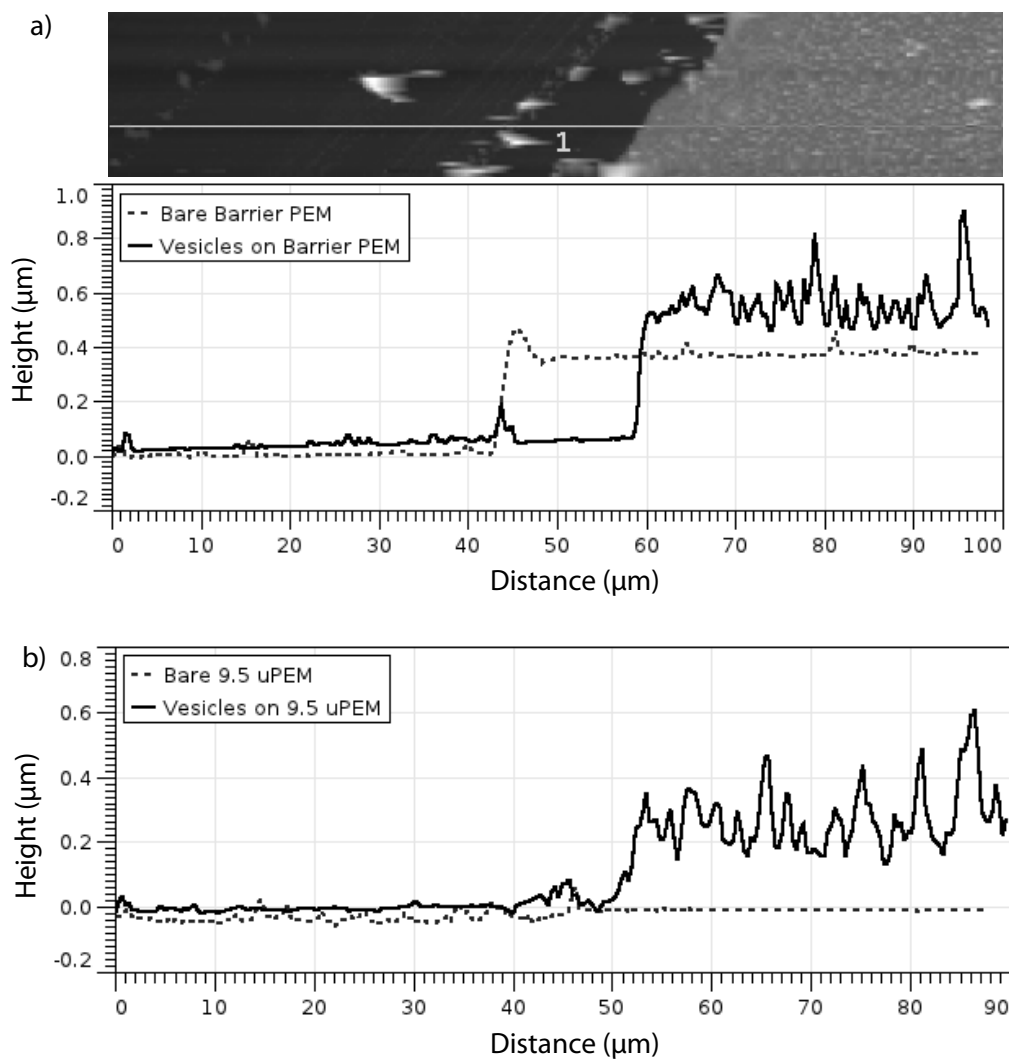


Figure 6.8: (a) AFM image of vesicles adsorbed onto the barrier PEM $(\text{PLL/PSS})_{34}$ - $(\text{PAH/PSS})_7$ - $(\text{PLL/PSS})_9$ -PLL and cross sections of vesicles on barrier PEM and bare barrier PEM used to derive the increase in volume upon vesicle adsorption, (b) cross sections of vesicles adsorbed to 9.5 uPEM and of the bare 9.5 uPEM which is only 55 nm thick. It can be seen already from the cross sections, that the increase in thickness upon vesicle adsorption is approximately 200 - 400 nm, for both $(\text{PLL/PSS})_{34}$ - $(\text{PAH/PSS})_7$ - $(\text{PLL/PSS})_9$ -PLL and $(\text{PLL/PSS})_9$ -PLL.

Electrochemically Driven Delivery of Calcein to Cells on Top of the Platform

Parts of this chapter were published in N. Graf, A. Tanno, A. Dochter, N. Rothfuchs, J. Vörös, T. Zambelli; Electrochemically Driven Delivery to Cells from Vesicles Embedded in a Polyelectrolyte Multilayer, *Soft Matter*, DOI: 10.1039/c2sm07272f

After confirming that it was possible to release the dye in a controlled fashion, both in terms of place and time (Chapter 5) and we could increase the loading capacity up to 17 times (Chapter 6), we adapted the platform for cell adhesion to be able to release the dye from the vesicles to the cells growing on top of it.

7.1 Challenges, Strategies & Encountered Problems

Cell detachment by EC-induced dissolution of the underlying PEM film has been used to detach intact cell sheets from a surface for tissue engineering^[32]. Obviously, to deliver dye from the surface to cells growing on it, a dissolution of the PEM is not desired. This would break the contacts of the cells with the substrate and, therefore, result in cell desorption instead of in delivery of the dye to the cells. The cPEM was conceived to protect the vesicles in the platform from the environment and to avoid a premature contact of the cells with the platform and, thereby, the vesicles. However, the QCM-results in Figure 4.7 suggested that one can not exclude that parts of the cPEM desorb from the surface upon the application of the EC-stimulus. To check if the cPEM (PLL/PGA)₂ is affected by the EC stimulus, (PLL/PSS)₉PLL-vesicles-(PLL-FITC/PGA)₂ samples with fluorescent cPEMs were prepared and 5 $\mu\text{A}/\text{cm}^2$ were applied. Figure 7.1 shows a CLSM

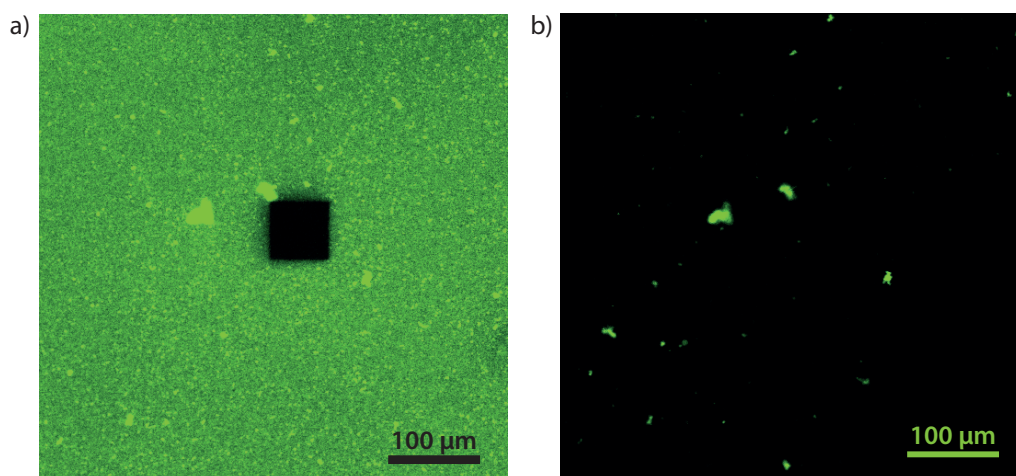


Figure 7.1: Fluorescent cPEM in a $(\text{PLL}/\text{PSS})_9\text{PLL}$ -vesicles- $(\text{PLL-FITC}/\text{PGA})_2$ buildup to see the effect of the EC application onto the cPEM. a) Before and b) after 70 min at $5 \mu\text{A}/\text{cm}^2$.

image a) before and b) after 70 min of EC application. The image becomes totally dark, indicating that the cPEM is most probably desorbing from the surface. It was important that the cPEM and, thereby, the cells remained on the surface upon EC application to enable the delivery of the vesicles' content to the cells.

A set of approaches was suggested to fulfill this new requirement (Figure 7.2).

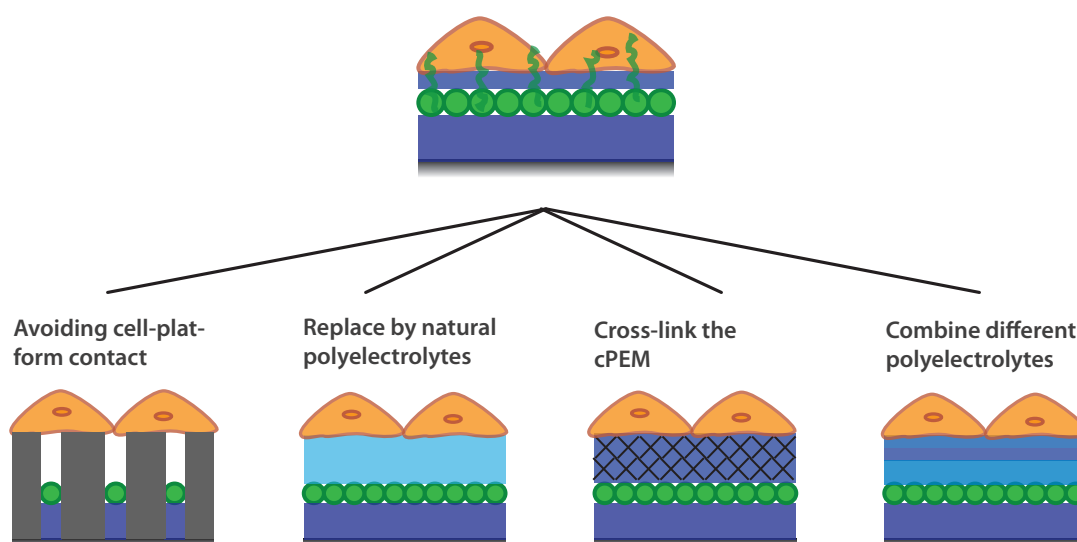


Figure 7.2: Approaches to assure the cells remain on the platform during the EC application. First, to pattern the substrate such that the cPEM is not in direct contact with the cells. Second, to replace the existing cPEM with natural polyelectrolytes such as hydrogels. Third, to chemically cross-link the cPEM to increase its pH-resistance, and fourth, to mix different polyelectrolytes to increase the stability of the cPEM without harming the vesicles underneath.

7.1.1 Avoiding Cell-Platform Contact: Micro-welled Substrate

The first approach was to circumvent the problem of cPEM dissolution by patterning of the substrate such that the PEM-vesicle-platform was not in direct contact with the cells. This would eliminate the need for a protective cPEM and also prevent a premature access of the cells to the dye.

To realize this approach, the most important issue was to avoid the adsorption of the platform directly on *top* of the pattern. Three options were discussed. First, one could deposit a channel-pattern on the surface, cover it with a cover-slip and assemble the platform by pipetting the components to the edge of the cover-slip. The liquid should then be transported to the inside by capillary forces and cover only the walls and bottom of the pattern. The disadvantage of this method would have been that the platform was built up not only on the ITO substrate but also on the walls of the channel possibly resulting in different behavior of the platform upon EC-stimulation.

Another idea was to add the platform normally onto the patterned substrate and remove it from the top of the pattern afterwards, for instance by the 'sticky-tape-approach'. After the deposition of the platform on the patterned substrate, the parts on *top* of the pattern could be removed by pressing a thin layer of agarose onto it and carefully removing it again. The agarose whose viscosity can be adjusted by temperature would serve as the 'sticky-tape'. However, the optimal temperature might be hard to find, if it was too liquid, the agarose would fill the holes of the pattern and if it was too solid it would not be sticky anymore.

Another option was to cover the patterned substrate first by PLL-*g*-PEG by electrostatic interactions. Then, one could apply an EC-stimulus and remove the PLL-*g*-PEG from the areas corresponding to the ITO substrate^[100,101]. Subsequently, the platform could be built up as usual and would (hopefully) only adsorb onto the bare ITO surfaces. This seemed to be the most straightforward approach. Yet, it was not clear if the PLL from the uPEM would adsorb competitively with the PLL-*g*-PEG on the surface.

Another important question was the dimension of the micro-wells such that the cells would not enter it and get in contact with the platform again. Franco et al.^[21] found that cells on patterned cubes of $1 \times 1 \times 1 \mu\text{m}^3$ still 'hang' down for 800 nm. Unfortunately, these structures were too small for our clean-room facility. Therefore we imaged cells on a previously created pattern of 6 μm thickness with 4 μm holes, to see how far down the cells can reach. Cells were grown on the SU-8 pattern for 4 hours and then labeled with

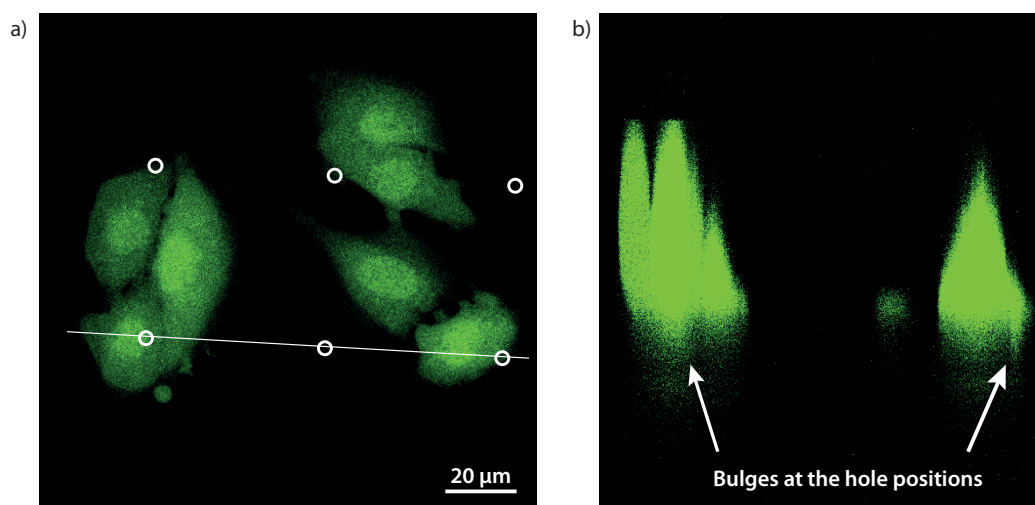


Figure 7.3: a) Area with cells spreading over the SU-8 micro-well pattern. The white circles indicate the position of the holes. The white line shows the position where the z-stack in b) was taken.

CellTrackerTM green and fixed with paraformaldehyde prior to the analysis by CLSM. Figure 7.3 a shows an area with cells spreading over the pattern. The white circles indicate the position of the holes. The white line shows the position where the z-stack in Figure 7.3 b was taken: The shape of the cells is slightly bulging at the position of the holes although the resolution was not good enough to see how deep the cells could reach. Therefore, we concluded that it was very likely that cells spread into the 4 μm holes and it was decided that this method did not seem to be straightforward to prevent a premature contact of the cells with the platform.

Consequently, the next approaches from Figure 7.2 dealing with the EC-stability of the cPEM came into play.

7.2 cPEM Optimization for Cell Adhesion

Since the strategy to avoid cell-platform contact by patterning was not successful we decided to combine the search for an EC-resistant cPEM with the one for a cPEM that favors cell-adhesion and does not affect the vesicle integrity upon deposition.

Many different cPEMs were systematically analyzed according to these criteria (Figure 7.4). Five categories were evaluated: the integrity of the vesicles after cPEM deposition, the resistance to the electrochemical stimulus, the attachment of cells on the cPEM, the separation between the vesicles and the cells and the ease of handling. We found

	Vesicles integrity	EC resistance	Cell attachment	Cell separation	Handling
Alginate with CaCl ₂ reservoir	--	++	n.t.	n.t.	--
Alginate no CaCl ₂ reservoir	n.t.	--	n.t.	n.t.	-
ECM gel	n.t.	n.t.	+	--	--
(PSS/PAH) ₂	--	n.t.	n.t.	n.t.	++
(PLL/HA) ₂	++	--	n.t.	n.t.	++
Cross-linked (PLL/HA) ₂ PLL	n.t.	-	n.t.	n.t.	-
Cross-linked (PLL/HA) ₁₂ PLL	++	++	+	++	-
Cross-linked (PLL/HA) ₁₂ PLL-g-PEG-RGD	++	++	++	++	-

++ very good, + good, - not good, -- bad, n.t. not tested

Figure 7.4: Table showing the different cPEMs that were analyzed as possible candidate for the use of the platform for the delivery to cells. Five categories were evaluated. The integrity of the vesicles after cPEM deposition, the resistance to the electrochemical stimulus, the attachment of cells on the cPEM, the separation between the vesicles and the cells, and the ease of handling. Extra cellular matrix (ECM) gel is primarily composed of laminin, collagen type IV, heparan sulfate proteoglycan and entactin (Sigma Aldrich, E1270)

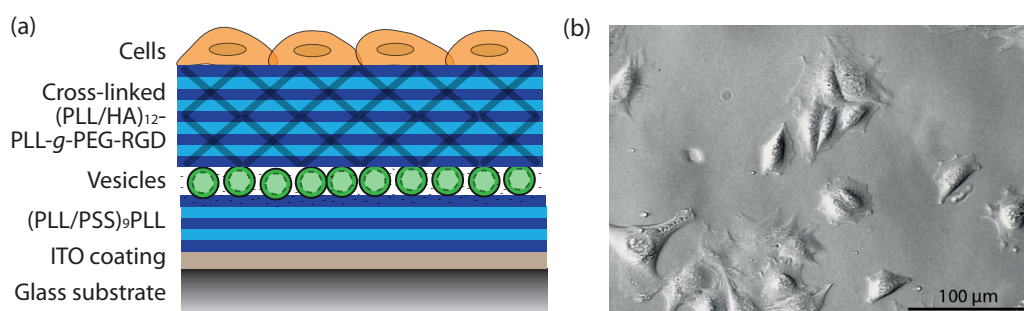


Figure 7.5: (a) Schematic drawing of the setup used for cell experiments. A cross-linked cPEM was added in order to provide an optimal support for cell growth and a separation from the active substance. (b) Microscopy image of cells grown for 3 h on a cross-linked (PLL/HA)₁₂PLL-g-PEG-RGD.

that cross-linked (PLL/HA)₁₂PLL-g-PEG-RGD was the most suitable candidate for these constraints. Figure 7.5 shows (a) a scheme of the used setup for the cell experiments and

(b) the cell attachment after letting them grow for 3 h on such a cPEM. The cells spread well on the sample showing that they are in close contact to the surface and adhere well to it.

7.3 Finding an Appropriate Factor to be Delivered

Even though, the optimal cPEM for cell delivery was found, before starting the cell experiments, the appropriate dye to be delivered had to be chosen. Figure 7.7 shows a collection of possible candidates. The dyes were also evaluated according to several criteria.

Leakage vs. Uptake

The first and most important criteria, was to find a dye that remains in the vesicles as long as no EC stimulus was applied but was at the same time spontaneously labeling the cells once released. The risk was that any dye which was able to be easily taken up by the cell, because it was spontaneously penetrating lipid bilayers, would actually leak out of the vesicles before any stimulus was applied. Nevertheless, this category of dyes was designed such that they were only fluorescent after entering the cell due to an enzymatic cleavage within the cell. This enabled to clearly distinguish whether the dye really was inside of the cell. Thus, since the lipid bilayer composition of the cells was not the same as the composition of the used vesicles, we still tried one of these dyes (CellTracker greenTM) to check if it was leaking out of the vesicles or not. Experiments showed that, indeed, the dye leaked out of the vesicles immediately and could, therefore, not be delivered by an external stimulus.

Binding to the Cell Surface

Since the leakage from the vesicles and the spontaneous uptake by the cells appeared to be strongly interconnected, we decided to try a dye which was known to bind to the *surface* of the cell. Therefore, we loaded the vesicles with cholera toxin Alexa Fluor 488 and cultivated cells on top of the platform. Figure 7.6 shows the evolution of the fluorescent intensity before and during the EC-application of $25 \mu\text{A}/\text{cm}^2$. Since Alexa Fluor dyes are well known to be very resistant to photobleaching, it was not possible to bleach a reference spot in the beginning. Therefore, the contrast settings were not optimal.

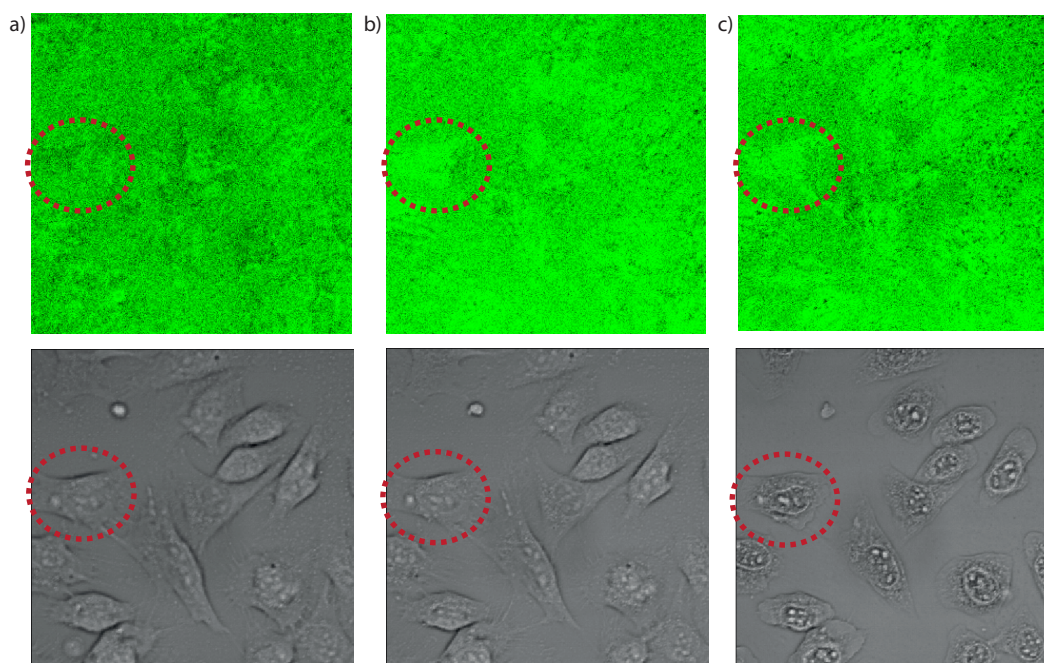


Figure 7.6: CLSM images for the EC-triggered delivery of cholera toxin Alexa Fluor 488 to cells growing on top of the platform. a) Before EC-application of $25 \mu\text{A}/\text{cm}^2$, b) after 1 min of EC application, c) after 12 min of EC-application. The red circles show a cell which became slightly greener during the EC-application. However the overall signal-to-noise-ratio is very poor.

Nevertheless, at least one of the cells became slightly greener during the EC-application. However, the cells did not look so healthy after 12 min of current application (Figure 7.6 b). We concluded that we needed higher concentrations of the cholera toxin within the vesicles and probably higher currents to release it faster and avoid harming the cells. Unfortunately, cholera toxin Alexa Fluor 488 was very expensive, so that one experiment would have cost approximately 500-1000 CHF!

Dilution Issues

The experiment with labeled cholera toxin underlined the importance of the dilution. Upon release the dye would be diluted by approximately 100-10'000 times as calculated from the total vesicle volume on a uPEM with 9.5 (PLL/PSS) bilayers in Chapter 6. Therefore, it was important to incorporate the dye at high concentrations in the vesicles. Nevertheless, after the release, the dye now at unavoidable low concentration must yet reach the cells and color them in a detectable way. It would, moreover, be advantageous if the dye was not too expensive. We decided to try the QTracker cell labeling kit, since QDots are well known to show strong fluorescence even in very small dilutions.

Unfortunately, experiments with QTrackers revealed leakage before the EC-stimulus was applied.

Diffusion through cPEM

Another issue was that the dye should easily be able to diffuse through the cross-linked cPEM. Thus, we excluded dyes that were attached to big molecules such as antibodies as well as molecules with lots of charges such as DNA or proteins.

7.4 Calcein for the Delivery to Cells

Since calcein disodium sulfate was used for all the preliminary experiments for the platform optimization, we discovered by accident that the cells eventually also turned green when working with calcein. Even though the calcein is negatively charged we found that it did not remain within the PEM (Chapter 4), which might be because the negative charges of the DOPS lipids which were most probably compensated by migrating PLL chains (see Subsection 4.2.2), occupy most of the 'free' positive charges of the PLL. We therefore, decided to try calcein for the further cell-experiments.

7.4.1 Needed Concentration

First, we checked the cells' reaction when they were exposed to different concentrations of calcein. 40'000 cells per cm² were seeded onto cell culture dishes and different calcein concentrations were pipetted into the medium. Figure 7.8 shows fluorescent images of the cells after exposure to calcein. Different microscopy settings were used for the three concentrations to find the lowest concentration where we could still see a difference of the cells and the background. One can see that down to a dilution of 500 μ M calcein, the cells still show fluorescence. Assuming that the dilution of calcein within the direct cell micro-environment will only be around 10–100, an initial concentration of 50 mM calcein in the vesicles was chosen. This should then be sufficient to stain the cells upon EC-triggered release.

Dye	Leak from Vesicles?	Cell Attach./Uptake?	Recognition	Diffusion through cPEM?	Other advantages	Other disadvantages
CellTracker green	Likely	Free diffusion / active uptake	Only fluorescent within cell	Likely	- Rel. cheap	
CellTracker orange	Likely	Free diffusion / active uptake	Only fluorescent within cell	Likely		
Calcein AM	Likely	Free diffusion / active uptake	Only fluorescent within cell	Likely	- Live staining	
Tubulin Tracker Green	Likely	Free diffusion / active uptake	Only fluorescent within cell	Likely		
Neutral red	Likely	Free diffusion / active uptake	Fluorescence dependant on pH	Likely		
Trypan blue	Very unlikely	Attaches to ECM	Normal fluorescence	Likely	- Cheap - Live-Dead staining	- Weak fluorescence - Toxic (~3 min)
Fluorescent Gelatin	Unlikely	Attach. to collagen recept. & fibronectin	Normal fluorescence	Likely		
BODIPY FL LDL	Unlikely	Receptor mediated endocytosis	Normal fluorescence	Likely	- Cancer drug transporter	- Very expensive - Designed for <i>human cells</i>
Antibody - integrin	Unlikely	Attachment - specific to integrin	Normal fluorescence	Possible	- Available with dye	- Not tripsin resistant
Qtracker 605 Cell Labeling Kit	Unlikely	Unspecific transport mechanism	Normal fluorescence	Possible		- Very expensive
Cholera toxin – Alexa Fluor 488	Unlikely	Bind to lipid rafts of the membrane	Normal fluorescence	Likely		- probably not tripsin resistant - Expensive
DiD	Very likely	Free diffusion	Only bright in lipid bilayer	Unlikely		
HSP-DiOC	Possible	Diffusion	Only bright in lipid bilayer	Likely		- very expensive
Transferrin – Texas red	Unlikely	Receptor mediated endocytosis (active)	Always bright	Likely	- Available with other dyes	- Is released by cell as fast as it's taken up
MitoTracker Red	Likely	Passive diffusion	Fluorescent if oxidized	Likely		- Only stains mitochondria
Calcein disodium salt	Very unlikely	Unknown	Always bright	Likely	- Cheap	

Figure 7.7: List showing the different dyes as possible candidates to be delivered from liposomes to the cells. The dyes with green background were the ones we actually tried in cell-experiments.

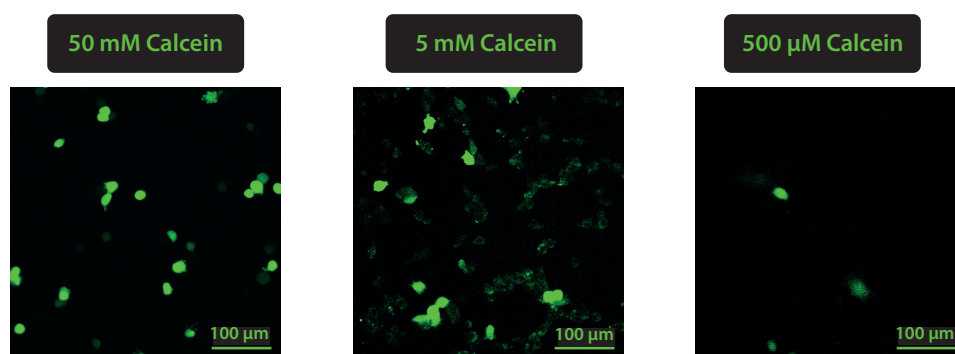


Figure 7.8: A dilution series where $40'000 \text{ cells/cm}^2$ were exposed to different concentrations of calcein. Cells were still fluorescent down to a concentration of $500 \mu\text{M}$ calcein.

7.4.2 Applying the Current: Released Calcein into the Cells

The vesicles were filled with 50 mM calcein and the platform was then built up according to the scheme in Figure 7.5. After mounting the platform into the flow cell, the cells were grown on the cPEM for at least 3 h. Then, an area in the middle of the sample was photobleached to determine the background intensity. Before the EC experiments were performed, a reference experiment was done where the evolution of the fluorescent intensity without applying EC was analyzed to check the stability of the platform. The fluorescent intensity remained at 99% for more than 90 minutes showing that the platform was stable as long as no EC was applied. Then the EC experiments were carried out. After bleaching the reference area, the sample was imaged and a current density of $50 \mu\text{A/cm}^2$ was applied. During the current application a fluorescent and a transmission image was taken every minute. A typical example of such an experiment is shown in Figure 7.9. Already after 2 minutes the cells clearly appeared green in the fluorescent image. Because the cells already turned clearly green after 3 min, the current was stopped to avoid harming the cells unnecessarily. At the same time the vesicles in the PEM became darker. This indicated that the dye is successfully released from the vesicles and delivered to the cells, which was the objective of our work. Note that even in the bleached area which remained completely black during the experiment preparation of at least 20 min (data not shown), the cells became green only after the current application. This shows that the release of the dye is indeed triggered by the application of current. Furthermore, it shows that the released dye is also diffusing laterally to the cells. No change in the phase contrast image could be observed during the 3 min of current application, indicating the lack of major damage to the cells. Dead staining 20 min after the experiment revealed that the 3 min

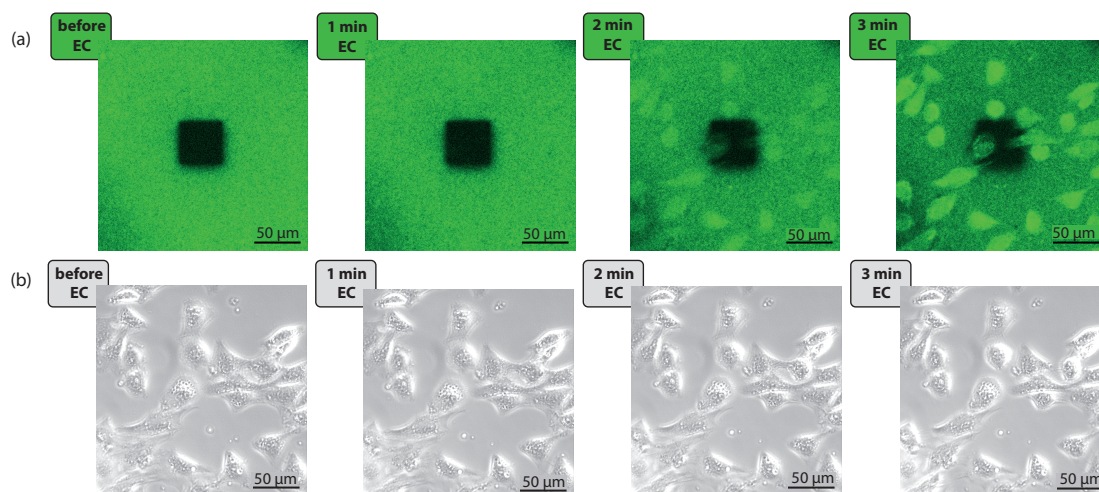


Figure 7.9: Time series of a current application of $50 \mu\text{A}/\text{cm}^2$ for 3 min. (a) Evolution of fluorescent intensity and (b) phase contrast images of the cells.

current application had no significant effect on the viability of the cells, which was found to be $98.9 \pm 1.6 \%$.

To quantify the results of the EC-driven delivery, the experiment was repeated 3 times and the fluorescent intensity of the cells in the bleached area as well as of the vesicles was monitored. Figure 7.10 shows the evolution of the fluorescent intensity during the 3 min of current application. The intensity of the vesicles decreased to approximately 55 % and at the same time the intensity of the cells in the bleached area increased to 25 % of the original intensity of the vesicles. Since the original intensity of the vesicles represents the maximum possible intensity on the surface, one can not expect the fluorescent intensity in the cells to become similarly strong. Therefore, we assumed that 25 % of the original intensity might already be close to the maximum intensity the cells can get and stopped the current to avoid any possible current-induced damage to the cells.

The last question we addressed was if the released dye only remained attached to the cell-membrane or if it actually was inside the cells. Hence, high magnification CLSM-images were taken after the EC-delivery to the cells. Figure 7.11 shows a representative cell on a bleached area after the electrochemical stimulus was applied for less than 3 min. For a membrane-labeling we would expect that the fluorescence is 1) higher at the edges of the cell, since these are the areas where the membranes overlap in the image and 2) more homogeneously distributed. However, because the fluorescence intensity is not bright at all at the borders of the cell, we concluded that it is very likely that the dye was taken up by the cells. However, the spotted, inhomogeneous appearance of the fluorescence suggests

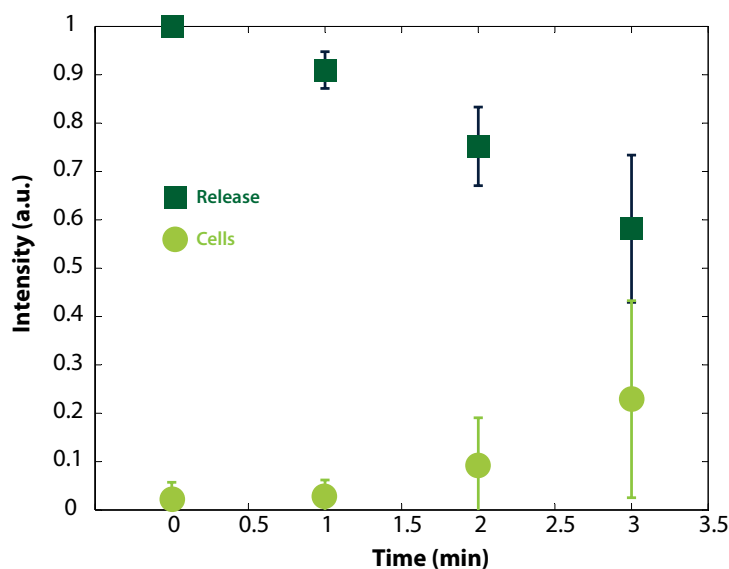


Figure 7.10: Quantification of dye release and cellular uptake within the bleached areas.

that the released calcein was taken up by endocytosis and remained in endosomes within the cell.

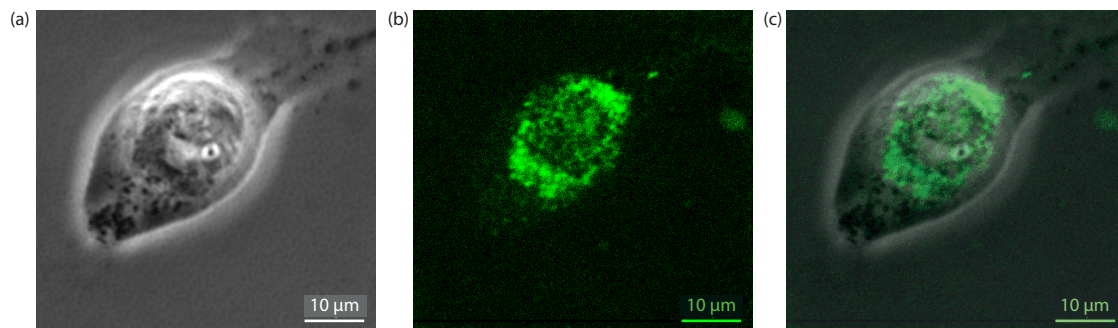


Figure 7.11: A high resolution image of a cell after applying an electrochemical stimulus for less than 3 min: (a) phase contrast image, (b) fluorescent image, (c) overlay of both.

7.5 Chapter Conclusion

We fabricated a simple, functional surface coating that serves as a platform suited for delivery to cells growing on top of it. It was demonstrated that the optimization of the platform enabled cell-growth, and a dye could be delivered to the adhered cells. Moreover, we showed that we can control location and the kinetics of the released substance. This

platform could be used for surface-mediated drug delivery or as an 'artificial synapse' chemically triggering the response of neurons.

Conclusion and Outlook

In this thesis a functional surface coating was planned, designed, developed and fabricated. We succeeded in triggering the release from the vesicles by the application of an electrochemical stimulus. The dye diffused out of the platform and was taken up by cells growing on top of the coating by endocytosis. The coating consisted of three main parts: 1) an underlying PEM (uPEM) made of (PLL/PSS)₉PLL which was resistant to pH and current application, 2) pH-sensitive DOPS liposomes which encapsulated a dye and were adsorbed to the uPEM and 3) a covering PEM (cPEM) made of cross-linked (PLL/HA)₁₂PLL-*g*-PEG-RGD stabilizing and protecting the vesicles from the environment. This cPEM, furthermore, supported the adhesion and growth of cells on it.

Moreover, we found a way to adsorb intact vesicles on PEMs without further stabilization which was not discovered before. Further investigation of this phenomena revealed that the PLL in the uPEM plays a crucial role for the vesicle stabilization enabling us even to adsorb spontaneous multilayers of vesicles. By patterning of the substrate we could further increase the control over the release from the platform. This also allowed for the parallelization of the experiments, increasing efficiency and reliability. Additionally, we found that the speed of the release can be tailored by the variation of the applied current density.

Such functional coatings serve as new tools for addressing basic research questions as well as solving issues for future *in vitro* and maybe even *in vivo* applications. However, the most probable and feasible applications will be in basic research. One example would be to increase the variety of triggers for the release. Many different triggers for the release from vesicles were explored such as magnetic, ultrasound, light, IR, and many more (see

Chapter 1). A very interesting way to trigger the release could also be by mechanical force, namely by stretching, resulting in a mechano-transductive surface coating. This concept is well known in nature, for example the formation of muscle or the hardening of bone tissue as a reaction to heavy work or exercise. In these processes, the mechanical load, such as friction on the skin, or the load on muscle tissue, elicits a biological change in the respective tissue. This change is possible due to transduction of mechanical information to chemical changes, i.e. mechano-chemical transduction, in the body. Mertz and coworkers managed to embed proteins in a surface coating such that the reactive sites of the proteins are prominent to the environment only when the surface is stretched rendering the surface mechano-transductive^[65–67]. The use of this concept could lead to a functional surface coating acting 'self-repairing' for example by releasing monomers upon mechanical stress which polymerize when they come in contact with the surrounding material, thus repairing the surface^[93].

Another basic research application would be to create 'artificial synapses' whereas substances can be released from vesicles and taken up by other vesicles mimicking the natural way signals are transmitted between neuronal cells. This application would require the refill of the vesicles. So far we could not achieve this. There might be a chance to try other parameters such as using non-charged dye, no cPEM and/or other current densities. Once this obstacle is overcome, one might start to work with different distances between the electrodes to assure that the dilution upon release is not too much and the material can still be taken up by the empty vesicles.

One option for an *in vitro* application could be to monitor and influence neuronal activity, by depositing the coating on a micro electrode array (MEA) and growing neurons on it. If one succeeds in the incorporation of neurotransmitters in liposomes, one could selectively stimulate the release to certain neurons and at the same time monitor the reaction of the neurons by the other electrodes around. Many people in our group already work with the monitoring of the activity, being an ideal pool of knowledge and experience in this field.

Another *in vitro* application would be drug screening experiments whereas neurotransmitters are loaded into the vesicles and neurons grow on top of the platform. The neurotransmitters could then be released in the presence of several drugs in order to see, if the drug inhibits or enhances the effect of the neurotransmitter. This application is not straightforward, since it is not yet clear what drugs and neurotransmitters are compatible

with the platform. As Chapter 7 underlined, it was rather difficult to find an appropriate dye for the proof of principle.

When thinking about *in vivo* applications, I always envisioned the coating of implants with the here developed platform. However, the components were never tested for their biocompatibility^[63] which depends not only on the chemistry but also on the concentration of the material. Additionally, even though the vesicles are actually intact upon adsorption, their content is still slowly released with time (Figure 4.10) weakening the advantage of the triggered release for long-term applications. Thus, before the platform can be used *in vivo*, these issues have to be solved.

During the work with this subject we learned many things. First of all, even if one works with well-known materials, the combination of them can lead to a highly complex system requiring many different complementary techniques to assess the interplay between the different materials. Apart from that I - of course - also learned many things in administrative areas such as the planning and organization of experiments and, more importantly, to find the right balance between implementing new ideas and staying on track for the envisioned goal.

References

- [1] The ancient girl with the golden eye: 5000 year old priestess found. <http://www.digitaljournal.com/article/123458>, December 2012.
- [2] J. M. Anderson. Biological Responses to Materials. *Annual Review of Materials Research*, 31:81–110, Aug. 2001.
- [3] J. M. Anderson, A. Rodriguez, and D. T. Chang. Foreign body reaction to biomaterials. *Seminars in immunology*, 20(2):86–100, Apr. 2008.
- [4] J. I. Anzai, Y. Kobayashi, N. Nakamura, M. Nishimura, , and T. Hoshi. Layer-by-Layer Construction of Multilayer Thin Films Composed of Avidin and Biotin-Labeled Poly(amine)s. *Langmuir*, 15:221–226, 1999.
- [5] T. Boudou, T. Crouzier, R. Auzély-Velty, K. Glinel, and C. Picart. Internal composition versus the mechanical properties of polyelectrolyte multilayer films: the influence of chemical cross-linking. *Langmuir*, 25(24):13809–13819, Dec. 2009.
- [6] T. Boudou, T. Crouzier, K. Ren, G. Blin, and C. Picart. Multiple functionalities of polyelectrolyte multilayer films: new biomedical applications. *Advanced Materials*, 22(4):441–467, Jan. 2010.
- [7] F. Boulmedais and P. Schaaf. Secondary Structure of Polypeptide Multilayer Films: An Example of Locally Ordered Polyelectrolyte Multilayers. *Langmuir Notes*, 18:4523–4525, 2002.
- [8] F. Boulmedais, C. S. Tang, B. Keller, and J. Vörös. Controlled Electrodissolution of Polyelectrolyte Multilayers: A Platform Technology Towards the Surface-Initiated Delivery of Drugs. *Advanced Functional Materials*, 16(1):63–70, Jan. 2006.
- [9] S. C. Bürgel, O. Guillaume-Gentil, L. Zheng, J. Vörös, and M. Bally. Zirconium ion mediated formation of liposome multilayers. *Langmuir*, 26(13):10995–11002, July 2010.
- [10] N. A. Campbell and J. B. Reece. *Campbell: Biology. 6th - Google Scholar*. Benjamin Cummings, 6 edition, 2002.
- [11] S. Chen, L. Liu, and S. Jiang. Strong resistance of oligo(phosphorylcholine) self-assembled monolayers to protein adsorption. *Langmuir*, 22(6):2418–2421, Mar. 2006.

- [12] J. Connor, M. B. Yatvin, and L. Huang. pH-sensitive liposomes: acid-induced liposome fusion. *Proceedings of the National Academy of Sciences of the United States of America*, 81(6):1715–1718, Mar. 1984.
- [13] G. Decher. Fuzzy nanoassemblies: toward layered polymeric multicomposites. *Science*, 277(5330):1232–1237, 1997.
- [14] G. Decher and D. J. Schmidt. Fine-Tuning of the film thickness of ultrathin multilayer films composed of consecutively alternating layers of anionic and cationic polyelectrolytes. *Progress in Colloid & Polymer Science*, 89:160–164, 1992.
- [15] M. Decker. *Protein Architecture: Interfacing Molecular Assemblies and Immobilization Biotechnology*. New York, New York, 2000.
- [16] L. Diéguez, N. Darwish, N. Graf, J. Vörös, and T. Zambelli. Electrochemical tuning of the stability of PLL/DNA multilayers. *Soft Matter*, 5:2415–2421, Feb. 2009.
- [17] T. Dinh and R. Tuch. Drug eluting stent, Patent Nr. 5,591,227. 1997.
- [18] T. Dinh and R. Tuch. Drug eluting stent, Patent Nr. 5,697,967. 1997.
- [19] D. L. Elbert, C. Herbert, and J. A. Hubbell. Thin polymer layers formed by polyelectrolyte multilayer techniques on biological surfaces. *Langmuir*, 15(16):5355–5362, 1999.
- [20] H. Ellens, J. Bentz, and F. C. Szoka. pH-induced destabilization of phosphatidylethanolamine-containing liposomes: role of bilayer contact. *Biochemistry*, 23(7):1532–1538, Mar. 1984.
- [21] D. Franco, M. Klingauf, M. Bednarzik, M. Cecchini, V. Kurtcuoglu, J. Gobrecht, D. Poulidakos, and A. Ferrari. Control of initial endothelial spreading by topographic activation of focal adhesion kinase. *Soft Matter*, 7(16):7313, 2011.
- [22] R. A. Frazier, G. Matthijs, M. C. Davies, C. J. Roberts, E. Schacht, and S. J. Tendler. Characterization of protein-resistant dextran monolayers. *Biomaterials*, 21(9):957–966, May 2000.
- [23] M. Gabi, A. Larmagnac, P. Schulte, and J. Vörös. Electrically controlling cell adhesion, growth and migration. *Colloids and Surfaces, B: Biointerfaces*, 79(2):365–371, Sept. 2010.
- [24] M. Gabi, T. Sannomiya, and A. Larmagnac. Influence of applied currents on the viability of cells close to microelectrodes. *Integrative Biology*, 1:108–115, 2009.
- [25] K. Glasmästar, C. Larsson, F. Höök, and B. Kasemo. Protein adsorption on supported phospholipid bilayers. *J. Colloid Interface Sci.*, 246(1):40–47, Feb. 2002.
- [26] N. Graf, F. Albertini, T. Petit, E. Reimhult, J. Vörös, and T. Zambelli. Electrochemically Stimulated Release from Liposomes Embedded in a Polyelectrolyte Multilayer. *Advanced Functional Materials*, 21(9):1666–1672, Mar. 2011.
- [27] A. Granéli, J. Benkoski, and F. Höök. Characterization of a proton pumping transmembrane protein incorporated into a supported *Analytical biochemistry*, 367:87–94, 2007.
- [28] A. Granéli, M. Edvardsson, and F. Höök. DNA-Based Formation of a Supported, Three-Dimensional Lipid Vesicle Matrix Probed by QCM-D and SPR. *Chemphyschem : a European journal of chemical physics and physical chemistry*, 5(5):729–733, May 2004.
- [29] C. Gretzer, L. Emanuelsson, E. Liljensten, and P. Thomsen. The inflammatory cell influx and cytokines changes during transition from acute inflammation to fibrous repair around implanted materials. *J. Biomater. Sci. Polym. Ed*, 17(6):669–687, 2006.

-
- [30] D. Grieshaber, J. Vörös, T. Zambelli, V. Ball, P. Schaaf, J.-C. Voegel, and F. Boulmedais. Swelling and contraction of ferrocyanide-containing polyelectrolyte multilayers upon application of an electric potential. *Langmuir*, 24(23):13668–13676, Dec. 2008.
- [31] O. Guillaume-Gentil, D. Abbruzzese, E. Thomasson, J. Vörös, and T. Zambelli. Chemically Tunable Electrochemical Dissolution of Noncontinuous Polyelectrolyte Assemblies: An In Situ Study Using ecAFM. *ACS Applied Materials & Interfaces*, 2(12):3525–3531, Dec. 2010.
- [32] O. Guillaume-Gentil, Y. Akiyama, and J. Vörös. Polyelectrolyte Coatings with a Potential for Electronic Control and Cell Sheet Engineering. *Advanced Materials*, 20:560–565, 2008.
- [33] O. Guillaume-Gentil, M. Gabi, M. Zenobi-Wong, and J. Vörös. Electrochemically switchable platform for the micro-patterning and release of heterotypic cell sheets. *Biomedical microdevices*, 13(1):221–230, Feb. 2011.
- [34] O. Guillaume-Gentil, N. Graf, F. Boulmedais, P. Schaaf, J. Vörös, and T. Zambelli. Global and local view on the electrochemically induced degradation of polyelectrolyte multilayers: from dissolution to delamination. *Soft Matter*, 6(17):4246–4254, 2010.
- [35] O. Guillaume-Gentil, R. Zahn, S. Lindhoud, N. Graf, J. Vörös, and T. Zambelli. From nanodroplets to continuous films: how the morphology of polyelectrolyte multilayers depends on the dielectric permittivity and the surface charge of the supporting substrate. *Soft Matter*, 7(8):3861–3871, 2011.
- [36] J. Harris. *Poly (ethylene glycol) Chemistry and Biological Applications*. American Chemical Society, Washington DC, 1997.
- [37] Y. J. Hong, H. Y. Lee, and J.-C. Kim. Alginate beads containing pH-sensitive liposomes and glucose oxidase: glucose-sensitive release. *Colloid And Polymer Science*, 287(10):1207–1214, 2009.
- [38] L. Hosta-Rigau, B. Städler, Y. Yan, E. C. Nice, J. K. Heath, F. Albericio, and F. Caruso. Capsosomes with Multilayered Subcompartments: Assembly and Loading with Hydrophobic Cargo. *Advanced Functional Materials*, 20(1):59–66, Jan. 2010.
- [39] A. Izquierdo, S. Ono, J.-C. Voegel, P. Schaaf, and G. Decher. Dipping versus spraying: Exploring the deposition conditions for speeding up layer-by-layer assembly. *Langmuir*, 21:7558–7567, 2005.
- [40] N. Jessel, M. Oulad-Abdelghani, F. Meyer, P. Lavalle, Y. Haikel, P. Schaaf, and J.-C. Voegel. Multiple and time-scheduled in situ DNA delivery mediated by beta-cyclodextrin embedded in a polyelectrolyte multilayer. *Proceedings of the National Academy of Sciences of the United States of America*, 103(23):8618–8621, June 2006.
- [41] C. Jewell and D. M. Lynn. Multilayered polyelectrolyte assemblies as platforms for the delivery of DNA and other nucleic acid-based therapeutics. *Advanced Drug Delivery Reviews*, 60(9):979–999, June 2008.
- [42] C. Jewell and D. M. Lynn. Surface-Mediated Delivery of DNA: Cationic Polymers Take Charge. *Current Opinion in Colloid & Interface Science*, 13(6):395–402, Dec. 2008.
- [43] C. Jewell, J. Zhang, N. J. Fredin, and D. M. Lynn. Multilayered polyelectrolyte films promote the direct and localized delivery of DNA to cells. *Journal of controlled release*, 106(1-2):214–223, Aug. 2005.
- [44] X. Jiang, R. Ferrigno, M. Mrksich, and G. M. Whitesides. Electrochemical desorption of self-assembled monolayers noninvasively releases patterned cells from geometrical confinements. *Journal of the American Chemical Society*, 125(9):2366–2367, Mar. 2003.

- [45] T. R. Khan, H. M. Grandin, A. Mashaghi, M. Textor, E. Reimhult, and I. Reviakine. Lipid redistribution in phosphatidylserine-containing vesicles adsorbing on titania. *Biointerphases*, 3(2):FA90–FA95, 2008.
- [46] B. S. Kim, H. I. Lee, Y. Min, Z. Poon, and P. T. Hammond. Hydrogen-bonded multilayer of pH-responsive polymeric micelles with tannic acid for surface drug delivery. *Chemical Communications*, 28:4194, 2009.
- [47] B. S. Kim, S. W. Park, and P. T. Hammond. Hydrogen-Bonding Layer-by-Layer-Assembled Biodegradable Polymeric Micelles as Drug Delivery Vehicles from Surfaces. *ACS Nano*, 2(2):386–392, Feb. 2008.
- [48] J. A. Kopechek, T. M. Abruzzo, B. Wang, S. M. Chrzanowski, D. A. B. Smith, P. H. Kee, S. Huang, J. H. Collier, D. D. McPherson, and C. K. Holland. Ultrasound-Mediated Release of Hydrophilic and Lipophilic Agents From Echogenic Liposomes. *Journal Of Ultrasound In Medicine*, 27(11):1597–1606, 2008.
- [49] N. Kotov. Layer-by-layer self-assembly: The contribution of hydrophobic interactions. *Nanostructured Materials*, 12(5-8):789–796, 1999.
- [50] L. Krasemann and B. Tieke. Selective ion transport across self-assembled alternating multilayers of cationic and anionic polyelectrolytes. *Langmuir*, 16(2):287–290, 2000.
- [51] I. C. Kwon, Y. H. Bae, and S. W. Kim. Heparin release from polymer complex. *Journal of controlled release*, 30:155–159, 1994.
- [52] P. Lavalle, C. Picart, J. Mutterer, C. Gergely, H. Reiss, J.-C. Voegel, B. Senger, and P. Schaaf. Modeling the buildup of polyelectrolyte multilayer films having exponential growth. *Journal of physical chemistry B*, 108(2):635–648, 2004.
- [53] E. Leguen, A. Chassepot, G. Decher, P. Schaaf, J.-C. Voegel, and N. Jessel. Bioactive coatings based on polyelectrolyte multilayer architectures functionalized by embedded proteins, peptides or drugs. *Biomolecular Engineering*, 24(1):33–41, Feb. 2007.
- [54] Y. Y. Luk, M. Kato, and M. Mrksich. Self-Assembled Monolayers of Alkanethiolates Presenting Mannitol Groups Are Inert to Protein Adsorption and Cell Attachment. *Langmuir*, 16(24):9604–9608, Nov. 2000.
- [55] D. T. Luttkhuizen, M. C. Harmsen, and M. J. A. Van Luyn. Cellular and molecular dynamics in the foreign body reaction. *Tissue Engineering*, 12(7):1955–1970, 2006.
- [56] Y. Lvov, K. Ariga, and T. Kunitake. Layer-by-Layer Assembly of Alternate Protein/Polyion Ultrathin Films. *Chemistry Letters*, (12):2323–2326, 1994.
- [57] Y. Lvov, G. Decher, and G. Sukhorukov. Assembly of thin films by means of successive deposition of alternate layers of DNA and poly(allylamine). *Macromolecules*, 26(20):5396–5399, Sept. 1993.
- [58] Y. Lvov, H. Haas, G. Decher, and H. Moehwald. Successive deposition of alternate layers of polyelectrolytes and a charged virus. *Langmuir*, 10(11):4232–4236, 1994.
- [59] R. C. MacDonald, S. A. Simon, and E. Baer. Ionic influences on the phase transition of dipalmitoylphosphatidylserine. *Biochemistry*, 15(4):885–891, Feb. 1976.
- [60] M. Malmsten. Ellipsometry Studies of Protein Adsorption at Lipid Surfaces. *Journal Of Colloid And Interface Science*, 168(1):247–254, Nov. 1994.

-
- [61] R. E. Marchant, S. Yuan, and G. Szakalas-Gratzl. Interactions of plasma proteins with a novel polysaccharide surfactant physisorbed to polyethylene. *J. Biomater. Sci. Polym. Ed*, 6(6):549–564, 1994.
- [62] N. G. Maroudas. Polymer exclusion, cell adhesion and membrane fusion. *Nature*, 254(5502):695–696, Apr. 1975.
- [63] J. S. Martinez, T. C. S. Keller, and J. B. Schlenoff. Cytotoxicity of free versus multilayered polyelectrolytes. *Biomacromolecules*, 12(11):4063–4070, Nov. 2011.
- [64] S. L. McArthur, K. M. McLean, P. Kingshott, H. A. W. St John, R. C. Chatelier, and H. J. Griesser. Effect of polysaccharide structure on protein adsorption. *Colloids and Surfaces, B: Biointerfaces*, 17(1):37–48, Jan. 2000.
- [65] D. Mertz, J. Hemmerlé, F. Boulmedais, J.-C. Voegel, P. Lavallo, and P. Schaaf. Polyelectrolyte multilayer films under mechanical stretch. *Soft Matter*, 3(11):1413–1420, 2007.
- [66] D. Mertz, J. Hemmerlé, J. Mutterer, S. Ollivier, J.-C. Voegel, P. Schaaf, and P. Lavallo. Mechanically responding nanovalves based on polyelectrolyte multilayers. *Nano letters*, 7(3):657–662, 2007.
- [67] D. Mertz, C. Vogt, J. Hemmerlé, J. Mutterer, V. Ball, J.-C. Voegel, P. Schaaf, and P. Lavallo. Mechanotransductive surfaces for reversible biocatalysis activation. *Nature materials*, 8(9):731–735, Sept. 2009.
- [68] M. Michel, Y. Arntz, G. Fleith, J. Toquant, Y. Haikel, J.-C. Voegel, P. Schaaf, and V. Ball. Layer-by-Layer Self-Assembled Polyelectrolyte Multilayers with Embedded Liposomes: Immobilized Sub-micronic Reactors for Mineralization. *Langmuir*, 22(5):2358–2364, 2006.
- [69] M. Michel, A. Izquierdo, G. Decher, J.-C. Voegel, P. Schaaf, and V. Ball. Layer by layer self-assembled polyelectrolyte multilayers with embedded phospholipid vesicles obtained by spraying: Integrity of the vesicles. *Langmuir*, 21(17):7854–7859, 2005.
- [70] M. Michel, D. Vautier, J.-C. Voegel, P. Schaaf, and V. Ball. Layer by Layer Self-Assembled Polyelectrolyte Multilayers with Embedded Phospholipid Vesicles. *Langmuir*, 20:4835–4839, 2004.
- [71] H. Mjahed, J.-C. Voegel, B. Senger, A. Chassepot, A. Rameau, V. Ball, P. Schaaf, and F. Boulmedais. Hole formation induced by ionic strength increase in exponentially growing multilayer films. *Soft Matter*, 5(11):2269, 2009.
- [72] S. Morgenthaler. *Surface Chemical Gradients*. PhD thesis, ETH Zürich, July 2007.
- [73] M. Mrksich. A surface chemistry approach to studying cell adhesion. *Chem Soc Rev*, 29(4):267–273, 2000.
- [74] M. Mrksich and G. M. Whitesides. Using Self-Assembled Monolayers to Understand the Interactions of Man-made Surfaces with Proteins and Cells. *Annual Review of Biophysics and Biomolecular Structure*, 25(1):55–78, June 1996.
- [75] S. Nappini, F. B. Bombelli, M. Bonini, B. Norden, and P. Baglioni. Magnetoliposomes for controlled drug release in the presence of low-frequency magnetic field. *Soft Matter*, 6(1):154–162, 2010.
- [76] W. Ong, Y. Yang, A. C. Cruciano, and R. L. McCarley. Redox-Triggered Contents Release from Liposomes. *Journal of the American Chemical Society*, 130(44):14739–14744, 2008.

- [77] E. Österberg, K. Bergström, K. Holmberg, J. A. Riggs, J. M. Van Alstine, T. P. Schuman, N. L. Burns, and J. M. Harris. Comparison of polysaccharide and poly(ethylene glycol) coatings for reduction of protein adsorption on polystyrene surfaces. *Colloids and Surfaces A: Physicochemical and Engineering Aspects*, 77(2):159–169, Sept. 1993.
- [78] C. Pale-Grosdemange, E. S. Simon, K. L. Prime, and G. M. Whitesides. Formation of self-assembled monolayers by chemisorption of derivatives of oligo(ethylene glycol) of structure HS(CH₂)₁₁(OCH₂CH₂)_mOH on gold. *Journal of the American Chemical Society*, 113(1):12–20, Jan. 1991.
- [79] C. Picart, J. Mutterer, L. Richert, Y. Luo, G. D. Prestwich, P. Schaaf, J.-C. Voegel, and P. Lavallo. Molecular basis for the explanation of the exponential growth of polyelectrolyte multilayers. *Proceedings of the National Academy of Sciences of the United States of America*, 99(20):12531–12535, Oct. 2002.
- [80] E. Reimhult, F. Höök, and B. Kasemo. Vesicle adsorption on SiO₂ and TiO₂: Dependence on vesicle size. *Journal of chemical physics*, 117(16):7401–7404, 2002.
- [81] L. Richert, F. Boulmedais, P. Lavallo, and J. Mutterer. Improvement of stability and cell adhesion properties of polyelectrolyte multilayer films by chemical cross-linking. *Biomacromolecules*, 5:248–294, 2004.
- [82] L. Richert, A. Engler, D. Discher, and C. Picart. Elasticity of native and cross-linked polyelectrolyte multilayer films. *Biomacromolecules*, 5:1908–1916, 2004.
- [83] L. Richert, P. Lavallo, D. Vautier, B. Senger, J. Stoltz, P. Schaaf, J.-C. Voegel, and C. Picart. Cell interactions with polyelectrolyte multilayer films. *Biomacromolecules*, 3(6):1170–1178, 2002.
- [84] M. Rodahl and B. Kasemo. A simple setup to simultaneously measure the resonant frequency and the absolute dissipation factor of a quartz crystal microbalance. *Review of Scientific Instruments*, 67(9):3238–3241, 1996.
- [85] G. Rydzek, J.-S. Thomann, N. Ben Ameer, L. Jierry, P. Mésini, A. Ponche, C. Contal, A. E. El Haitami, J.-C. Voegel, B. Senger, P. Schaaf, B. Frisch, and F. Boulmedais. Polymer Multilayer Films Obtained by Electrochemically Catalyzed Click Chemistry. *Langmuir*, 26(4):2816–2824, Feb. 2010.
- [86] J. B. Schlenoff, S. T. Dubas, and T. Farhat. Sprayed Polyelectrolyte Multilayers. *Langmuir*, 16:9968–9969, 2000.
- [87] A. Schneider, G. Francius, R. Obeid, and P. Schwinte. Polyelectrolyte Multilayers with a Tunable Young's Modulus: Influence of Film Stiffness on Cell Adhesion. *Langmuir*, 22:1193–1200, 2006.
- [88] A. Schroeder, R. Honen, K. Turjeman, A. Gabizon, J. Kost, and Y. Barenholz. Ultrasound triggered release of cisplatin from liposomes in murine tumors. *Journal of controlled release*, 137(1):63–68, July 2009.
- [89] A. Schroeder, J. Kost, and Y. Barenholz. Ultrasound, liposomes, and drug delivery: principles for using ultrasound to control the release of drugs from liposomes. *Chemistry and Physics of Lipids*, 162(1-2):1–16, 2009.
- [90] T. Segura, M. J. Volk, and L. D. Shea. Substrate-mediated DNA delivery: role of the cationic polymer structure and extent of modification. *Journal of controlled release*, 93(1):69–84, Nov. 2003.
- [91] U. Seifert. Configurations of fluid membranes and vesicles. *Advances In Physics*, 46(1):13–137, 1997.

-
- [92] A. Sharma and U. S. Sharma. Liposomes in drug delivery: Progress and limitations. *International Journal of Pharmaceutics*, 154(2):123–140, Aug. 1997.
- [93] G. D. Shchukin and H. Möhwald. Self-Repairing Coatings Containing Active Nanoreservoirs. *Smart materials*, 3:926–943.
- [94] B. S. Shim, P. Podsiadlo, D. G. Lilly, A. Agarwal, J. Leet, Z. Tang, S. Ho, P. Ingle, D. Paterson, W. Lu, and N. A. Kotov. Nanostructured thin films made by diwetting method of layer-by-layer assembly. *Nano letters*, 7(11):3266–3273, 2007.
- [95] Y. Shimazaki, M. Mitsuishi, S. Ito, , and M. Yamamoto. Preparation of the Layer-by-Layer Deposited Ultrathin Film Based on the Charge-Transfer Interaction. *Langmuir*, 13:1385–1387, 1997.
- [96] W. B. Stockton and M. Rubner. Molecular-Level Processing of Conjugated Polymers. 4. Layer-by-Layer Manipulation of Polyaniline via Hydrogen-Bonding Interactions. *Macromolecules*, 30(9):2717–2725, 1997.
- [97] X. Su, B. Kim, S. KIM, P. T. Hammond, and D. Irvine. Layer-by-Layer-Assembled Multilayer Films for Transcutaneous Drug and Vaccine Delivery. *ACS Nano*, Oct. 2009.
- [98] J. Sun, T. Wu, Y. Sun, Z. Wang, X. Zhang Jiacong Shen, J. Sun, and W. Cao. Fabrication of a covalently attached multilayer via photolysis of layer-by-layer self-assembled films containing diazo-resins. *Chemical Communications*, pages 1853–1854, 1998.
- [99] J. D. Swalen. Langmuir-Blodgett Films. *Science*, 249(4966):305–306, July 1990.
- [100] C. Tang, M. Dusseiller, S. Makohliso, M. Heuschkel, S. Sharma, B. Keller, and J. Voros. Dynamic, electronically switchable surfaces for membrane protein microarrays. *Analytical chemistry*, 78(3):711–717, 2006.
- [101] C. Tang, L. Feller, P. Rossbach, B. Keller, J. Voros, S. Tosatti, and M. Textor. Adsorption and electrically stimulated desorption of the triblock copolymer poly(propylene sulfide-bl-ethylene glycol) (PPS-PEG) from indium tin oxide (ITO) surfaces. *Surface Science*, 600(7):1510–1517, 2006.
- [102] Z. Tang, Y. Wang, P. Podsiadlo, and N. A. Kotov. Biomedical applications of layer-by-layer assembly: From biomimetics to tissue engineering. *Advanced Materials*, 18(24):3203–3224, 2006.
- [103] A. Tezcaner, D. Hicks, F. Boulmedais, J. Sahel, P. Schaaf, J.-C. Voegel, and P. Lavallo. Polyelectrolyte multilayer films as substrates for photoreceptor cells. *Biomacromolecules*, 7(1):86–94, 2006.
- [104] P. Thevenot, W. Hu, and L. Tang. Surface chemistry influences implant biocompatibility. *Current topics in medicinal chemistry*, 8(4):270–280, 2008.
- [105] V. Torchilin and V. Weissig. *Liposomes: a practical approach*. Oxford University Press, 2 edition, 2003.
- [106] T. S. Troutman, S. J. Leung, and M. Romanowski. Light-Induced Content Release from Plasmon-Resonant Liposomes. *Advanced Materials*, 21(22):2334–2338, 2009.
- [107] P. Tryoen-Tóth, D. Vautier, Y. Haikel, J.-C. Voegel, P. Schaaf, J. Chluba, and J. Ogier. Viability, adhesion, and bone phenotype of osteoblast-like cells on polyelectrolyte multilayer films. *Journal of biomedical materials research*, 60(4):657–667, June 2002.
- [108] D. Vautier, V. Karsten, C. Egles, J. Chluba, P. Schaaf, J.-C. Voegel, and J. Ogier. Polyelectrolyte multilayer films modulate cytoskeletal organization in chondrosarcoma cells. *J. Biomater. Sci. Polym. Ed.*, 13(6):713–732, 2002.

- [109] P. Venugopalan, S. Jain, S. Sankar, P. Singh, A. Rawat, and S. Vyas. pH-Sensitive liposomes: mechanism of triggered release to drug and gene delivery prospects. *Pharmazie*, 57(10):659–671, 2002.
- [110] P. Vermette and L. Meagher. Interactions of phospholipid- and poly(ethylene glycol)-modified surfaces with biological systems: relation to physico-chemical properties and mechanisms. *Colloids and Surfaces, B: Biointerfaces*, 28(2-3):153–198, Apr. 2003.
- [111] C. Vodouhe, M. Schmittbuhl, F. Boulmedais, D. Bagnard, D. Vautier, P. Schaaf, C. Egles, J.-C. Voegel, and J. Ogier. Effect of functionalization of multilayered polyelectrolyte films on motoneuron growth. *Biomaterials*, 26(5):545–554, Feb. 2005.
- [112] D. V. Volodkin, Y. Arntz, P. Schaaf, H. Moehwald, J.-C. Voegel, and V. Ball. Composite multilayered biocompatible polyelectrolyte films with intact liposomes: stability and temperature triggered dye release. *Soft Matter*, 4(1):122–130, 2008.
- [113] D. V. Volodkin, P. Schaaf, H. Moehwald, J.-C. Voegel, and V. Ball. Effective embedding of liposomes into polyelectrolyte multilayered films: the relative importance of lipid-polyelectrolyte and interpolyelectrolyte interactions. *Soft Matter*, 5(7):1394–1405, 2009.
- [114] D. V. Volodkin, A. G. Skirtach, and H. Moehwald. Near-IR Remote Release from Assemblies of Liposomes and Nanoparticles. *Angewandte Chemie International Edition*, 48(10):1807–1809, 2009.
- [115] D. V. Volodkin, A. G. Skirtach, and H. Moehwald. LbL Films as Reservoirs for Bioactive Molecules. In *Advances in Polymer Science 1*. Springer Berlin Heidelberg, Berlin, Heidelberg, 2011.
- [116] L. Vroman. *Blood*. Surface activity in blood coagulation. Natural History Press, New York, 1967.
- [117] C. R. Wittmer, J. A. Phelps, C. M. Lepus, W. M. Saltzman, M. J. Harding, and P. R. Van Tassel. Multilayer nanofilms as substrates for hepatocellular applications. *Biomaterials*, 29(30):4082–4090, Oct. 2008.
- [118] K. C. Wood, H. F. Chuang, R. D. Batten, D. M. Lynn, and P. T. Hammond. Controlling interlayer diffusion to achieve sustained, multiagent delivery from layer-by-layer thin films. *Proceedings of the National Academy of Sciences of the United States of America*, 103(27):10207–10212, July 2006.
- [119] A. Yavlovich, A. Singh, S. Tarasov, J. Capala, R. Blumenthal, and A. Puri. Design of liposomes containing photopolymerizable phospholipids for triggered release of contents. *Journal Of Thermal Analysis And Calorimetry*, 98(1):97–104, 2009.
- [120] J. Zasadzinski, R. Viswanathan, L. Madsen, J. Garnæs, and D. Schwartz. Langmuir-Blodgett films. *Science*, 263(5154):1726–1733, Mar. 1994.
- [121] A. N. Zelikin. Drug Releasing Polymer Thin Films: New Era of Surface-Mediated Drug Delivery. *ACS Nano*, 4(5):2494–2509, May 2010.
- [122] Y. W. Zhiyong Tang and N. A. Kotov. Biomedical Applications of Layer-by-Layer Assembly: From Biomimetics to Tissue Engineering. *Advanced Materials*, 16:3203–3224, 2006.

Curriculum Vitae

Personal

Name: Norma Magdalena Graf
Date of Birth: March, 24, 1983
Nationality: Swiss, Citizen of Bleienbach (BE)
Present Address: Emil Klöti-Strasse 6
CH-8406 Winterthur
Switzerland

Education and Practical Experience

- 04. 2008 - 04. 2012 Doctoral student at the Laboratory of Biosensors and Bioelectronics, Institute for Biomedical Engineering, Department of Information Technology and Electrical Engineering, ETH Zürich
- 10. 2002 - 02. 2008 Studies of Material Sciences at ETH Zürich, Graduation with the degree Master of Sciences ETH
- 08. 2007 - 02. 2008 Master Thesis at the Laboratory of Surface Sciences and Technology, ETH Zürich in collaboration with CIBA Basel
- 05. 2007 - 03. 2008 Researcher at WW Technology, Schlieren, Switzerland
- 09. 2005 - 04. 2006 Internship at Philips Research Campus in Eindhoven, Netherlands
- 08. 2002 - 09. 2002 Internship at EMPA, Dübendorf, Switzerland

08. 1996 - 08. 2002 Gymnasium in Immensee, Switzerland, with focus on mathematics and physics

Publications Related to this Thesis

Presentations

- N. Graf, F. Albertini, T. Petit, J. Vörös, T. Zambelli; Electrochemically Stimulated Release From Liposomes Embedded in a Polyelectrolyte Multilayer, ISP International Symposium on Polyelectrolytes, Shanghai, China, November 2010
- N. Graf, F. Albertini, T. Petit, J. Vörös, T. Zambelli; Electrochemically Stimulated Release From Liposomes Embedded in a Polyelectrolyte Multilayer, MRC Graduate Symposium, Zürich, Switzerland, May 2010
- N. Graf, F. Albertini, T. Petit, J. Vörös, T. Zambelli; Towards Electrically Induced Release of Bioactive Molecules Into Living Cells, WACBE World Congress on Bioengineering 2009, 26 - 29 July 2009 The Hong Kong Polytechnic University, Hong Kong

Posters

- N. Graf, F. Albertini, T. Petit, J. Vörös, T. Zambelli; Electrochemically triggered Release of Dye from Liposomes Embedded in Polyelectrolyte Multilayers, European Material Research Symposium (EMRS), 9.-14.5.2011, Nice, France
- N. Graf, J. Vörös, T. Zambelli; Electrochemically Triggered Release of Bioactive Molecules from Liposomes, 20th International Symposium on Bioelectrochemistry and Bioenergetics, 10.-14.05.2009, Sibiu, Romania. This Poster received the 'BES 2009 Best Poster' Award.
- N. Graf, F. Pianezzi, J. Vörös, T. Zambelli; Electrochemically Triggered Release of Bioactive Molecules from Liposomes
- N. Graf, F. Pianezzi, J. Vörös, T. Zambelli; Joining Forces: Sensing and Manipulating in Live Cells, 07.11.2008, Zürich, Switzerland

- N. Graf, F. Pianezzi, J. Vörös, T. Zambelli; Electrochemically Triggered Rupture of Phosphocholine Vesicles, SBE's 4th International Conference on Bioengineering and Nanotechnology, 22.-24.07.2008, Dublin, Ireland
- N. Graf, O. Guillaume-Gentil, D. Abbruzzese, R. Zahn, J. Vörös, T. Zambelli; Polyelectrolyte Multilayers as Interface for Biomedical Applications, 7th International Symposium on Polyelectrolytes, 16.-19.6.2008, Coimbra, Portugal

Publications

- N. Graf, A. Tanno, A. Dochter, N. Rothfuchs, J. Vörös, T. Zambelli; Electrochemically Driven Delivery to Cells from Vesicles Embedded in a Polyelectrolyte Multilayer, *Soft Matter*, DOI: 10.1039/c2sm07272f
- N. Graf, E. Thomasson, A. Tanno, J. Vörös, T. Zambelli; Spontaneous Formation of a Vesicle Multilayer on Top of an Exponentially Growing Polyelectrolyte Multilayer Mediated by Diffusing Poly-l-lysine, *Journal of Physical Chemistry B*, 2011
- O. Guillaume-Gentil, R. Zahn, S. Lindhoud, N. Graf, J. Vörös and T. Zambelli; From Nanodroplets to Continuous Films: How the Morphology of Polyelectrolyte Multilayers Depends on the Dielectric Permittivity and the Surface Charge of the Supporting Substrate, *Soft Matter*, 2011, 7, 3861
- N. Graf, F. Albertini, T. Petit, E. Reimhult, J. Vörös, T. Zambelli; Electroactive Platform for Stimulated Release from Liposomes Embedded in Polyelectrolyte Multilayers, *Advanced Functional Materials*, 2011, 21, 1666-1672
- O. Guillaume-Gentil, N. Graf, F. Boulmedais, P. Schaaf, J. Vörös, and T. Zambelli; Global and Local View on the Electrochemically Induced Degradation of Polyelectrolyte Multilayers: from Dissolution to Delamination, *Soft Matter*, 6, 4246-4254, 2010
- L. Diéguez, N. Darwish, N. Graf, J. Vörös, T. Zambelli; Electrochemically Controlled Deposition and Dissolution of PLL/DNA Multilayers, *Soft Matter* 5, 2415-2421, 2009

Supervised Student Projects

- Alexander Tanno (Master Thesis); Platform for Surface-Mediated Drug Delivery: Adaption for Improved Cell Attachment and Triggered Release from Liposomes to Living Cells
- Nuria Rothfuchs (Semester Thesis); Adapting a Delivery Platform for Local and Temporal Release Control
- Alexandre Dochter (Master Thesis); Study of a Polyelectrolyte Multilayer Based Release System for Spatial and Temporal Release Control
- Luca Hirt (Semester Thesis); Stretching as an Alternative Triggering Mechanism for Dye Release from Liposomes Embedded in Polyelectrolyte Multilayers
- Alexander Tanno (Semester Thesis); Design Strategies for Electrochemically Triggered Release of Dyes to Cells
- Francesco Albertini (Semester Thesis); Investigation of Lipid Composition for pH-Sensitive Liposomes
- Tristan Petit (Semester Thesis); Protocols for Embedding Intact Vesicles into a Polyelectrolyte Multilayer